TR-795-716
APRIL 1970

DERIVATION OF EQUATIONS FOR A 6-D TRAJECTORY WITH 3-D ELASTIC BODY VEHICLE DYNAMICS

PREPARED FOR:

NATIONAL AERONAUTICS AND SPACE ADMINISTRATION
GEORGE C. MARSHALL SPACE FLIGHT CENTER
Aero-Astrodynamics Laboratory

UNDER CONTRACT NAS8-24920

NORTHROP CORPORATION
ELECTRO-MECHANICAL DIVISION
P. O. BOX 1484
HUNTSVILLE, ALABAMA 35807
TELEPHONE (205)837-0580

DERIVATION OF EQUATIONS FOR A 6-D TRAJECTORY WITH 3-D ELASTIC BODY VEHICLE DYNAMICS

April 1970

By

G. A. Aramayo
K. L. Clark
J. H. Kincaid
J. T. Lyons
C. M. Pearson

PREPARED FOR:

NATIONAL AERONAUTICS AND SPACE ADMINISTRATION
GEORGE C. MARSHALL SPACE FLIGHT CENTER
AERO-ASTRODYNAMICS LABORATORY

Under Contract NAS8-24920

REVIEWED AND APPROVED BY:

C. M. Pearson, General Supervisor
Structural Dynamics Branch

M. A. Sloan, Jr., Director
Dynamics Analysis Section

NORTHROP CORPORATION
HUNTSVILLE, ALABAMA

FOREWORD

This report was developed under NASA Contract NAS8-24920, "Derivation of Equations for a 6-D Trajectory with 3-D Elastic Body Vehicle Dynamics". The report documents the derivation of all subsystem dynamics equations which are logically grouped for simulation purposes into separate modules described in an earlier companion report (ref. 1). Those equations in this report that are enclosed by straight lines are those equations that appear in the Simulation Diagrams of reference 1.

The NASA Technical Coordinator was Mr. D. K. Mowery, Aero-Astrodynamics Laboratory, George C. Marshall Space Flight Center, Huntsville, Alabama. The study program was conducted by Northrop-Huntsville's Dynamics Analysis Section.

ABSTRACT

This report contains the derivation of equations for the following subsystem dynamics:

- elastic body (3-D)
- trajectory (6-D)
- initialization
- gravitation
- slosh
- rigid body rotation
- aerodynamics
- propulsion and engine dynamics
- loads
- guidance and control

Each set of subsystem dynamics equations is presented in a form amenable to inclusion within a simulation module. The modules may then be assembled to provide an overall mathematical model for use in simulating the flight dynamics of space shuttle vehicles during boost-phase flight.

TABLE OF CONTENTS

TABLE OF CONTENTS (Concluded)

LIST OF ILLUSTRATIONS

LIST OF ILLUSTRATIONS (Concluded)

Section I
INTRODUCTION

In general, space vehicle dynamics are closely approximated by assuming that the vehicle is symmetrical. Past problems encountered on the Saturn V vehicle flights have shown a strong deficiency in predicting correct vehicle dynamics under this symmetry assumption. These critical assumptions may be eliminated by rederiving total system equations with limiting restrictions. These equations may be developed logically and presented in a step-by-step and subsystem-by-subsystem approach (refs. 2, 3) enabling a quick simplification or change to any subsystem. The formulation and modularization of these subsystem dynamics equations will provide the necessary elements or modules (ref. 1) of a mathematical model for use in simulating space vehicle flight dynamics. Success with this approach has been demonstrated by a previous simulation (ref. 4).

The derivation of subsystem equations for a 6-D trajectory using 3-D elastic vehicle mode shapes is presented in Sections II through XI. Section XII presents conclusions and recommendations, and a listing of a few important references may be found in Section XIII.

Section II
ELASTIC BODY EQUATIONS

2.1 GENERAL

Space vehicle dynamics have been approximated with some success by assuming that the vehicle is symmetrical. For conventional vehicles having a high degree of axial symmetry, there is usually negligible coupling between the pitch and yaw lateral elastic modes, as well as between lateral and longitudinal or torsional elastic modes. Thus, an analysis of the planar elastic properties of the vehicle is usually sufficient for purposes of control system analysis.

However, understanding the bending dynamics of advanced space vehicles which may possess large numbers of vehicular asymmetries, particularly during boost-phase flight, requires among other things, that the investigator

(1) Accurately determine the vehicle's three-dimensional vibration characteristics called 3-D modal data,

(2) Provide tractable equations suitable for mathematically representing the vehicle's elastic body dynamics, and

(3) Correctly use the 3-D modal data (generalized masses, natural frequencies, modal displacements, modal slopes) as parametric inputs vital to the solution of the elastic body equations.

2.2 ASSUMPTIONS

It has been assumed that the 3-D modal data that are to be used with the elastic body equations have been previously determined by using a vehicle bending model that includes/excludes the following:

Includes	Excludes
• empty airframe	• engine masses
• non-slosh propellants	
• slosh propellants (frozen)	

Important consequences of using this type of 3-D modal data are described in Section VI - Propellant Slosh Equations, and Section IX - Propulsion and Engine Dynamics.

2.3 EQUATION DEVELOPMENT

2.3.1 Elastic Body Equations

It is the purpose of the elastic body equations to determine bending at specified vehicle stations due to forces and moments at those stations. Each bending mode is modeled as a linear second-order dynamic system with a characteristic natural frequency and damping as follows:

$$\ddot{\bar{\eta}} + 2\,\zeta\omega\,\dot{\bar{\eta}} + \omega^2\,\bar{\eta} = M^{-1}\,\bar{Q} \qquad (2\text{-}1)$$

where

$\ddot{\bar{\eta}}$ = n-vector of generalized accelerations
(Note: n is the number of bending modes)

$\dot{\bar{\eta}}$ = n-vector of generalized velocities

$\bar{\eta}$ = n-vector of generalized displacements

ζ = n x n diagonal damping coefficient matrix

ω = n x n diagonal undamped natural frequency matrix

M = n x n diagonal modal mass (generalized mass) matrix

M^{-1} = n x n diagonal inverse of M

$\bar{Q}$ = n-vector of generalized forces

2.3.2 Generalized Forces

The generalized force Q is considered to have contributions from aerodynamics, slosh, engine thrust, and engine inertia, as follows:

$$Q = Q_A + Q_S + Q_T + Q_E \qquad (2\text{-}2)$$

where the generalized forces Q_A, Q_S, Q_T, and Q_E are discussed in the following subsections.

2.3.2.1 Generalized Force Due to Aerodynamics, Q_A

$$Q_A = Q_{AF} + Q_{AM} \tag{2-3}$$

$$= \sum_{\beta} \sum_{j=1}^{N_{A_\beta}} \Phi_\xi^T (\bar{R}_{A_{\beta_j}}) \bar{F}^B_{A_{\beta_j}} + \sum_{\beta} \sum_{j=1}^{N_{A_\beta}} \Phi_\gamma^T (\bar{R}_{A_{\beta_j}}) \bar{M}^B_{A_{\beta_j}} \tag{2-4}$$

2.3.2.2 Generalized Force Due to Propellant Slosh, Q_S

$$Q_S = Q_{SF} + Q_{SFL} + Q_{SM} + Q_{SML} \tag{2-5}$$

$$= \sum_{j=1}^{Ns} \Phi_\xi^T (\bar{R}_{S_j}) \bar{F}^B_{S_j} + \sum_{j=1}^{Ns} \Phi_\xi^T (\bar{R}_{L_j}) \bar{F}^B_{L_j} +$$

$$\sum_{j=1}^{Ns} \Phi_\gamma^T (\bar{R}_{S_j}) \bar{M}^B_{S_j} + \sum_{j=1}^{Ns} \Phi_\gamma^T (\bar{R}_{L_j}) \bar{M}^B_{L_j} \tag{2-6}$$

2.3.2.3 Generalized Force Due to Engine Thrust, Q_T

$$Q_T = Q_{TF} \tag{2-7}$$

$$= \sum_{j=1}^{N_E} \Phi_\xi^T (\bar{R}_{E_j}) \bar{F}^B_{T(b)_j} \tag{2-8}$$

2.3.2.4 Generalized Force Due to Engine Inertia, Q_E

$$Q_E = Q_{EF} + Q_{EM} \tag{2-9}$$

$$= \sum_{j=1}^{N_E} \Phi_\xi^T (\bar{R}_{E_j}) \bar{F}^B_{E(b)_j} + \sum_{j=1}^{N_E} \Phi_\gamma^T (\bar{R}_{E_j}) \bar{M}^B_{E(b)_j} \tag{2-10}$$

NOTE: Refer to subsection 2.5 GLOSSARY OF TERMS

Substituting equations (2-4), (2-6), (2-8), and (2-10) into equation (2-2) results in a form for the total generalized force that is amenable to simulation, as follows:

$$
\begin{aligned}
Q = &\sum_{\beta} \sum_{j=1}^{N_{A_\beta}} \Phi_\xi^T (\bar{R}_{A_{\beta_j}}) \bar{F}^B_{A_{\beta_j}} + \sum_{\beta} \sum_{j=1}^{N_{A_\beta}} \Phi_\gamma^T (\bar{R}_{A_{\beta_j}}) \bar{M}^B_{A_{\beta_j}} \\
&+ \sum_{j=1}^{N_S} \Phi_\xi^T (\bar{R}_{S_j}) \bar{F}^B_{S_j} + \sum_{j=1}^{N_S} \Phi_\xi^T (\bar{R}_{L_j}) \bar{F}^B_{L_j} \\
&+ \sum_{j=1}^{N_S} \Phi_\gamma^T (\bar{R}_{S_j}) \bar{M}^B_{S_j} + \sum_{j=1}^{N_S} \Phi_\gamma^T (\bar{R}_{L_j}) \bar{M}^B_{L_j} \\
&+ \sum_{j=1}^{N_E} \Phi_\xi^T (\bar{R}_{E_j}) \bar{F}^B_{T(b)_j} \\
&+ \sum_{j=1}^{N_E} \Phi_\xi^T (\bar{R}_{E_j}) \bar{F}^B_{E(b)_j} + \sum_{j=1}^{N_E} \Phi_\gamma^T (\bar{R}_{E_j}) \bar{M}^B_{E(b)_j}
\end{aligned}
\tag{2-11}
$$

2.4 GENERALIZED ACCELERATION, VELOCITY, AND DISPLACEMENT

Equation (2-1) can be rearranged to provide the form

$$\ddot{\bar{\eta}} = M^{-1}Q - 2\zeta\omega\dot{\bar{\eta}} - \omega^2\bar{\eta} \tag{2-12}$$

or the equivalent modal form

$$\begin{bmatrix} \ddot{\eta}_1 \\ \cdot \\ \cdot \\ \cdot \\ \ddot{\eta}_n \end{bmatrix} = \begin{bmatrix} \frac{Q_1}{M_1} - 2\zeta_1\omega_1\dot{\eta}_1 - \omega_1^2\eta_1 \\ \cdot \\ \cdot \\ \cdot \\ \frac{Q_n}{M_n} - 2\zeta_n\omega_n\dot{\eta}_n - \omega_n^2\eta_n \end{bmatrix} \tag{2-13}$$

Generalized accelerations $\ddot{\eta}_i$ (i=1, n) are calculated algebraically. The $\ddot{\eta}_i$'s are successively integrated to provide the generalized velocity

$$\dot{\eta}_i = \int_o^t \ddot{\eta}_i \, dt + \dot{\eta}_i(0) \qquad i = 1, n \tag{2-14}$$

and the generalized displacement

$$\eta_i = \int_o^t \dot{\eta}_i \, dt + \eta_i(0) \qquad i = 1, n \tag{2-15}$$

where $\dot{\eta}_i(o)$ and $\eta_i(o)$ are generalized velocity and displacement at time t=0.

2.5 GLOSSARY OF TERMS

SYMBOL	DEFINITION	UNIT
$\bar{F}^{B}_{A_{\beta j}} = \begin{bmatrix} F^{B}_{A\beta X_j} \\ F^{B}_{A\beta Y_j} \\ F^{B}_{A\beta Z_j} \end{bmatrix}$	Vector force at the j^{th} aerodynamic station (aero panel) of the β-body, where β = f (fuselage), w (wing), h (horizontal stabilizer), and v (vertical stabilizer).	N
$\bar{F}^{B}_{E(b)_j} = \begin{bmatrix} F^{B}_{E(b)X_j} \\ F^{B}_{E(b)Y_j} \\ F^{B}_{E(b)Z_j} \end{bmatrix}$	Vector force of the j^{th} engine inertia	N
$\bar{F}^{B}_{L_j} = \begin{bmatrix} F^{B}_{LX_j} \\ F^{B}_{LY_j} \\ F^{B}_{LZ_j} \end{bmatrix}$	Vector force of the j^{th} tank longitudinal slosh mass inertia	N
$\bar{F}^{B}_{S_j} = \begin{bmatrix} F^{B}_{SX_j} \\ F^{B}_{SY_j} \\ F^{B}_{SZ_j} \end{bmatrix}$	Vector force of the j^{th} tank lateral slosh mass inertia	N

SYMBOL	DEFINITION	UNIT
$\bar{F}^{B}_{T(b)_j} = \begin{bmatrix} F^{B}_{T(b)X_j} \\ F^{B}_{T(b)Y_j} \\ F^{B}_{T(b)Z_j} \end{bmatrix}$	Vector force of the j^{th} engine thrust	N
$M = \begin{bmatrix} M_{b1} & & 0 \\ & \ddots & \\ 0 & & M_{bn} \end{bmatrix}$	Modal mass (generalized mass) matrix	kg
$M^{-1} = \begin{bmatrix} \frac{1}{M_{b1}} & & 0 \\ & \ddots & \\ 0 & & \frac{1}{M_{bn}} \end{bmatrix}$	Inverse modal mass matrix	1/kg
$\bar{M}^{B}_{A_{\beta j}} = \begin{bmatrix} M^{B}_{A\beta X_j} \\ M^{B}_{A\beta Y_j} \\ M^{B}_{A\beta Z_j} \end{bmatrix}$	Aerodynamic vector moment at the j^{th} aero station of the β-body, where β = f (fuselage) w (wing), h (horizontal stabilizer), and v (vertical stabilizer)	N-m

SYMBOL	DEFINITION	UNIT
$\bar{M}^B_{E(b)_j} = \begin{bmatrix} M^B_{E(b)X_j} \\ M^B_{E(b)Y_j} \\ M^B_{E(b)Z_j} \end{bmatrix}$	Vector moment of the j^{th} engine inertial force	N-m
$\bar{M}^B_{L_j} = \begin{bmatrix} M^B_{LX_j} \\ M^B_{LY_j} \\ M^B_{LZ_j} \end{bmatrix}$	Vector moment of the j^{th} tank longitudinal slosh mass	N-m
$\bar{M}^B_{S_j} = \begin{bmatrix} M^B_{SX_j} \\ M^B_{SY_j} \\ M^B_{SZ_j} \end{bmatrix}$	Vector moment at the j^{th} slosh mass inertia	N-m
$Q = \begin{bmatrix} Q_1 \\ \cdot \\ \cdot \\ \cdot \\ Q_n \end{bmatrix}$	Generalized forces	N

SYMBOL	DEFINITION	UNIT
$\zeta = \begin{bmatrix} \zeta_{b1} & & 0 \\ & \ddots & \\ 0 & & \zeta_{bn} \end{bmatrix}$	Damping coefficient matrix	unitless
$\ddot{\eta} = \begin{bmatrix} \ddot{\eta}_1 \\ \vdots \\ \ddot{\eta}_n \end{bmatrix}$	Generalized accelerations (NOTE: The subscript n represents the number of bending modes)	m/sec^2
$\dot{\eta} = \begin{bmatrix} \dot{\eta}_1 \\ \vdots \\ \dot{\eta}_n \end{bmatrix}$	Generalized velocities	m/sec
$\eta = \begin{bmatrix} \eta_1 \\ \vdots \\ \eta_n \end{bmatrix}$	Generalized displacements	m

SYMBOL	DEFINITION	UNIT
$\Phi_{\ell}^{T}(\bar{R}_{A_{\beta_j}}) = \begin{bmatrix} \phi_{1X}(\bar{R}_{A_{\beta_j}}) & \phi_{1Y}(\bar{R}_{A_{\beta_j}}) & \phi_{1Z}(\bar{R}_{A_{\beta_j}}) \\ \vdots & \vdots & \vdots \\ \phi_{nX}(\bar{R}_{A_{\beta_j}}) & \phi_{nY}(\bar{R}_{A_{\beta_j}}) & \phi_{nZ}(\bar{R}_{A_{\beta_j}}) \end{bmatrix}$	Matrix transpose of modal displacement coefficient matrix (order: n x 3, where n is the number of bending modes considered), at the j^{th} aero station of the β-body (where β = f (fuselage), w (wing), h (horizontal stabilizer), and v (vertical stabilizer), defined by position vector $\bar{R}_{A_{\beta_j}}$ $j = 1, N_{A_\beta}$, where N_{A_β} is the total number of aero stations considered on the β-body	m/m unitless
$\Phi_{E}^{T}(\bar{R}_{E_j}) = \begin{bmatrix} \phi_{1X}(\bar{R}_{E_j}) & \phi_{1Y}(\bar{R}_{E_j}) & \phi_{1Z}(\bar{R}_{E_j}) \\ \vdots & \vdots & \vdots \\ \phi_{nX}(\bar{R}_{E_j}) & \phi_{nY}(\bar{R}_{E_j}) & \phi_{nZ}(\bar{R}_{E_j}) \end{bmatrix}$	Matrix transpose of modal displacement coefficient matrix at the j^{th} engine attach point defined by position vector $\bar{R}_{E_j}$ $j = 1, N_E$ where N_E is the total number of engine attach point locations	m/m unitless
$\Phi_{S}^{T}(\bar{R}_{L_j}) = \begin{bmatrix} \phi_{1X}(\bar{R}_{L_j}) & \phi_{1Y}(\bar{R}_{L_j}) & \phi_{1Z}(\bar{R}_{L_j}) \\ \vdots & \vdots & \vdots \\ \phi_{nX}(\bar{R}_{L_j}) & \phi_{nY}(\bar{R}_{L_j}) & \phi_{nZ}(\bar{R}_{L_j}) \end{bmatrix}$	Matrix transpose of modal displacement coefficient matrix at the lower bulkhead of the j^{th} tank defined by the position vector $\bar{R}_{L_j}$ $j = 1, N_S$ where N_S is the total number of tanks considered in slosh	m/m unitless
$\Phi_{E}^{T}(\bar{R}_{S_j}) = \begin{bmatrix} \phi_{1X}(\bar{R}_{S_j}) & \phi_{1Y}(\bar{R}_{S_j}) & \phi_{1Z}(\bar{R}_{S_j}) \\ \vdots & \vdots & \vdots \\ \phi_{nX}(\bar{R}_{S_j}) & \phi_{nY}(\bar{R}_{S_j}) & \phi_{nZ}(\bar{R}_{S_j}) \end{bmatrix}$	Matrix transpose of modal displacement coefficient matrix at the j^{th} slosh mass location defined by position vector $\bar{R}_{S_j}$ $j = 1, N_s$	m/m unitless
$\Phi_{\gamma}^{T}(\bar{R}_{A_{\beta_j}}) = \begin{bmatrix} \phi'_{1X}(\bar{R}_{A_{\beta_j}}) & \phi'_{1Y}(\bar{R}_{A_{\beta_j}}) & \phi'_{1Z}(\bar{R}_{A_{\beta_j}}) \\ \vdots & \vdots & \vdots \\ \phi'_{nX}(\bar{R}_{A_{\beta_j}}) & \phi'_{nY}(\bar{R}_{A_{\beta_j}}) & \phi'_{nZ}(\bar{R}_{A_{\beta_j}}) \end{bmatrix}$	Matrix transpose of modal rotational coefficient matrix at the j^{th} aero station of the β-body defined by position vector $\bar{R}_{A_{\beta j}}$ $j = 1, N_{A_\beta}$	rad/m
$\Phi_{\gamma}^{T}(\bar{R}_{E_j}) = \begin{bmatrix} \phi'_{1X}(\bar{R}_{E_j}) & \phi'_{1Y}(\bar{R}_{E_j}) & \phi'_{1Z}(\bar{R}_{E_j}) \\ \vdots & \vdots & \vdots \\ \phi'_{nX}(\bar{R}_{E_j}) & \phi'_{nY}(\bar{R}_{E_j}) & \phi'_{nZ}(\bar{R}_{E_j}) \end{bmatrix}$	Matrix transpose of modal rotational coefficient matrix at the j^{th} engine attach point location defined by position vector $\bar{R}_{E_j}$ $j = 1, N_E$	rad/m
$\Phi_{\gamma}^{T}(\bar{R}_{L_j}) = \begin{bmatrix} \phi'_{1X}(\bar{R}_{L_j}) & \phi'_{1Y}(\bar{R}_{L_j}) & \phi'_{1Z}(\bar{R}_{L_j}) \\ \vdots & \vdots & \vdots \\ \phi'_{nX}(\bar{R}_{L_j}) & \phi'_{nY}(\bar{R}_{L_j}) & \phi'_{nZ}(\bar{R}_{L_j}) \end{bmatrix}$	Matrix transpose of modal rotational coefficient matrix at the lower bulkhead of the j^{th} tank defined by the position vector $\bar{R}_{L_j}$ $j = 1, N_S$	rad/m

SYMBOL	DEFINITION	UNIT
$\bar{\phi}'_{r}(\bar{R}_{S_j}) = \begin{bmatrix} \phi'_{1X}(\bar{R}_{S_j}) & \phi'_{1Y}(\bar{R}_{S_j}) & \phi'_{1Z}(\bar{R}_{S_j}) \\ \vdots & \vdots & \vdots \\ \phi'_{nX}(\bar{R}_{S_j}) & \phi'_{nY}(\bar{R}_{S_j}) & \phi'_{nZ}(\bar{R}_{S_j}) \end{bmatrix}$	Matrix transpose of modal rotational coefficient matrix at the j^{th} slosh mass location defined by position vector $\bar{R}_{S_j}$ $j = 1, N_S$	rad/m
$\Omega_b = \begin{bmatrix} \omega_{b1} & & 0 \\ & \ddots & \\ 0 & & \omega_{bn} \end{bmatrix}$	Undamped natural frequency matrix	rad/sec

Section III
VEHICLE TRAJECTORY

3.1 GENERAL

A vehicle's acceleration relative to an inertial frame may be found through the use of Newton's laws of motion, and the principle of superposition of forces. Successive integration of this acceleration will render the vehicle's velocity and position relative to the inertial frame. These in turn can be used to calculate significant parameters of the vehicle relative to the rotating earth.

The development of equations and coordinate transformations used in simulating a vehicle's trajectory during boost phase flight in the earth's atmosphere is outlined in the following subsections. Those equations that are boxed in are presented in the Simulation Diagram of the Trajectory Module described in a companion report (ref. 1).

3.2 DERIVATION OF EQUATIONS

Newton's laws of motion, combined with the principle of superposition of forces, states that the sum of the forces acting on a body equals the mass of the body times its acceleration (assuming all quantities are measured in an inertial frame). If the B-frame, fixed in the body, is assumed to be rotating slowly enough to be considered inertial, the above law states that

$$\sum \bar{F}^B = m_T \bar{A}^B \tag{3-1}$$

This is convenient for finding the acceleration due to body forces, $\bar{A}^B$. Rearranging equation (3-1), it follows that

$$\bar{A}^B = \frac{1}{m_T} \sum \bar{F}^B \tag{3-2}$$

Considering the body forces $\bar{F}_A^B$ (aerodynamics), $\bar{F}_E^B$ (engine inertia), $\bar{F}_S^B$ (propellant slosh), and $\bar{F}_T^B$ (engine thrust) one can reduce the summation form of equation (3-2) to the following form:

$$\bar{A}^B = \frac{1}{m_T} (\bar{F}_A^B + \bar{F}_E^B + \bar{F}_S^B + \bar{F}_T^B) \tag{3-3}$$

To this must be added the acceleration due to gravity, $\bar{A}_G$, which is easily calculated in the Plumbline Frame. To do this, $\bar{A}$ is first changed to Plumbline coordinates by using A^{PB*}, the Body-to-Plumbline transformation:

$$\bar{A}^P = A^{PB} \bar{A}^B \tag{3-4}$$

Then the total acceleration acting on the vehicle is

$$\bar{A}_T^P = \bar{A}^P + \bar{A}_G^P \tag{3-5}$$

This is integrated to obtain $\dot{\bar{R}}^P$, the vehicle's velocity in the Plumbline Frame

$$\dot{\bar{R}}^P = \int_0^t \bar{A}_T^P \, dt + \dot{\bar{R}}^P(0) \tag{3-6}$$

and integrated again to obtain $\bar{R}^P$, the vehicle's position in the Plumbline Frame:

$$\bar{R}^P = \int_0^t \dot{\bar{R}}^P \, dt + \bar{R}^P(0) \tag{3-7}$$

The magnitude of $\dot{\bar{R}}^P$ can be found in a straightforward manner, from the definition of a dot product:

$$V = (\dot{\bar{R}}^P \cdot \dot{\bar{R}}^P)^{1/2} \tag{3-8}$$

The velocity of the vehicle relative to the earth can be found by subtracting out the rotation of the earth from the vehicle's orbital velocity:

$$\bar{V}_E^P = \dot{\bar{R}}^P - \bar{\Omega}^P \times \bar{R}^P \tag{3-9}$$

---

* *See Subsection 3.3, Coordinate Transformations*

For the purposes of this simulation skew-symmetric (tilde) 3 x 3 matrices are used to effect cross products, since matrix multiplication is easier to implement. In this case, the tilde matrix is

$$\tilde{\Omega}^P = \begin{bmatrix} 0 & -\Omega_Z^P & \Omega_Y^P \\ \Omega_Z^P & 0 & -\Omega_X^P \\ -\Omega_Y^P & \Omega_X^P & 0 \end{bmatrix} \tag{3-10}$$

Then equation (3-9) can be written as

$$\boxed{\bar{V}_E^P = \dot{\bar{R}}^P - \tilde{\Omega}^P \bar{R}^P} \tag{3-11}$$

Similarly to equation (3-8), the magnitude of $\bar{R}^P$ is

$$\boxed{R = (\bar{R}^P \cdot \bar{R}^P)^{1/2}} \tag{3-12}$$

The coordinates of $\bar{R}$ in the Inertial Equatorial Frame may be found through the use of A^{PI*}, the I - to -P transformation:

$$\bar{R}^I = [A^{PI}]^{-1} \bar{R}^P \tag{3-13}$$

But A^{PI} is an orthogonal transformation, so that

$$[A^{PI}]^{-1} = [A^{PI}]^T \tag{3-14}$$

Then equation (3-13) can be written as

$$\boxed{\bar{R}^I = [A^{PI}]^T \bar{R}^P} \tag{3-15}$$

The vehicle's geocentric latitude, ϕ', is defined to be the angle between the earth's equatorial plane and the vector from the earth's geometric center to the vehicle's CG ($\bar{R}$), positive north of the equator. Referring to Figure 3-1, this is seen to be

---

* *See Section IV, Initialization*

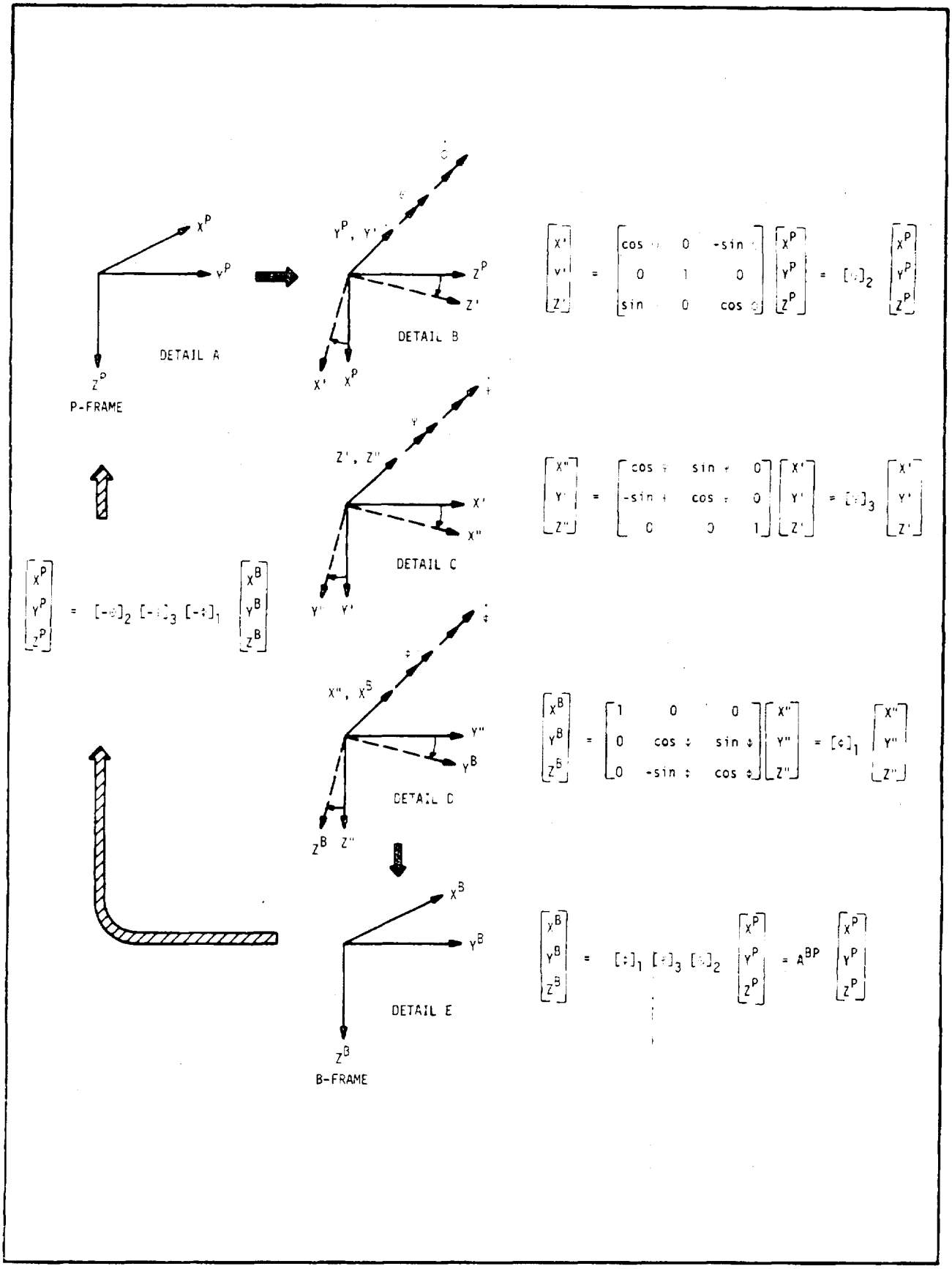

Figure 3-1. PLUMBLINE ➡ BODY AND BODY ➪ PLUMBLINE TRANSFORMATIONS

$$\phi' = \sin^{-1}\left(\frac{R_Z^I}{R}\right) \tag{3-16}$$

The vehicle's altitude, h, is defined as the height above the surface of the earth; in the Fischer model, it is the height above the earth's reference ellipsoid. At geocentric latitude ϕ', the reference ellipsoid has a radius of

$$\frac{b_e}{\sqrt{1 - \varepsilon_e^2 \cos^2 \phi'}} \tag{3-17}$$

where b_e is the ellipsoids semi-minor axis (polar radius) and ε_e is its eccentricity.

Then h is found to be

$$h = R - \frac{b_e}{\sqrt{1 - \varepsilon_e^2 \cos^2 \phi'}}$$

The vehicle's longitude, λ, is defined to be the angle between the Greenwich meridian and the vehicle's meridian, positive east of Greenwich. Since the I-frame is inertial and the Greenwich meridian is on the rotating earth, this rotation must be taken into account. Then it can be seen from Figure 3-1 that

$$\lambda = \tan^{-1}\left(\frac{R_Y^I}{R_X^I}\right) - \Omega_e (t + t_{GRR}) \tag{3-19}$$

The vehicle's geodetic latitude, ϕ, is defined to be the angle between the earth's equatorial plane and the normal to the reference ellipsoid at a point directly below the vehicle, with direction positive north of the equator. The latitude ϕ differs from ϕ' because of the changing curvature of the ellipsoid, and is related to ϕ' by the equation:

$$\phi = \tan^{-1}\left[\frac{a_e^2}{b_e^2} \tan \phi'\right] \tag{3-20}$$

3.3 COORDINATE TRANSFORMATIONS

Since the acceleration due to body forces is computed in the Body Frame but is needed in the Plumbline Frame, the proper Body-to-Plumbline transformation, A^{PB}, must be found. The derivation of this transformation is outlined in the following subsections.

3.3.1 Plumbline to Body (P-to-B)

The P-frame (Plumbline) having coordinate axes X^P, Y^P, Z^P, is shown in Figure 3-1 (Detail A). A right-hand rotation about the Y^P-axis (Figure 3-1, Detail B) through an angle θ can be represented by the transformation

$$\begin{bmatrix} X' \\ Y' \\ Z' \end{bmatrix} = \begin{bmatrix} \cos\theta & 0 & -\sin\theta \\ 0 & 1 & 0 \\ \sin\theta & 0 & \cos\theta \end{bmatrix} \begin{bmatrix} X^P \\ Y^P \\ Z^P \end{bmatrix} = [\theta]_2 \begin{bmatrix} X^P \\ Y^P \\ Z^P \end{bmatrix} \tag{3-21}$$

Note that $\dot{\theta}$ is on the Y' axis (Figure 3-1, Detail B).

A similar right-hand rotation about the Z'-axis (Figure 3-1, Detail C) through an angle ψ can be represented by the transformation

$$\begin{bmatrix} X'' \\ Y'' \\ Z'' \end{bmatrix} = \begin{bmatrix} \cos\psi & \sin\psi & 0 \\ -\sin\psi & \cos\psi & 0 \\ 0 & 0 & 1 \end{bmatrix} \begin{bmatrix} X' \\ Y' \\ Z' \end{bmatrix} = [\psi]_3 \begin{bmatrix} X' \\ Y' \\ Z' \end{bmatrix} \tag{3-22}$$

Note that $\dot{\psi}$ is on the Z'' axis (Figure 3-1, Detail C).

A final right-hand rotation about the X''-axis (Figure 3-1, Detail D) through an angle ϕ can be represented by the transformation

$$\begin{bmatrix} X^B \\ Y^B \\ Z^B \end{bmatrix} = \begin{bmatrix} 1 & 0 & 0 \\ 0 & \cos\phi & \sin\phi \\ 0 & -\sin\phi & \cos\phi \end{bmatrix} \begin{bmatrix} X'' \\ Y'' \\ Z'' \end{bmatrix} = [\phi]_1 \begin{bmatrix} X'' \\ Y'' \\ Z'' \end{bmatrix} \tag{3-23}$$

Note that $\dot{\phi}$ is on the X^B axis (Figure 3-1, Detail D).

The three successive rotations of equations (3-21), (3-22), and (3-23) provide a transformation matrix that relates a vector $\bar{a}^P$ in the P-frame to the vector $\bar{a}^B$ in the B-frame as follows:

$$\bar{a}^B = [\Phi]_1 [\Psi]_3 [\Theta]_2 \bar{a}^P = A^{BP} \bar{a}^P \tag{3-24}$$

3.3.2 Body to Plumbline (B–to–P)

The Euler angles Φ, Ψ, and Θ are considered positive for the P-to-B transformation and negative for the B-to-P transformation. The B-to-P transformation may be written as follows:

$$\bar{a}^P = \{[\Phi]_1 [\Psi]_3 [\Theta]_2\}^{-1} \bar{a}^B = [A^{BP}]^{-1} \bar{a}^B \tag{3-25}$$

where the matrix inverse may be expressed as

$$[A^{BP}]^{-1} = [\Theta]_2^{-1} [\Psi]_3^{-1} [\Phi]_1^{-1} \tag{3-26}$$

$$= [\Theta]_2^T [\Psi]_3^T [\Phi]_1^T \tag{3-27}$$

$$= [-\Theta]_2 [-\Psi]_3 [-\Phi]_1 \tag{3-28}$$

$$= A^{PB} \tag{3-29}$$

where

$$[-\Theta]_2 = \begin{bmatrix} \cos(-\Theta) & 0 & -\sin(-\Theta) \\ 0 & 1 & 0 \\ \sin(-\Theta) & 0 & \cos(-\Theta) \end{bmatrix} \tag{3-30}$$

$$[-\Psi]_3 = \begin{bmatrix} \cos(-\Psi) & \sin(-\Psi) & 0 \\ -\sin(-\Psi) & \cos(-\Psi) & 0 \\ 0 & 0 & 1 \end{bmatrix} \tag{3-31}$$

$$[-\Phi]_1 = \begin{bmatrix} 1 & 0 & 0 \\ 0 & \cos(-\Phi) & \sin(-\Phi) \\ 0 & -\sin(-\Phi) & \cos(-\Phi) \end{bmatrix} \qquad (3\text{-}32)$$

3.4 GLOSSARY OF TERMS

SYMBOL	DEFINITION	UNIT
$\bar{a}$	Any arbitrary vector, see equation (3-24)	arbitrary
a_e	Semi-major axis of the earth	m
$\bar{A}$	Acceleration due to body forces	m/sec^2
$\bar{A}_G$	Gravitational acceleration	m/sec^2
A^{BP}	Plumbline-to-Body coordinate transformation matrix	unitless
A^{PB}	Body-to-Plumbline coordinate transformation matrix	unitless
b_e	Semi-minor axis of the earth	m
$\bar{F}$	Any distance force acting on the vehicle	N
$\bar{F}_A$	Total aerodynamic force acting on the vehicle	N
$\bar{F}_E$	Total engine inertial force acting on the vehicle	N
$\bar{F}_S$	Total slosh force acting on the vehicle	N
$\bar{F}_T$	Total engine thrust force acting on the vehicle	N
h	Vehicle's altitude above the surface of the earth	m
m_T	Total mass of the vehicle	kg
R	Scalar distance of the vehicle CG from the earth's geometric center	m
$\bar{R}$	Position vector of the vehicle CG	m
$\bar{R}(0)$	Position vector of the vehicle CG at initialization	m
$\dot{\bar{R}}$	Velocity vector of the vehicle	m/sec
$\dot{\bar{R}}(0)$	Velocity vector of the vehicle at initialization	m/sec
t	Instantaneous time	sec
t_{GRR}	Time of Guidance Reference Release	sec
V	Scalar velocity of the vehicle	m/sec
$\bar{V}_E$	Vehicle's velocity vector relative to the earth's surface	m/sec
ε_e	Eccentricity of the earth	unitless
Φ	Euler rotation about the Y^P axis	rad
λ	Longitude of the vehicle's position	rad

SYMBOL	DEFINITION	UNIT
ϕ	Geodetic latitude of the vehicle's position	rad
ϕ'	Geocentric latitude of the vehicle's position	rad
ψ	Euler rotation about the X^B axis	rad
θ	Euler rotation about the Z' axis	rad
$\bar{\Omega}$	Earth's vector angular velocity	rad/sec
$\tilde{\Omega}$	Skew-symmetric Ω matrix: equivalent to the vector cross product operation "$\bar{\Omega}$ x ( )"	rad/sec

Section IV
INITIALIZATION

4.1 GENERAL

The initial parameters of a simulation, as given, must be converted into a more usable form in order to be implemented. In particular, the angles which determine the launch site must be converted into a transformation matrix, the earth's angular rate must be converted into a vector, and all of these then converted into the vehicle's initial position and velocity.

4.2 DERIVATION OF EQUATIONS

The earth's angular rate, Ω_e, is given as parametric input. Since by definition the vector angular velocity is aligned along the Z^I axis, it follows that

$$\bar{\Omega}^I = \begin{bmatrix} 0 \\ 0 \\ \Omega_e \end{bmatrix} \tag{4-1}$$

Since this is more useful in Plumbline coordinates, the Inertial Equatorial-to-Plumbline transformation, A^{PI*}, may be used to obtain

$$\bar{\Omega}^P = [A^{PI}] \begin{bmatrix} 0 \\ 0 \\ \Omega_e \end{bmatrix} \tag{4-2}$$

At launch the vehicle is at rest with respect to the earth, so that any inertial velocity it has is due to the earth's rotation. Then this velocity is

$$\dot{\bar{R}}^P_L = \bar{\Omega}^P \times \bar{R}^P_L \tag{4-3}$$

* *See subsection 4.3*

4.3 COORDINATE TRANSFORMATIONS

4.3.1 Inertial Equatorial–to–Plumbline Transformation

The I-to-P coordinate transformation matrix, A^{PI}, may be computed by using the angles which reference the launch site's position to the Greenwich meridian, the equator, and true north, at GRR: λ_L, ϕ_L, and A_{ZL}, respectively (See Figures 4-1 and 4-2).

The launch longitude, λ_L, is the angle between the launch meridian and the Greenwich meridian, which contains X^I. Then a right-hand rotation of λ_L radians about Z^I, true north, will rotate X^I into the launch meridian, with the new X still lying on the equator. This rotation is represented by the symbol $[\lambda_L]_3$, as defined below:

$$[\lambda_L]_3 = \begin{bmatrix} \cos\lambda_L & \sin\lambda_L & 0 \\ -\sin\lambda_L & \cos\lambda_L & 0 \\ 0 & 0 & 1 \end{bmatrix} \tag{4-4}$$

The launch geodetic latitude, ϕ_L, is the angle between the equator and X^P. Since the new Y created above is on the equator perpendicular to the launch meridian, a right-hand rotation of $-\phi_L$ radians about the new Y will rotate the new X into coincidence with X^P. This rotation is represented by the symbol $[-\phi_L]_2$ as defined below:

$$[-\phi_L]_2 = \begin{bmatrix} \cos(-\phi_L) & 0 & -\sin(-\phi_L) \\ 0 & 1 & 0 \\ \sin(-\phi_L) & 0 & \cos(-\phi_L) \end{bmatrix} \tag{4-5}$$

The launch azimuth, A_{ZL}, is the angle between the $X^P - Z^P$ plane and the launch meridian. Then a right-hand rotation of $-A_{ZL}$ radians will bring the new Z created above into coincidence with Z^P and the new Y with Y^P, thus completing the transformation of the I-frame into the P-frame. This rotation is represented by the symbol $[-A_{ZL}]_1$, as defined below:

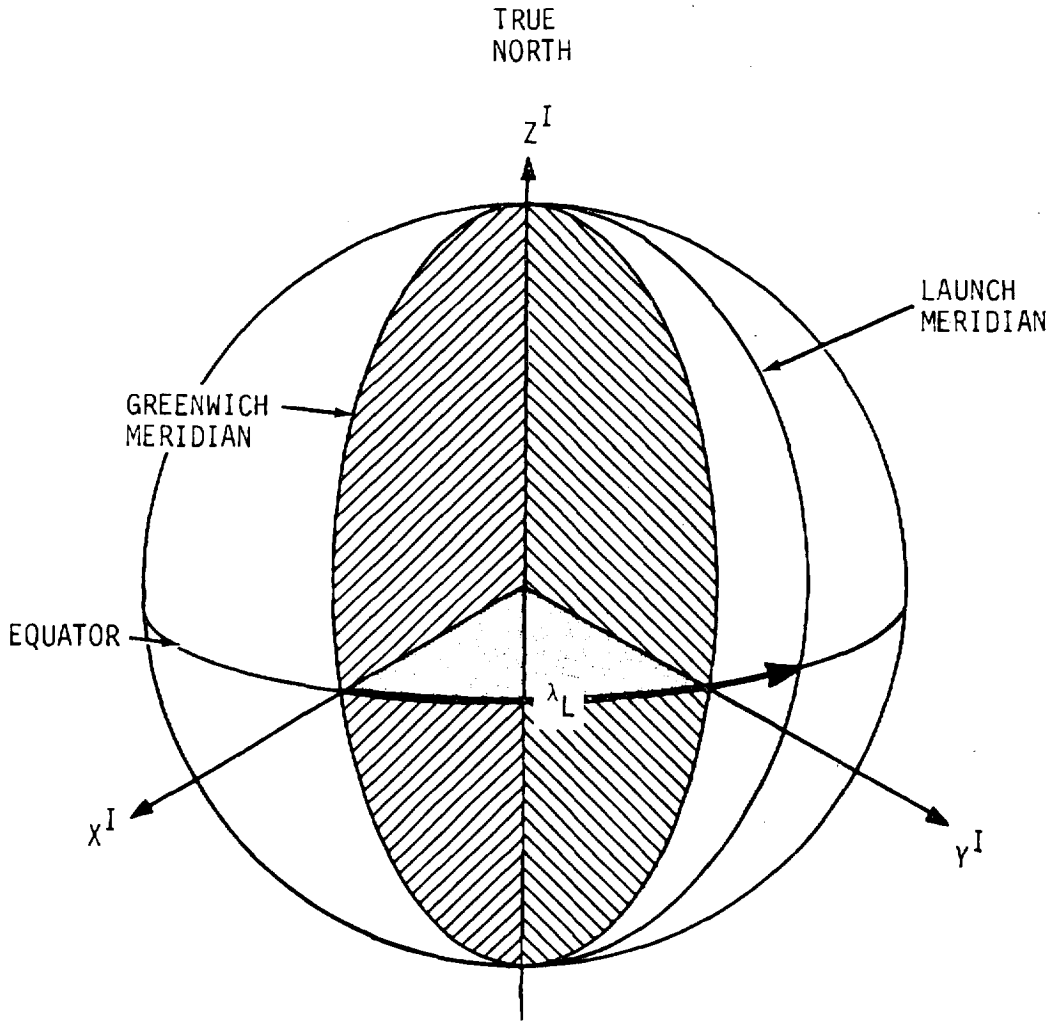

X^I, Y^I, Z^I

ORIGIN: EARTH'S GEOMETRIC CENTER

X AXIS: IN THE EQUATORIAL PLANE, POSITIVE AT THE GREENWICH MERIDIAN AT TIME OF GRR

Z AXIS: POSITIVE ALONG THE EARTH'S MEAN SPIN VECTOR (TRUE NORTH)

Y AXIS: COMPLETING A RIGHT-HAND FRAME

Figure 4-1. INERTIAL EQUATORIAL FRAME

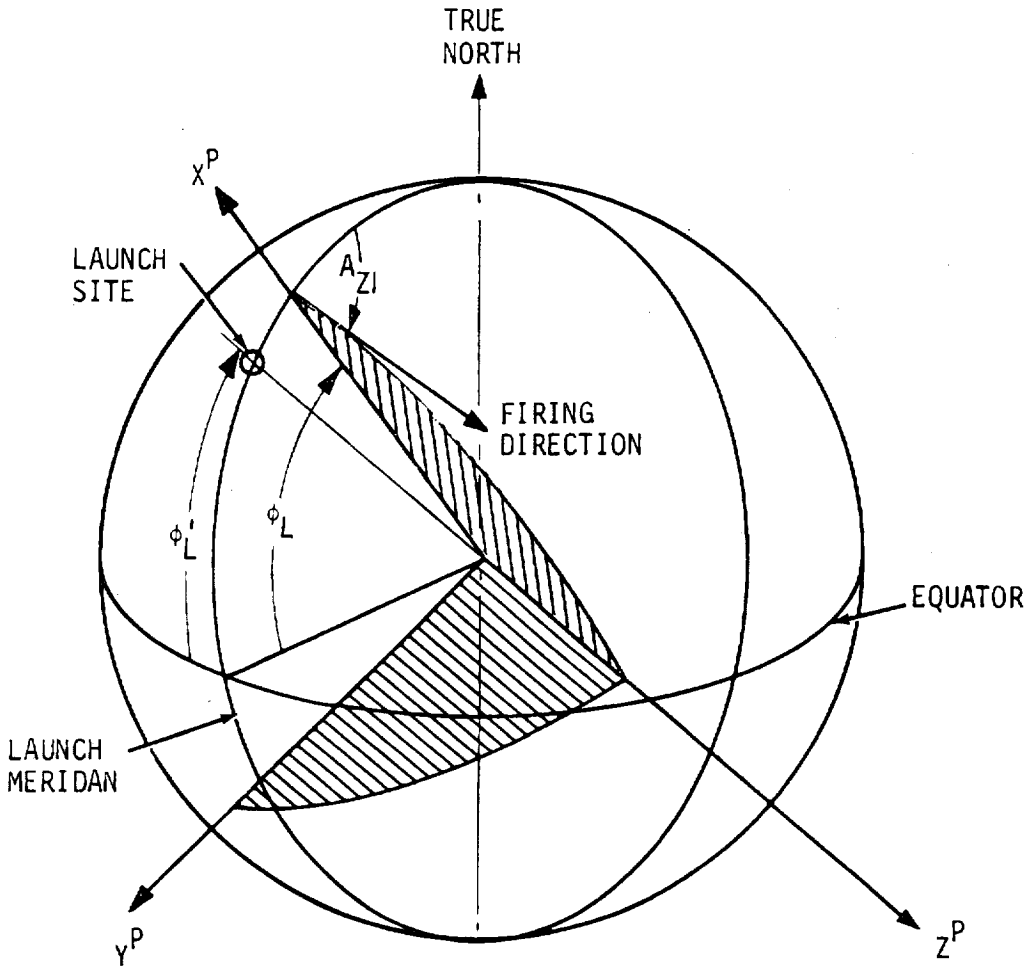

X^P, Y^P, Z^P

ORIGIN: EARTH'S GEOMETRIC CENTER

X-AXIS: PARALLEL TO GRAVITY GRADIENT OF LAUNCH SITE

Z-AXIS: POSITIVE IN DIRECTION OF LAUNCH AZIMUTH (FIRING DIRECTION)

Y-AXIS: COMPLETING A RIGHT-HAND FRAME

Figure 4-2. PLUMBLINE FRAME

$$[-A_{ZL}]_1 = \begin{bmatrix} 1 & 0 & 0 \\ 0 & \cos(-A_{ZL}) & \sin(-A_{ZL}) \\ 0 & -\sin(-A_{ZL}) & \cos(-A_{ZL}) \end{bmatrix} \tag{4-6}$$

Thus, the I-to-P transformation, A^{PI}, is given by

$$A^{PI} = [-A_{ZL}]_1 \; [-\phi_L]_2 \; [\lambda_L]_3 \tag{4-7}$$

4.3.2 Launch Position Transformation

Four parameters are used to calculate the vehicle's initial position in the Plumbline Frame: A_{ZL}, ϕ_L, ϕ_L', and R_L, the scalar distance of the vehicle CG from the earth's geometric center. The vehicle's position vector, $\bar{R}_L$, is first considered to be in the REN Frame, where

$\hat{R}$ is defined by the direction of $\bar{R}_L$
$\hat{E}$ is on the equatorial plane and perpendicular to $\hat{R}$, such that $\hat{R} \times \hat{E}$ is in the earth's northern hemisphere (Local East)
$\hat{N}$ completes the right-hand frame (Local North)

(See Figure 4-3.) Then

$$\bar{R}_L^{REN} = \begin{bmatrix} R_L \\ 0 \\ 0 \end{bmatrix} \tag{4-8}$$

The difference of the launch geodetic and geocentric latitudes, $\phi_L' - \phi_L$, is the angle between R and X^P. It follows from the definition of E that this axis is perpendicular to both $\hat{R}$ and X^P. Then a right-hand rotation of $(\phi_L' - \phi_L)$ radians about the $\hat{E}$ axis will bring $\hat{R}$ into coincidence with X^P, so that both $\hat{E}$ and the new $\hat{N}$ are now in the $Y^P - Z^P$ plane. This rotation is represented by the symbol $(\phi_L' - \phi_L]_2$, as defined below:

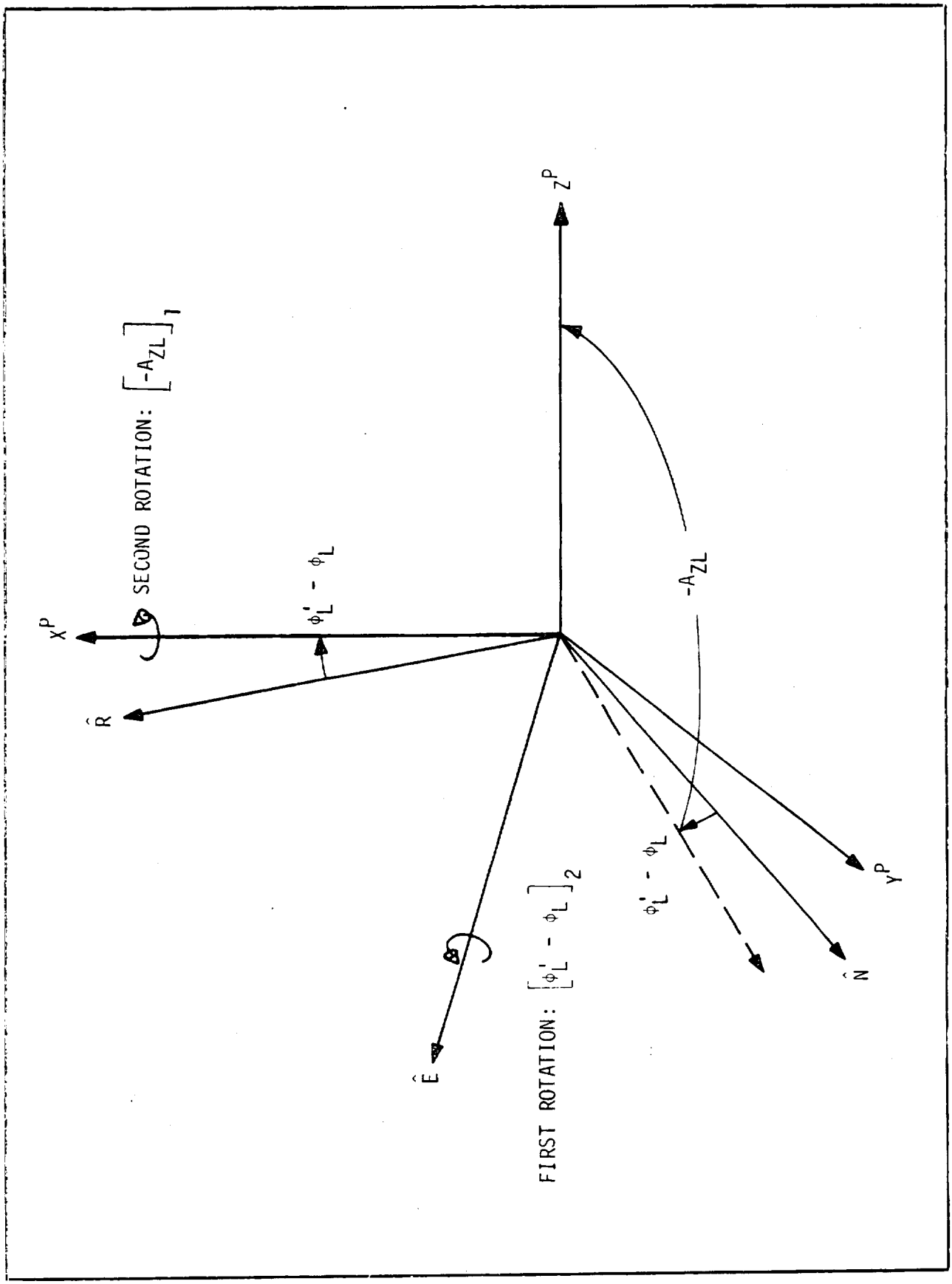

Figure 4-3. RELATION OF REN LAUNCH FRAME TO X^P-Y^P-Z^P (PLUMBLINE) FRAME

$$[\phi'_L - \phi_L]_2 = \begin{bmatrix} \cos(\phi'_L - \phi_L) & 0 & -\sin(\phi'_L - \phi_L) \\ 0 & 1 & 0 \\ \sin(\phi'_L - \phi_L) & 0 & \cos(\phi'_L - \phi_L) \end{bmatrix} \tag{4-9}$$

The launch azimuth, A_{ZL}, is the angle between the X^P - Z^P plane and the launch meridian (the X^P - $\hat{N}$ plane). Note that X^P is now perpendicular to both $\hat{E}$ and the new $\hat{N}$, as well as Y^P and Z^P. Then a right-hand rotation of $-A_{ZL}$ radians about X^P (the new $\hat{R}$) will bring the new $\hat{N}$ created above into coincidence with Z^P and $\hat{E}$ with Y^P, and thus complete the transformation of the REN Frame into the P-frame. This rotation is represented by the symbol $[-A_{ZL}]_1$, as defined below:

$$[-A_{ZL}]_1 = \begin{bmatrix} 1 & 0 & 0 \\ 0 & \cos(-A_{ZL}) & \sin(-A_{ZL}) \\ 0 & -\sin(-A_{ZL}) & \cos(-A_{ZL}) \end{bmatrix} \tag{4-10}$$

Thus, $\bar{R}_L$ in Plumbline coordinates is found to be

$$\bar{R}^P_L = [-A_{ZL}]_1 \, [\phi'_L - \phi_L]_2 \begin{bmatrix} R_L \\ 0 \\ 0 \end{bmatrix} \tag{4-11}$$

4.3.3 Restart Option #1

Restart Option #1 is designed to take as parametric input the following earth-related parameters, evaluated at restart: ϕ'_o, λ_o, R_o, t_o, A_{Zo}, γ_o, and V_o. It then computes the vehicle's initial position and velocity vectors, resolved in the Plumbline Frame: $\bar{R}^P_o$ and $\dot{\bar{R}}^P_o$, respectively.

4.3.3.1 Restart Position Transformation. Similar to the Launch Option, $\bar{R}_o$ is first considered to be in the REN Frame, defined above. (See Figure 4-4.)

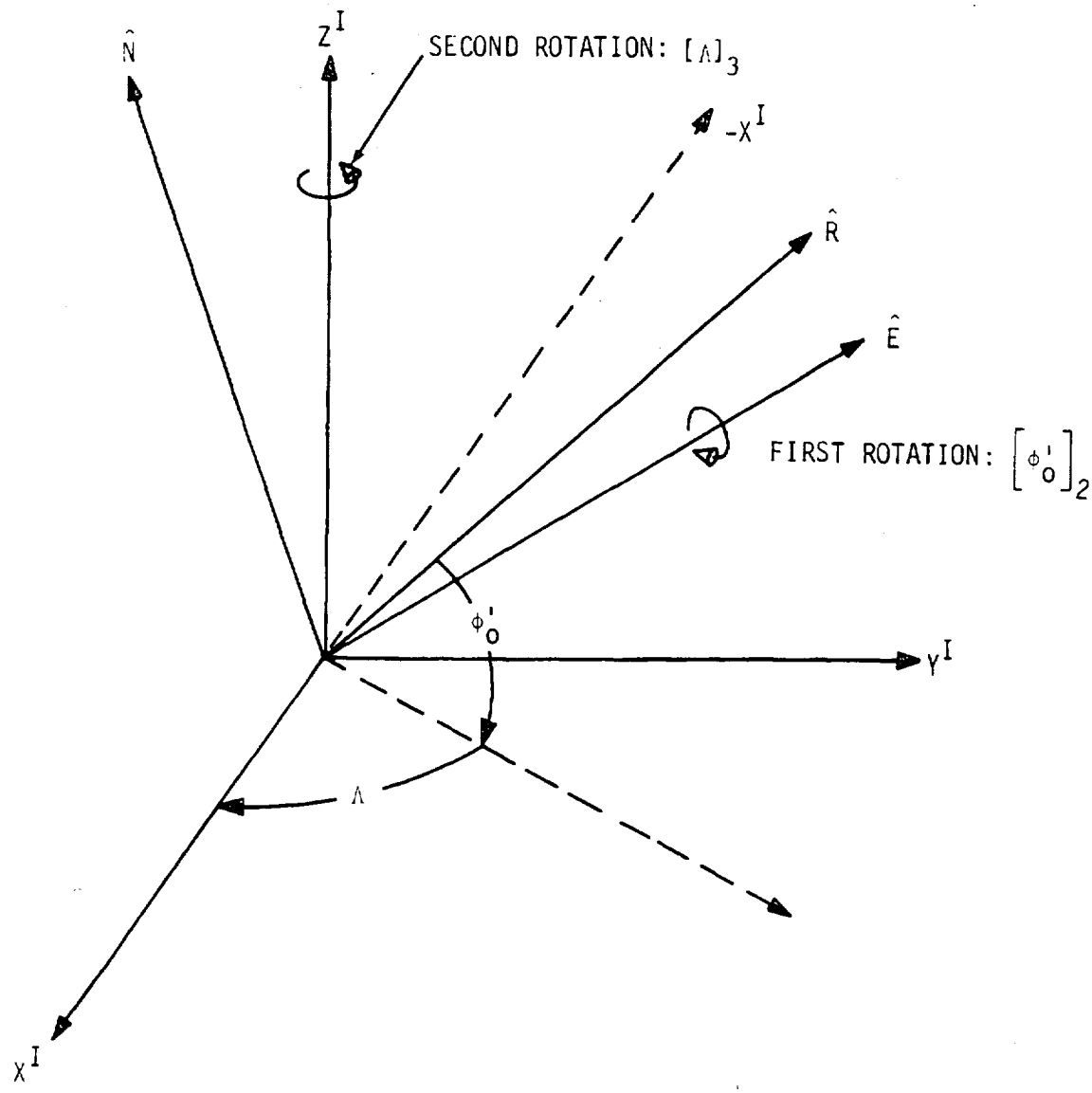

Figure 4-4. RELATION OF REN FRAME TO X^I-Y^I-Z^I (INERTIAL EQUATORIAL) FRAME

As before,

$$\bar{R}_o^{REN} = \begin{bmatrix} R_o \\ 0 \\ 0 \end{bmatrix} \tag{4-12}$$

The vehicle's geocentric latitude at restart, ϕ'_o, is the angle between $\hat{R}$ and the equatorial plane (the $X^I - Y^I$ plane). Since $\hat{E}$ is on the $X^I - Y^I$ plane it is perpendicular to Z^I, and also perpendicular to $\hat{R}$ by definition. Then a right-hand rotation of ϕ'_o radians about the $\hat{E}$ axis will place $\hat{R}$ on the equator, and bring $\hat{N}$ into coincidence with Z^I. This rotation is represented by the symbol $[\phi'_o]_2$, as defined below:

$$[\phi'_o]_2 = \begin{bmatrix} \cos\phi'_o & 0 & -\sin\phi'_o \\ 0 & 1 & 0 \\ \sin\phi'_o & 0 & \cos\phi'_o \end{bmatrix} \tag{4-13}$$

The angle between X^I and the new $\hat{R}$, above, is related to the vehicle's longitude at restart, λ_o. Longitude, λ_o, is referenced to the rotating earth and not directly to the inertially fixed I-frame; i.e., the rotation of the earth since the I-frame was fixed (at GRR) has been subtracted out. (See equation (3-19.) To relate $\hat{R}$ to X^I directly then, the earth's rotation must be added back. To simplify the notation, a new parameter is defined:

$$\Lambda = -(\lambda_o + \Omega_e\ (t_o + t_{GRR})) \tag{4-14}$$

Note that Λ is the negative of the angle from X^I to the new $\hat{R}$. Since both $\hat{E}$ and $\hat{R}$ are now on the equator, Z^I is now perpendicular to both. Then a right-hand rotation of Λ radians about Z^I will bring the new $\hat{R}$ into coincidence with X^I and $\hat{E}$ with Y^I, thus completing the transformation of the REN Frame into the I-frame. This rotation is represented by the symbol $[\Lambda]_3$, as defined below:

$$[\Lambda]_3 = \begin{bmatrix} \cos\Lambda & \sin\Lambda & 0 \\ -\sin\Lambda & \cos\Lambda & 0 \\ 0 & 0 & 1 \end{bmatrix} \tag{4-15}$$

The transformation matrix, A^{PI} is used to resolve the vector R_o into Plumbine coordinates.

$$\bar{R}_o^P = [A^{PI}]\ [\Lambda]_3\ [\phi'_o]_2 \begin{bmatrix} R_o \\ 0 \\ 0 \end{bmatrix} \tag{4-16}$$

4.3.3.2 Restart Velocity Transformation. The vehicle's velocity vector, $\dot{\bar{R}}_o$, is first considered to be in the VJK Frame, where

$\hat{V}$ is defined by the direction of $\dot{\bar{R}}_o$

$\hat{J}$ is in the direction of $\hat{V} \times \hat{R}$

$\hat{K}$ completes the right-hand frame.

Then

$$\dot{\bar{R}}_o^{VJK} = \begin{bmatrix} V_o \\ 0 \\ 0 \end{bmatrix} \tag{4-17}$$

(See Figure 4-5.)

The vehicle's flight path angle at restart, γ_o, is the angle between $\hat{V}$ and the $\hat{E} - \hat{N}$ plane (local horizontal). Thus $\frac{\pi}{2} - \gamma_o$ is the angle between $\hat{V}$ and $\hat{R}$. Note from the definition that $\hat{J}$ is perpendicular to both $\hat{V}$ and $\hat{R}$. Then a right-hand rotation of $(\frac{\pi}{2} - \gamma_o)$ radians about the $\hat{J}$ axis will bring $\hat{V}$ into coincidence with $\hat{R}$, and place $\hat{K}$ on the $\hat{E} - \hat{N}$ plane. This rotation is represented by the symbol $[\frac{\pi}{2} - \gamma_o]_2$, as defined below:

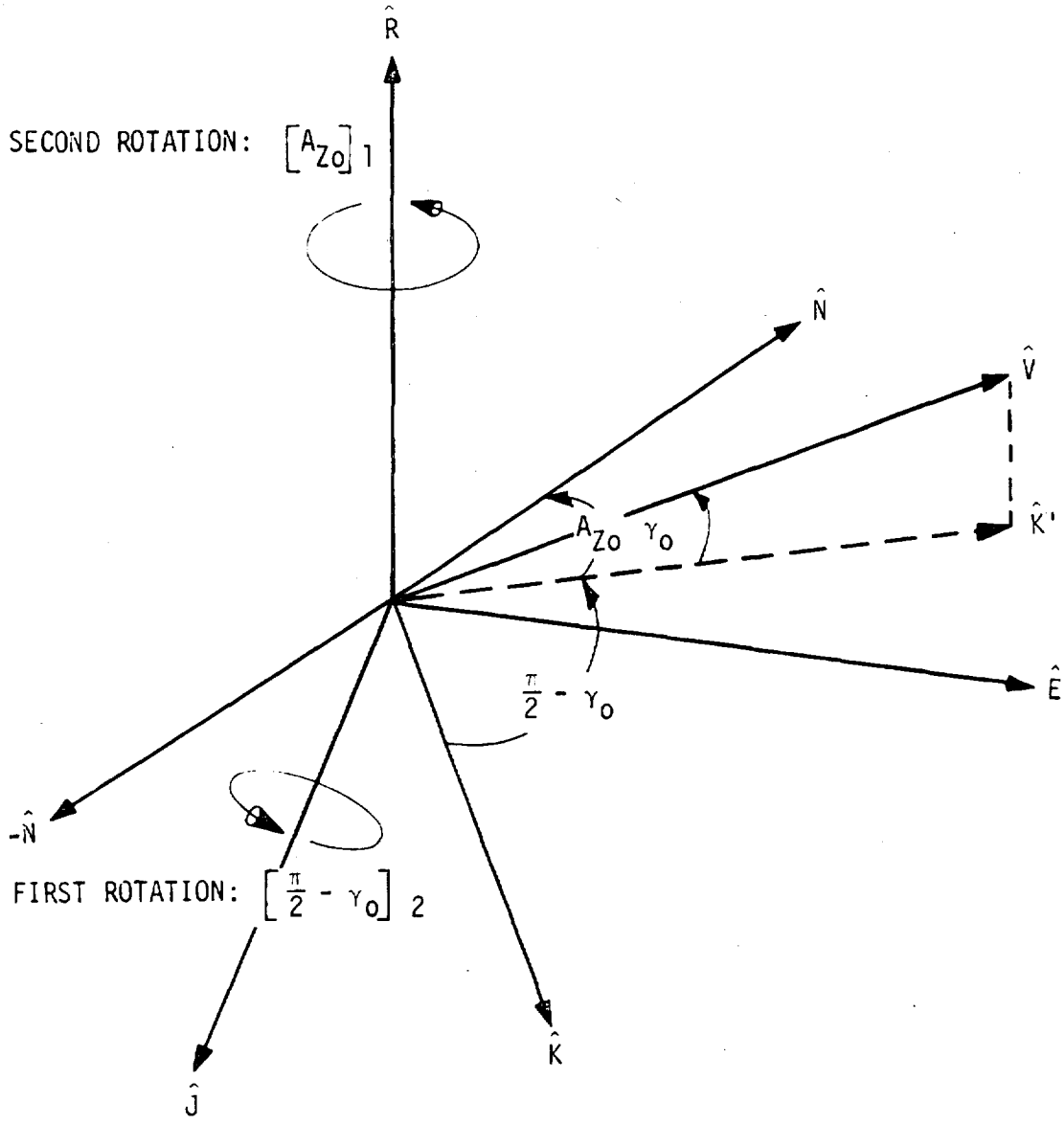

Figure 4-5. RELATION OF VJK FRAME TO REN FRAME

$$[\tfrac{\pi}{2} - \gamma_o]_2 = \begin{bmatrix} \cos(\frac{\pi}{2} - \gamma_o) & 0 & -\sin(\frac{\pi}{2} - \gamma_o) \\ 0 & 1 & 0 \\ \sin(\frac{\pi}{2} - \gamma_o) & 0 & \cos(\frac{\pi}{2} - \gamma_o) \end{bmatrix} \tag{4-18}$$

The vehicle's azimuth at restart, A_{Zo}, is the angle between the $\hat{R}$ - $\hat{V}$ plane (the restart meridian) and the $\hat{K}$ - $\hat{V}$ plane. Thus, it is also the angle between the new $\hat{K}$ and $\hat{N}$. Since the new $\hat{K}$ is on the $\hat{E}$ - $\hat{N}$ plane, $\hat{R}$ is now perpendicular to both $\hat{K}$ and $\hat{N}$. Then a right-hand rotation of A_{Zo} radians about the $\hat{R}$ axis (the new $\hat{V}$) will bring the new $\hat{K}$ into coincidence with $\hat{N}$ and $\hat{J}$ with $\hat{E}$, thus completing the VJK-to-REN transformation. This rotation is represented by the symbol $[A_{Zo}]_1$, as defined below:

$$[A_{Zo}]_1 = \begin{bmatrix} 1 & 0 & 0 \\ 0 & \cos A_{Zo} & \sin A_{Zo} \\ 0 & -\sin A_{Zo} & \cos A_{Zo} \end{bmatrix} \tag{4-19}$$

Then in REN coordinates $\dot{\bar{R}}_o$ is

$$\dot{\bar{R}}_o^{REN} = [A_{Zo}]_1 \, [\tfrac{\pi}{2} - \gamma_o]_2 \begin{bmatrix} V_o \\ 0 \\ 0 \end{bmatrix} \tag{4-20}$$

The transformation from REN to Plumbline coordinates, in equation (4-16), was found to be $[A^{PI}]\,[A]_3\,[\phi'_o]_2$. Then

$$\dot{\bar{R}}_o^{P} = [A^{PI}]\,[A]_3\,[\phi'_o]_2\;\dot{\bar{R}}_o^{REN} \tag{4-21}$$

$$\dot{\bar{R}}_o^{P} = [A^{PI}]\,[A]_3\,[\phi'_o]_2\,[A_{Zo}]_1\,[\tfrac{\pi}{2} - \gamma_o]_2 \begin{bmatrix} V_o \\ 0 \\ 0 \end{bmatrix} \tag{4-22}$$

4.4 GLOSSARY OF TERMS

SYMBOL	DEFINITION	UNIT
A^{PI}	Coordinate transformation matrix from the Inertial Equatorial Frame to the Plumbline Frame	unitless
A_{ZL}	Launch azimuth	rad
$[-A_{ZL}]_1$	Coordinate transformation matrix which represents a right-hand rotation about the X^P axis through an angle $(-A_{ZL})$	unitless
A_{Zo}	Restart azimuth	rad
$[A_{Zo}]_1$	Coordinate transformation matrix which represents a right-hand rotation about the R axis through an angle A_{Zo}	unitless
R_L	Scalar distance of the vehicle's CG from the earth's geometric center at launch	m
$\bar{R}_L$	Vector displacement of the vehicle's CG from the earth's geometric center at launch	m
$\dot{\bar{R}}_L$	Vector velocity of the vehicle's CG at launch	m/sec
R_o	Scalar distance of the vehicle's CG from the earth's geometric center at restart	m
$\bar{R}_o$	Vector displacement of the vehicle's CG from the earth's geometric center at restart	m
$\dot{\bar{R}}_o$	Vector velocity of the vehicle's CG at restart	m/sec
t_{GRR}	Time (positive) between guidance reference release and launch	sec
t_o	Time (positive) between launch and restart	sec
V_o	Scalar velocity of the vehicle's CG at restart	m/sec
γ_o	Flight path angle (angle of $\dot{\bar{R}}_o$ with respect to local horizontal) at restart	rad
$[\frac{\pi}{2} - \gamma_o]_2$	Coordinate transformation matrix which represents a right-hand rotation about the J axis through an angle $(\frac{\pi}{2} - \gamma_o)$	unitless
λ_L	Launch longitude	rad
$[\lambda_L]_3$	Coordinate transformation matrix representing a right-hand rotation about the Z^I axis through an angle λ_L	unitless

SYMBOL	DEFINITION	UNIT
λ_o	Restart longitude	rad
A	Intermediate parameter, defined in equation (4-14)	rad
$[A]_3$	Coordinate transformation matrix representing a right-hand rotation about the Z^I axis through an angle A	unitless
ϕ_L	Launch geodetic latitude	rad
$[-\phi_L]_2$	Coordinate transformation matrix representing a right-hand rotation about an intermediate Y axis through an angle $(-\phi_L)$	unitless
ϕ'_L	Launch geocentric latitude	rad
$[\phi'_L - \phi_L]_2$	Coordinate transformation matrix representing a right-hand rotation about the $\hat{E}$ axis through an angle $(\phi'_L - \phi_L)$	unitless
ϕ'_o	Restart geocentric latitude	rad
$[\phi'_o]_2$	Coordinate transformation matrix representing a right-hand rotation about the $\hat{E}$ axis through an angle ϕ'_o	unitless
Ω_e	Scalar rotational rate of the earth	rad/sec
$\bar{\Omega}$	Vector angular velocity of the earth	rad/sec

Section V
GRAVITATION

5.1 GENERAL

The gravitational acceleration acting on the vehicle may be found through use of the gravity potential equation, that is, the gravitational acceleration of a body at a certain point in the earth's gravitational potential field is equal to the field's gradient at that point.

5.2 DERIVATION OF EQUATIONS

In this simulation the Fischer oblate model of the earth is being used. The oblate potential of the earth is assumed to contain the first, second, third, and fourth spherical harmonics (i.e., pear-shaped earth):

$$U = \frac{\mu}{R}\left[1 + \frac{J}{3}\frac{a_e^2}{R^2}(1-3\sin^2\phi') + \frac{H}{5}\frac{a_e^3}{R^3}(3-5\sin^2\phi')\sin\phi' + \frac{D}{35}\frac{a_e^4}{R^4}(3-30\sin^2\phi' + 35\sin^4\phi')\right] \quad (5\text{-}1)$$

where μ is the gravitational coefficient of the earth and a_e is the earth's semi-major axis (equatorial radius).

The position vector of the vehicle's CG expressed in Plumbline coordinates, $\bar{R}^P$, is directed from the earth's center of mass. To obtain ϕ', the geocentric latitude, the position vector expressed in Inertial Equatorial coordinates must be obtained. Subsection 4.3 provides the necessary transformation, A^{PI}:

$$\bar{R}^I = [A^{PI}]^T \bar{R}^P \quad (5\text{-}2)$$

As in subsection 3.2,

$$\sin\phi' = \frac{R_Z^I}{R} = \frac{\bar{A}_{*3}^{PI} \cdot \bar{R}^P}{R} \quad (5\text{-}3)$$

To obtain the gravitational acceleration, ∇U is formed:

$$\nabla U = \left(\frac{\partial U}{\partial u_1}, \frac{\partial U}{\partial u_2}, \frac{\partial U}{\partial u_3}\right) \tag{5-4}$$

where $u_1 = R_X^P$, $u_2 = R_Y^P$, $u_3 = R_Z^P$. Each of the above partials is of the form:

$$\begin{aligned}\frac{\partial U}{\partial u_j} = &- \frac{\mu}{R^2}\frac{u_j}{R} - J\frac{\mu}{R^2}\frac{a_e^2}{R^2}\left[(1-5\sin^2\phi')\frac{u_j}{R} + 2\sin\phi' A_{j3}^{PI}\right] \\ &- H\frac{\mu}{R^2}\frac{a_e^3}{R^3}\left[(3-7\sin^2\phi')\sin\phi'\frac{u_j}{R} + \left(-\frac{3}{5} + 3\sin^2\phi'\right)A_{j3}^{PI}\right] \\ &- D\frac{\mu}{R^2}\frac{a_e^4}{R^4}\left\{\left[\frac{3}{7} - (6-9\sin^2\phi')\sin^2\phi'\right]\frac{u_j}{R}\right. \\ &\left. + \left(\frac{12}{7} - 4\sin^2\phi'\right)\sin\phi' A_{j3}^{PI}\right\}\end{aligned} \tag{5-5}$$

where $j = 1, 2, 3$.

The above equation can be rearranged into a coefficient, S_1, times u_j minus a coefficient, S_2, times A_{j3}^{PI} where

$$S_1 = -\frac{\mu}{R^3}\left\{1 + J\left(\frac{a_e}{R}\right)^2(1-5\sin^2\phi') + H\left(\frac{a_e}{R}\right)^3(3-7\sin^2\phi')\sin\phi' + D\left(\frac{a_e}{R}\right)^4\left[\frac{3}{7} - (6-9\sin^2\phi')\sin^2\phi'\right]\right\} \tag{5-6}$$

$$S_2 = \frac{\mu}{R^2}\left[2J\left(\frac{a_e}{R}\right)^2\sin\phi' - H\left(\frac{a_e}{R}\right)^3\left(\frac{3}{5} - 3\sin^2\phi'\right) + D\left(\frac{a_e}{R}\right)^4\left(\frac{12}{7} - 4\sin^2\phi'\right)\sin\phi'\right] \tag{5-7}$$

Since U is given in the form of equation (5-1) it follows from the definition of a potential field that the gravitational acceleration in Plumbline coordinates, $\bar{A}_G^P$, is

$$\bar{A}_G^P = \nabla U \tag{5-8}$$

Substituting equations (5-6), (5-7), and (5-8) into equations (5-4) and (5-5), this can be condensed to

$$\boxed{\bar{A}_G^P = S_1 \bar{R}^P - S_2 \bar{A}_{*3}^{PI}} \qquad (5\text{-}9)$$

5.3 GLOSSARY OF TERMS

SYMBOL	DEFINITION	UNIT
a_e	Semi-major axis of the earth	m
$\bar{A}_G = \begin{bmatrix} A_{GX} \\ A_{GY} \\ A_{GZ} \end{bmatrix}$	Gravitational acceleration vector	m/sec^2
A^{PI}	Transformation matrix (3x3) from Inertial Equatorial to Plumbline coordinates	unitless
$A_{*3}^{PI} = \begin{bmatrix} A_{13}^{PI} \\ A_{23}^{PI} \\ A_{33}^{PI} \end{bmatrix}$	Third column of A^{PI}	unitless
J,H,D	Harmonic coefficients in the Fischer model of the earth	unitless
R	Scalar distance from earth geometric center to vehicle CG	m
$\bar{R} = \begin{bmatrix} R_X \\ R_Y \\ R_Z \end{bmatrix}$	Position vector of the vehicle CG	m
S_1	Intermediate parameter used in computing $\bar{A}_G^P$	$1/sec^2$
S_2	Intermediate parameter used in computing $\bar{A}_G^P$	m/sec^2
$\begin{bmatrix} u_1 \\ u_2 \\ u_3 \end{bmatrix} = \begin{bmatrix} R_X^P \\ R_Y^P \\ R_Z^P \end{bmatrix}$	Alternate, indexed form of the position vector of the vehicle's CG, resolved in Plumbline coordinates	m
U	Gravity potential field of the earth	m^2/sec^2

SYMBOL	DEFINITION	UNIT
μ	Earth's gravitational coefficient	m^3/sec^2
ϕ'	Geocentric latitude of the vehicle CG	rad

Section VI
PROPELLANT SLOSH EQUATIONS

6.1 GENERAL

This section outlines the derivation of the equations that calculate the forces and moments of a contained liquid propellant when subjected to a periodic motion about its nominal flight trajectory.

The Lagrange formulation is used in the derivation of the forces and moments associated with a dynamically equivalent mechanical model composed of an assemblage of springs, dashpots, and masses.

6.2 ASSUMPTIONS

This subsection lists the assumptions and limitations made during the derivation of the equations. Both assumptions of the mechanical model and assumptions of the equations are given. The first part is related to the mechanical model assumptions.

The implicit assumption is made that there exists a mechanical model that yields forces and moments equivalent to those produced by a fluid in a container. This implies that the fluid in the tank is incompressible, it behaves as an irrotational liquid, and that the container has no sources or sinks.

The tank containing the sloshing fluid is subjected to a 6-D of freedom motion but it is implied that the forces can be dynamically simulated by 3 sets of harmonic oscillators, one in each tank direction, and that the coupling of the sloshing effects in one tank axis to any other is negligible.

Furthermore, one additional restriction is imposed on the model; the free surface of the quiescent liquid in the tank need not be perpendicular to the principal axis of the tank as seen in Figure 6-1. Thus, the axis of major constant acceleration may not be parallel to the major tank axis.

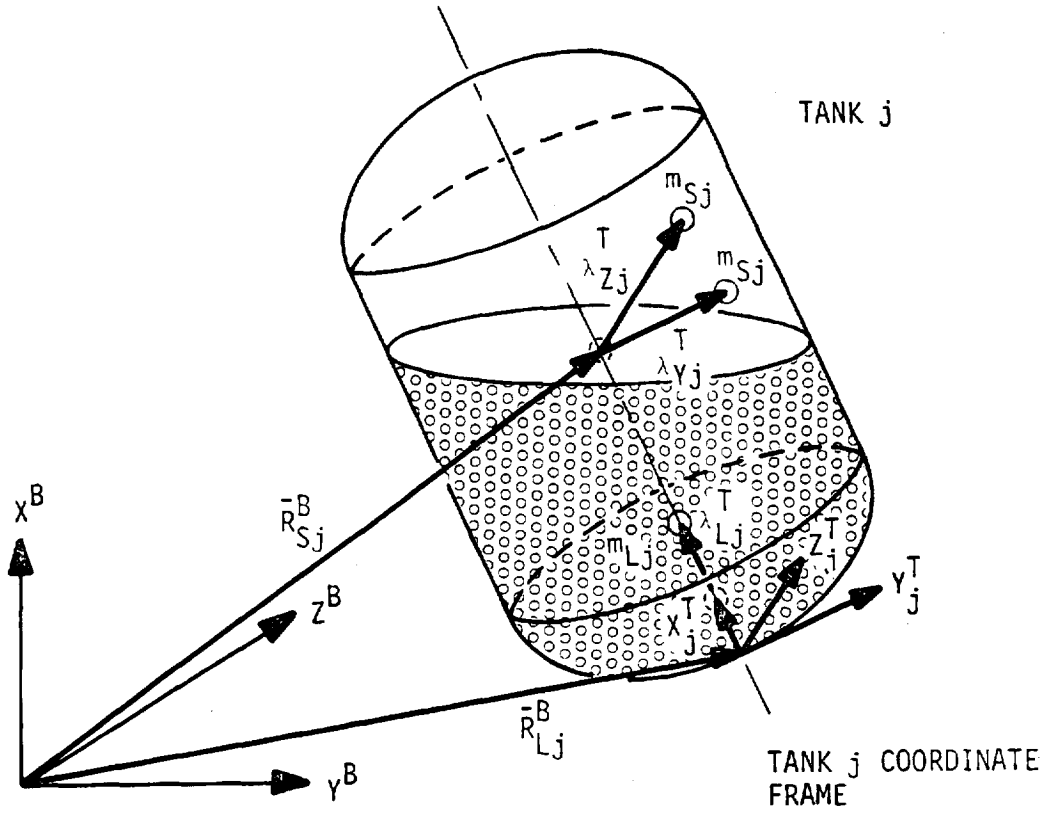

Figure 6-1. VECTOR GEOMETRY FOR THE j^{th} TANK

With due consideration to the above-mentioned assumptions, the equations of motion can be developed considering only the fundamental mode for each tank direction. Higher modes are neglected since their effects have less significance in the slosh-control-bending interaction.

As a matter of convenience, the equations developed in the next subsection are made for one tank only. Proper indexing makes the extension of this formulation to any number of tanks quite simple.

As a matter of information, the assumptions related to the mathematical model used in the derivation of the equations are presented below as follows:

- The bending data (refer to subsection 2.2) used in the formulation is to be generated with a mass profile that contains all the liquid propellant of the vehicle.
- The attachment point of the mechanical model for both lateral tank directions is assumed to be the same (located at centerline of tank). The attachment point of the longitudinal model is located at the base of the tank. This point is also the origin of each tank coordinate axis.
- The effects of vehicle excitation about the 3 axes (3 displacements and 3 rotations) are included in the formulation.
- The effects of cross coupling due to slosh are not considered (an uncoupled model is used for each tank axis).
- The effects of torsional or roll slosh are not considered.

6.3 DEVELOPMENT OF EQUATIONS

The equations of motion are derived using the Lagrange equations for a typical j^{th} tank.

The kinetic, potential, and dissipative energies for the fundamental mode of the dynamically similar mechanical model are computed first. Substitution of these energy expressions in the Lagrange equations yields the system equations of motion.

The energy of the system is a function of velocity and displacement of the mass of the system. In order to generalize the derivation, it is possible to express this quantity as a product of two quantities, one dependent on

time and the other dependent on the geometry of the system. If the matrix [C]* is DEFINED to be the geometry-dependent component of the velocity vector $\dot{\bar{\Delta}}$, of the slosh center of mass, and the time varying component, $\dot{\bar{Q}}$ has the form:

$$\dot{\bar{Q}}^T = [V_X^B \; V_Y^B \; V_Z^B \; \omega_X^B \; \omega_Y^B \; \omega_Z^B \; \dot{\eta}_1 \; \dot{\eta}_2 \cdots \dot{\eta}_n \; \dot{\lambda}_{Lj} \; \dot{\lambda}_{Yj} \; \dot{\lambda}_{Zj}] \tag{6-1}$$

then the vector, $\dot{\bar{\Delta}}_j$ is defined to be

$$\dot{\bar{\Delta}}_j = [C]_j \; \dot{\bar{Q}}_j \tag{6-2}$$

where the subscript j associates this vector with the j^{th} tank. The vector $\dot{\bar{\Delta}}$ is a 3x1 column where the first element is the displacement rate of the longitudinal slosh mass usually attached to the bottom of the tank; the other two components are the displacement rates of the lateral slosh masses in the Y and Z tank directions. It is observed that the vector $\bar{\Delta}$ is given in the tank coordinate system. The orientation of this system is related to the main vehicle axis as follows:

$$\overline{BODY} = [\tau]_j \; \overline{TANK}_j \tag{6-3}$$

Referring to equation (6-1), it can be seen that matrix $[C]_j$, as outlined in detail in Figure 6-2, is a constant with respect to time and is uniquely computed for each tank as a function of tank topology.

6.3.1 Kinetic Energy

The kinetic energy for the j^{th} tank is a quadratic of the generalized system velocities and is of the form:

$$T_j = \frac{1}{2} \dot{\bar{\Delta}}_j^T \; [m]_j \; \dot{\bar{\Delta}}_j \tag{6-4}$$

where the matrix [m] is as follows:

$$[m]_j = \begin{bmatrix} m_{Lj} & & 0 \\ & m_{Sj} & \\ 0 & & m_{Sj} \end{bmatrix} \tag{6-5}$$

and the vector $\dot{\bar{\Delta}}_j$ has the form

* *See subsection 6.4*

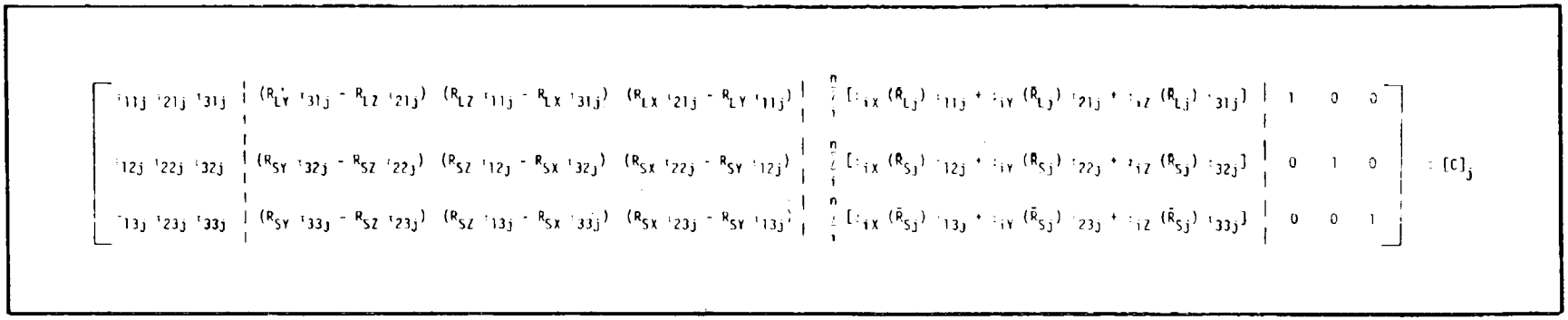

Figure 6-2. DEFINITION OF MATRIX [C]

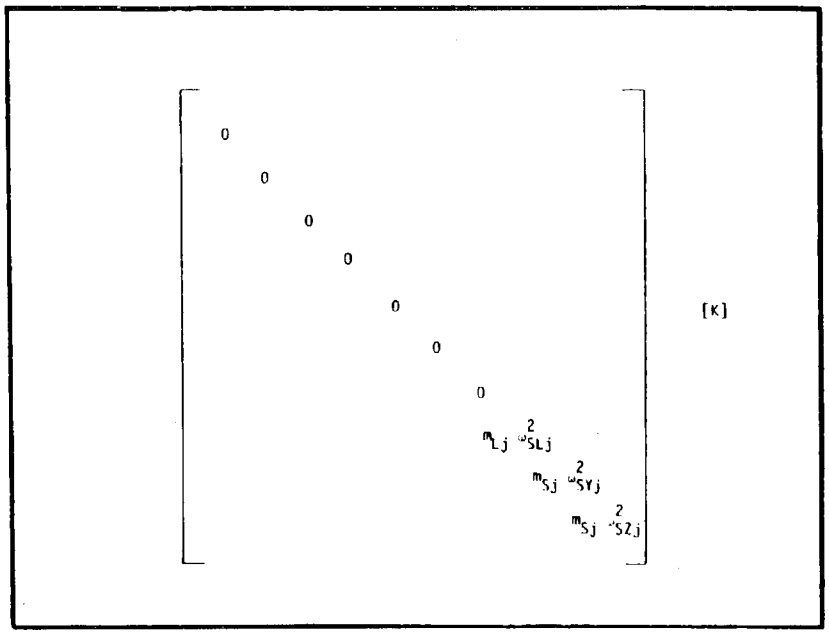

Figure 6-3. DEFINITION OF MATRIX [K]

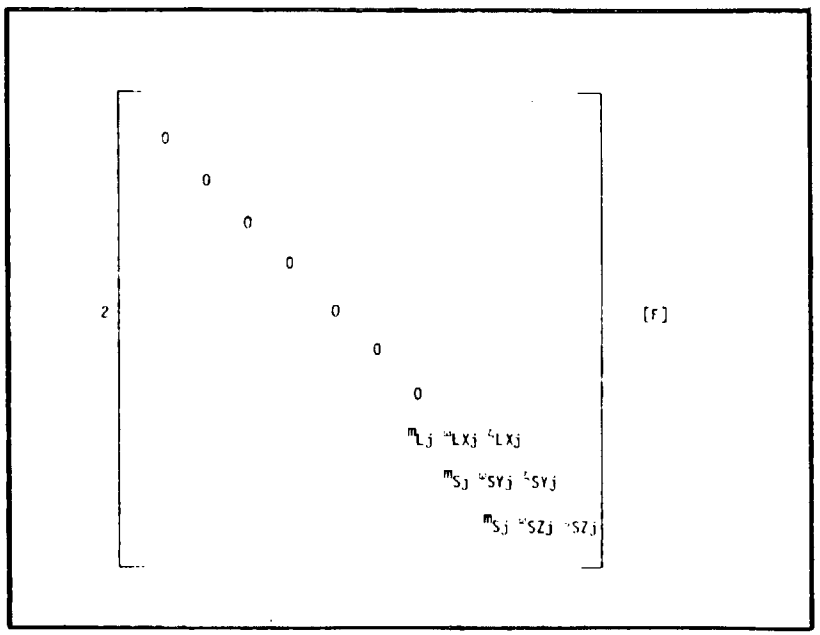

Figure 6-4. DEFINITION OF MATRIX [F]

$$\dot{\Lambda}_j = \frac{d}{dt}\left[[C]_j \bar{Q}_j \right] = [C]_j \dot{\bar{Q}}_j \qquad (6\text{-}6)$$

hence equation (6-4) becomes

$$T_j = \frac{1}{2} \dot{\bar{Q}}_j^T [C]_j^T [m] [C]_j \dot{\bar{Q}}_j \qquad (6\text{-}7)$$

6.3.2 Potential Energy

The potential energy for the j^{th} tank is a quadratic of the generalized system displacements, and is of the form:

$$V_j = \frac{1}{2} \bar{\Delta}_j^T [K]_j \bar{\Delta}_j \qquad (6\text{-}8)$$

where the matrix $[K]_j^*$ is DEFINED to be of the form as shown in Figure 6-3, and $\bar{\Delta}$ is the time-integral of the expression shown in equation (6-2). It should be remembered that the λ terms have been defined as relative motion from the deflected tank elastic axis.

Substitution of equation (6-2) in equation (6-8) yields the potential energy as a function of the generalized system displacements:

$$V_j = \frac{1}{2} \bar{Q}_j^T [C]_j^T [K]_j [C]_j \bar{Q}_j \qquad (6\text{-}9)$$

6.3.3 Dissipative Energy

The dissipative energy of the system is a quadratic of the generalized system velocities.

$$D_j = \frac{1}{2} \dot{\bar{\Delta}}^T [F]_j \dot{\bar{\Delta}} \qquad (6\text{-}10)$$

where the matrix $[F]_j$ is DEFINED to be of the form as shown in Figure 6-4. Substitution of equation (6-2) in equation (6-10) yields the dissipative energy as a function of the generalized system velocities:

$$D_j = \frac{1}{2} \dot{\bar{Q}}_j^T [C]_j^T [F]_j [C]_j \dot{\bar{Q}}_j \qquad (6\text{-}11)$$

---

* *See subsection 6.4*

6.3.4 Equations of Motion

The Lagrange equations state that:

$$\frac{d}{dt}\left(\frac{\partial T}{\partial \dot{q}_\ell}\right) + \frac{\partial V}{\partial q_\ell} + \frac{\partial T}{\partial q_\ell} + \frac{\partial D}{\partial \dot{q}_\ell} = 0 \qquad (6\text{-}12)$$

where $\partial T/\partial q_\ell = 0$ since the system kinetic energy is a quadratic in the generalized velocities only. Substitution of (6-7), (6-9), and (6-11) into (6-12) for a general term q_ℓ, and using the symmetrical properties of the equations, yields:

$$\frac{d}{dt}\left[\left(\frac{\partial \dot{\bar{Q}}}{\partial \dot{q}_\ell}\right)_j^T [C]_j^T [m] [C]_j \dot{\bar{Q}}_j\right] + \left(\frac{\partial \bar{Q}}{\partial q_\ell}\right)_j^T [C]_j^T [K]_j [C]_j \bar{Q}_j + \left(\frac{\partial \dot{\bar{Q}}}{\partial q_\ell}\right)_j^T [C]_j^T [F]_j [C]_j \dot{\bar{Q}}_j = 0 \qquad (6\text{-}13)$$

where q_ℓ takes the names of λ_{Lj}, λ_{Yj}, and λ_{Zj} for the slosh motion along the X, Y, and Z tank directions. Substitution of these variables in equation (6-13) and expansion yields for $q_\ell = \lambda_{Lj}$,

$$m_{Sj}\left[\ddot{\lambda}_{Lj} + 2\,\omega_{SLj}\,\zeta_{SLj}\,\dot{\lambda}_{Lj} + \omega_{SLj}^2\,\lambda_{Lj} + QX_j\right] = 0 \qquad (6\text{-}14)$$

for $q_\ell = \lambda_{Yj}$

$$m_{Sj}\left[\ddot{\lambda}_{Yj} + 2\,\omega_{SYj}\,\zeta_{SYj}\,\dot{\lambda}_{Yj} + \omega_{SYj}^2\,\lambda_{Yj} + QY_j\right] = 0 \qquad (6\text{-}15)$$

for $q_\ell = \lambda_{Zj}$

$$m_{Sj}\left[\ddot{\lambda}_{Zj} + 2\,\omega_{SZj}\,\zeta_{SZj}\,\dot{\lambda}_{Zj} + \omega_{SZj}^2\,\lambda_{Zj} + QZ_j\right] = 0 \qquad (6\text{-}16)$$

where the terms QX_j, QY_j, and QZ_j are the acceleration terms of the attachment points of the springs of the model in the X, Y, and Z tank directions. These terms are of the form:

$$QX_j = \tau_{11j}\,A_X^B + \tau_{21j}\,A_Y^B + \tau_{31j}\,A_Z^B + \sum_{i=1}^{n}\left[\phi_{iX}(\bar{R}_{Lj})\,\tau_{11j} + \phi_{iY}(\bar{R}_{Lj})\,\tau_{21j} + \phi_{iZ}(\bar{R}_{Lj})\,\tau_{31j}\right]\ddot{n}_i + (\dot{\omega}_Y^B\,R_{LZj}^B - \dot{\omega}_Z^B\,R_{LYj}^B)\,\tau_{11j} + (\dot{\omega}_Z^B\,R_{LXj}^B - \dot{\omega}_X^B\,R_{LZj}^B)\,\tau_{21j} + (\dot{\omega}_X^B\,R_{LYj}^B - \dot{\omega}_Y^B\,R_{LXj}^B)\,\tau_{31j} \qquad (6\text{-}17)$$

$$QY_j = \tau_{12j} A_X^B + \tau_{22j} A_Y^B + \tau_{32j} A_Z^B + \sum_{i=1}^{n} [\phi_{iX}(\bar{R}_{Sj}) \tau_{12j} + \phi_{iY}(\bar{R}_{Sj}) \tau_{22j} + \phi_{iZ}(\bar{R}_{Sj}) \tau_{32j}] \ddot{\eta}_i + (\dot{\omega}_Y^B R_{SZj}^B - \dot{\omega}_Z^B R_{SYj}^B) \tau_{12j} + (\dot{\omega}_Z^B R_{SXj}^B - \dot{\omega}_X^B R_{SZj}^B) \tau_{22j} + (\dot{\omega}_X^B R_{SYj}^B - \dot{\omega}_Y^B R_{SXj}^B) \tau_{32j} \quad (6\text{-}18)$$

$$QZ_j = \tau_{13j} A_X^B + \tau_{23j} A_Y^B + \tau_{33j} A_Z^B + \sum_{i=1}^{n} [\phi_{iX}(\bar{R}_{Sj}) \tau_{13j} + \phi_{iY}(\bar{R}_{Sj}) \tau_{23j} + \phi_{iZ}(\bar{R}_{Sj}) \tau_{33j}] \ddot{\eta}_i + (\dot{\omega}_Y^B R_{SZj}^B - \dot{\omega}_Z^B R_{SYj}^B) \tau_{13j} + (\dot{\omega}_Z^B R_{SXj}^B - \dot{\omega}_X^B R_{SZj}^B) \tau_{23j} + (\dot{\omega}_X^B R_{SYj}^B - \dot{\omega}_Y^B R_{SYj}^B) \tau_{33j} \quad (6\text{-}19)$$

where

i = 1, n

n = number of bending modes.

The total accelerations experienced by the slosh masses are:

X direction:

$$\ddot{\lambda}_{Lj} = -QX_j - 2\omega_{SLj} \zeta_{SLj} \dot{\lambda}_{Lj} - \omega_{SLj}^2 \lambda_{Lj} \quad (6\text{-}20)$$

Y direction:

$$\ddot{\lambda}_{Yj} = -QY_j - 2\omega_{SYj} \zeta_{SYj} \dot{\lambda}_{Yj} - \omega_{SYj}^2 \lambda_{Yj} \quad (6\text{-}21)$$

Z direction:

$$\ddot{\lambda}_{Zj} = -QZ_j - 2\omega_{XZj} \zeta_{SZj} \dot{\lambda}_{Zj} - \omega_{SZj}^2 \lambda_{Zj} \quad (6\text{-}22)$$

6.3.5 Forces and Moments

6.3.5.1 Forces and Moments Exciting Vehicle Bending. The forces on the vehicle that are due to the lateral slosh motion acting at the attachment point location are:

$$\bar{F}^{B}_{Sj} = \begin{bmatrix} F_{SXj} \\ F_{Syj} \\ F_{SZj} \end{bmatrix} = -m_{sj}[\tau]_j \begin{bmatrix} 0 \\ \ddot{\lambda}_{Yj} + QY_j \\ \ddot{\lambda}_{Zj} + QZ_j \end{bmatrix} \tag{6-23}$$

and those forces resulting from the longitudinal slosh motion acting at the bottom of each tank are

$$\bar{F}^{B}_{Lj} = \begin{bmatrix} F_{LXj} \\ F_{LYj} \\ F_{LZj} \end{bmatrix} = -m_{Lj}[\tau]_j \begin{bmatrix} \ddot{\lambda}_{Lj} + QX_j \\ 0 \\ 0 \end{bmatrix} \tag{6-24}$$

The vector forces $\bar{F}^{B}_{Sj}$ and $\bar{F}^{B}_{Lj}$ excite bending with point of application at the respective attachment points. In addition to these excitations, bending is also excited by moments that result when the inertia forces act on the offset produced by the sloshing motion. These moments also act through axes passing through the corresponding attachment points and are of the form presented below.

Moments due to lateral sloshing:

$$\bar{M}^{B}_{Sj} = \begin{bmatrix} M^{B}_{SXj} \\ M^{B}_{SYj} \\ M^{B}_{SZj} \end{bmatrix} = \begin{bmatrix} 0 \\ m_{Sj} A^{B}_{X} (\tau_{32j} \lambda_{Yj} + \tau_{33j} \lambda_{Zj}) \\ -m_{Sj} A^{B}_{X} (\tau_{22j} \lambda_{Yj} + \tau_{23j} \lambda_{Zj} \end{bmatrix} \tag{6-25}$$

Moments due to longitudinal sloshing:

$$\bar{M}^{B}_{Lj} = \begin{bmatrix} M^{B}_{LXj} \\ M^{B}_{LYj} \\ M^{B}_{LZj} \end{bmatrix} = \begin{bmatrix} m_{Lj} (A^{B}_{Y} \tau_{31j} \lambda_{Lj} - A^{B}_{Z} \tau_{21j} \lambda_{Lj}) \\ m_{Lj} A^{B}_{Z} \tau_{11j} \lambda_{Lj} \\ -m_{Lj} A^{B}_{Y} \tau_{11j} \lambda_{Lj} \end{bmatrix} \tag{6-26}$$

6.3.5.2 Forces and Moments Exciting Vehicle Rigid Body Motion. The forces that excite vehicle translational acceleration are those resulting when the vector forces $\bar{F}^B_{Sj}$ and $\bar{F}^B_{Lj}$ are transferred to the vehicle CM. The resultant of these vectors for each tank is given below.

$$\bar{\nu}^B_{Sj} = \begin{bmatrix} \nu^B_{SXj} \\ \nu^B_{XYj} \\ \nu_{SZj} \end{bmatrix} = \begin{bmatrix} F^B_{SXj} + F^B_{LXj} \\ F^B_{SYj} + F^B_{LYj} \\ F^B_{SZj} + F^B_{LZj} \end{bmatrix} \tag{6-27}$$

In a similar form, the moments that excite vehicle rotational acceleration are those resulting when the vector forces $\bar{F}^B_{Sj}$ and $\bar{F}^B_{Lj}$ are transferred to the vehicle CM and the vector moments that result from the inertia forces acting on the slosh offsets. These moments, given in vector form, are:

$$\bar{\mu}^B_{Sj} = \bar{M}^B_{Sj} + \bar{M}^B_{Lj} + \bar{R}^B_{Sj} \times \bar{F}^B_{Sj} + \bar{R}^B_{Lj} \times \bar{F}^B_{Lj} \tag{6-28}$$

and in component form:

$$\bar{\mu}^B_{Sj} = \begin{bmatrix} \mu^B_{SXj} \\ \mu^B_{SYj} \\ \mu^B_{SZj} \end{bmatrix} = \begin{bmatrix} (R^B_{SYj} F^B_{SZj} - R^B_{SZj} F^B_{SYj} + R^B_{LYj} F^B_{LZj} - R^B_{LZj} F^B_{LYj} + M^B_{LXj} + M^B_{SXj}) \\ (R^B_{SZj} F^B_{SXj} - R^B_{SXj} F^B_{SZj} + M^B_{SYj} + R^B_{LZj} F^B_{LXj} - R^B_{LXj} F^B_{LZj} + M_{LYj}) \\ (R^B_{SXj} F^B_{XYj} - R^B_{SYj} F^B_{SXj} + M^B_{SZj} + R^B_{LXj} F^B_{LYj} - R^B_{LYj} F^B_{LXj} + M^B_{LZj}) \end{bmatrix} \tag{6-29}$$

where the vectors $\bar{R}^B_{Sj}$ and $\bar{R}^B_{Lj}$ are the position vectors that locate the attachment points of the lateral and longitudinal slosh masses, respectively.

The total force and moment due to N_S tanks is the sum of the forces and moments produced by each tank.

$$\bar{F}_S^B = \sum_{j=1}^{N_S} \nu_{Sj}^B \tag{6-30}$$

and

$$\bar{M}_S^B = \sum_{j=1}^{N_S} \mu_{Sj}^B \tag{6-31}$$

6.4 TRANSFORMATION MATRICES

This section outlines the derivation of the transformation matrices utilized during the derivation. Explicitly the transformations appearing in expressions (6-2), (6-3), (6-8), and (6-10) are considered.

6.4.1 The $[C]_j$ Matrix

If the velocity of the center of mass of the sloshing mass is defined to be of the form shown in equation (6-2) and transcribed here as follows,

$$\dot{\bar{\Delta}}_j = [C]_j \dot{\bar{Q}}_j \tag{6-32}$$

it can be seen that the vector $\dot{\bar{Q}}_j$ is the generalized velocity vector of the system, and that the matrix $[C]_j$ is the space or geometry-dependent component of the velocity vector $\dot{\bar{\Delta}}$.

By referring to Figure 6-5, it can be seen that for the case when the tank coordinate system is parallel to the vehicle coordinate system, the velocity of the center of mass of the lateral slosh mass in the vehicle (or tank) Z direction, is (for the planar case):

$$\dot{\Delta}_{ZT} = (V_Z^B - R_{SX}\,\omega_Y^B + \sum_{i=1}^{n} \phi_{iZ}\,(\bar{R}_{Sj})\,\dot{r}_i) + \dot{\lambda}_{SZj} \tag{6-33}$$

The terms in parentheses are the velocity of the attachment point.

It can be shown that for a six-dimensional case, when the vehicle is translating in a three-demensional space and rotating simultaneously about

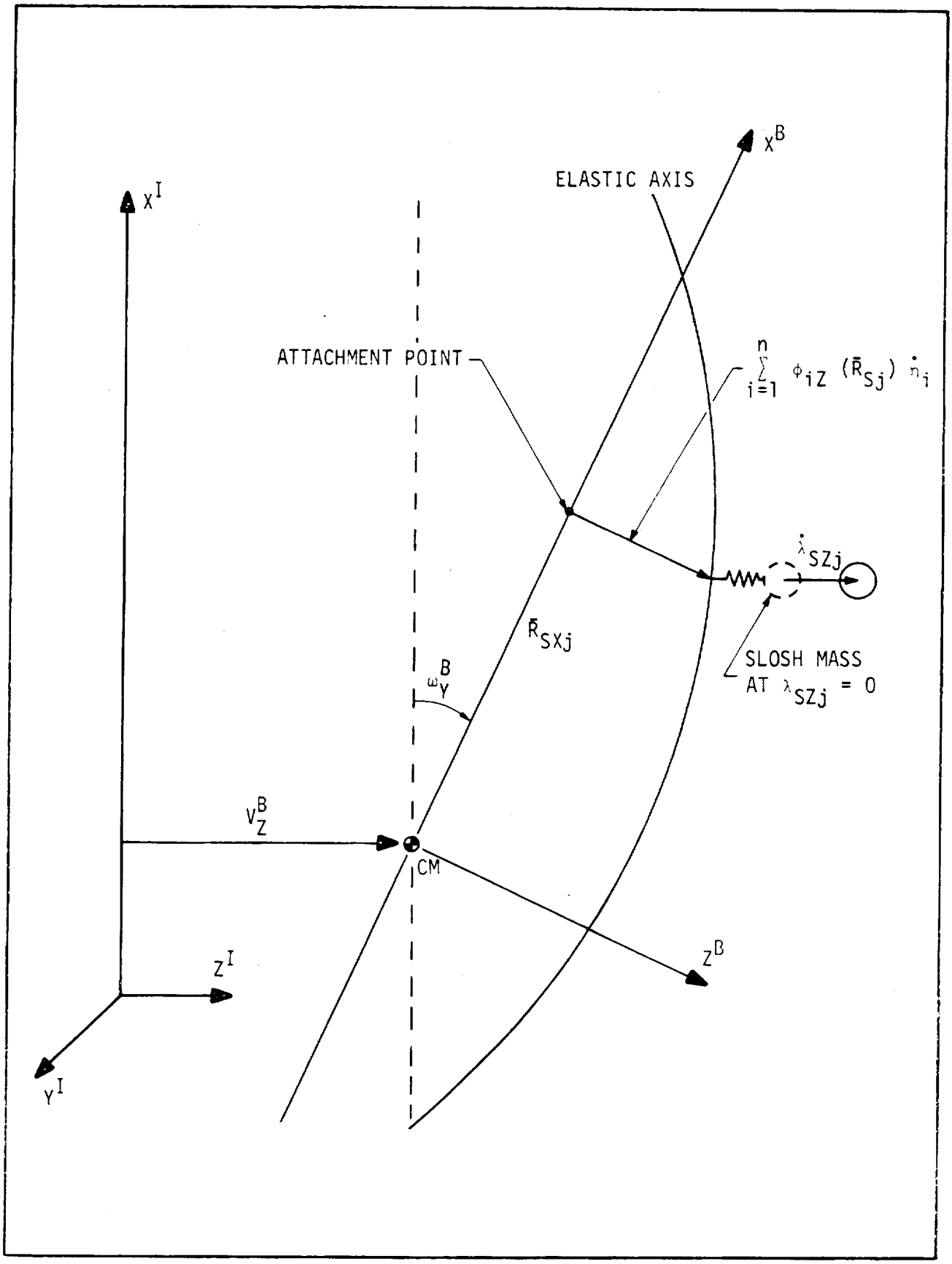

Figure 6-5. Z-VELOCITY COMPONENT OF THE j^{th} SLOSH MASS

three axes, equation (6-33) can be generalized as follows:

$$\dot{\Delta}_{ZT} = (V_Z^B + \left[\bar{\omega}^B \times \bar{R}_{Sj}\right]_Z + \sum_{i=1}^{n} \phi_{iZ}(\bar{R}_{Sj})\,\dot{n}_i) + \dot{\lambda}_{SZj} \qquad (6\text{-}34)$$

For the general case where the tank coordinate system is nonaligned to the vehicle coordinate system, the coordinate transformation

$$\overline{BODY} = [\tau]_j\ \overline{TANK} \qquad (6\text{-}35)$$

may be used in equation (6-34) to render the general form

$$\dot{\Delta}_{ZT} = \underbrace{[\tau_{13j}\ \tau_{23j}\ \tau_{33j}]}_{\tau_Z}\ [\bar{V}^B + \bar{\omega}^B \times \bar{R}_{Sj} + \Phi_\xi(\bar{R}_{Sj})\,\dot{\bar{n}}] + \dot{\lambda}_{SZj} \qquad (6\text{-}36)$$

where τ_Z is the 3rd column of the transformation $[\tau]_j$ in (6-35), $\bar{V}^B$ is the vector of velocities whose components are V_X^B, V_Y^B, and V_Z^B, and $\bar{\omega}^B$ is the vector of angular velocities with components ω_X^B, ω_Y^B, and ω_Z^B.

Expansion of equation (6-36) yields:

$$\begin{aligned}\dot{\Delta}_{ZT} = {} & \tau_{13j}\,V_X^B + \tau_{23j}\,V_Y^B + \tau_{33j}\,V_Z^B + (R_{SYj}^B\,\tau_{33j} - R_{SZj}^B\,\tau_{23j})\,\omega_X^B \\ & + (R_{SZj}^B\,\tau_{13j} - R_{SXj}^B\,\tau_{33j})\,\omega_Y^B + (R_{SXj}^B\,\tau_{23j} - R_{Syj}^B\,\tau_{13j})\omega_Z^B \\ & + \sum_{i}^{n} [\phi_{iX}(\bar{R}_{Sj})\,\tau_{13j} + \phi_{iY}(\bar{R}_{Sj})\,\tau_{23j} + \phi_{iZ}(\bar{R}_{Sj})\,\tau_{33j}]\,\dot{n}_i + \dot{\lambda}_{SZj}\end{aligned} \qquad (6\text{-}37)$$

This expression can be rewritten as follows:

$$\begin{aligned}\dot{\Delta}_{ZT} = {} & [\tau_{13j}\ \tau_{23j}\ \tau_{33j}\ (R_{SYj}^B\,\tau_{33j} - R_{SZj}^B\,\tau_{23j}) \\ & (R_{SZj}^B\,\tau_{13j} - R_{SXj}^B\,\tau_{33j})\ \ (R_{SXj}^B\,\tau_{23j} - R_{SYj}^B\,\tau_{13j}) \\ & \sum^{n} [\phi_{iX}(\bar{R}_{Sj})\,\tau_{13j} + \phi_{iY}(\bar{R}_{Sj})\,\tau_{23j} + \phi_{iZ}(\bar{R}_{Sj})\,\tau_{33j}] + 1]\,\dot{\bar{Q}}\end{aligned} \qquad (6\text{-}38)$$

where $\dot{\bar{Q}}$ is defined as follows (the transpose is shown here)

$$\dot{\bar{Q}}^T = [V_X^B \; V_Y^B \; V_Z^B \; \omega_X^B \; \omega_Y^B \; \omega_Z^B \; \dot{\eta}_i \; \dot{\eta}_2 \cdots \dot{\eta}_n \; \dot{\lambda}_{SZj}] \tag{6-39}$$

Expression (6-39) augmented to accommodate the slosh motion about the other two axes is shown in Figure 6-2. The expression (6-38) is the 3rd row of the matrix $(C]_j$ as shown in Figure 6-2.

The other two rows can be easily obtained by paralleling the development of expression (6-38).

6.4.2 The $[\tau]_j$ Matrix

The $[\tau]_j$ matrix is an orthogonal transformation that is used to transform vectors given in the Body coordinate system to vectors in the tank systems. This transformation is a parametric input and no derivation is required.

6.4.3 The $[K]_j$ Matrix

The matrix $[K]_j$ is a quadratic in the generalized displacement vector $\bar{\Delta}_j$. The exact nature of this matrix is of no interest at this time, only the terms associated with the sloshing degrees of freedom are given so that by definition the remaining terms are assumed to be zero.

The matrix $[K]_j$ is unique for each tank and is of the same order as the generalized vector $\bar{Q}$. The form of this matrix is shown in Figure 6-3.

6.4.4 The $[F]_j$ Matrix

The matrix $[F]_j$ is a quadratic in the generalized velocities. The same notes made for matrix $[K]_j$ apply to this matrix. The form of the $[F]_j$ matrix is shown in Figure 6-4.

6.5 GLOSSARY OF TERMS

SYMBOL	DEFINITION	UNIT
$\bar{A}^B$	Vector of vehicle rigid body acceleration	m/sec^2
$\bar{F}^B_{Lj}$	The j^{th} tank slosh force vector (longitudinal propellant slosh)	N
$\bar{F}^B_{Sj}$	The j^{th} slosh force vector (lateral propellant slosh)	N
$\bar{F}^B_S$	Total slosh vector at vehicle CM	N
$\bar{M}^B_{Lj}$	Vector moment of the j^{th} tank longitudinal slosh mass, exciting bending at location $\bar{R}_{Lj}$	N-m
m_{Lj}	Longitudinal slosh mass for the j^{th} tank	Kg
$\bar{M}^B_S$	Total slosh moment vector about vehicle CM	N-m
$\bar{M}^B_{Sj}$	Vector moment of the j^{th} tank lateral slosh mass, exciting bending at location $\bar{R}_{Sj}$	N-m
m_{Sj}	Lateral slosh mass for the j^{th} tank	Kg
N_S	Number of tanks in vehicle	unitless
n	Number of bending modes	unitless
QX_j	Acceleration of the j^{th} tank longitudinal slosh mass attachment point in the X^T_j direction	m/sec^2
QY_j	Acceleration of the j^{th} tank lateral slosh mass attachment point in the Y^T_j direction	m/sec^2
QZ_j	Acceleration of the j^{th} tank lateral slosh mass attachment point in the Z^T_j direction	m/sec^2
$\bar{RL}^B_j$	Position vector of the j^{th} longitudinal slosh mass attachment point (lower bulkhead)	m
$\bar{R}^B_{Sj}$	Position vector of the j^{th} tank lateral slosh-mass attachment point	m
ζ_{SY}	Fundamental damping coefficient (yaw plane slosh mass-spring model)	unitless
ζ_{SZ}	Fundamental damping coefficient (pitch plane slosh mass-spring model)	unitless
ζ_{SL}	Fundamental damping coefficient (longitudinal axis mass-spring model)	unitless
$\ddot{\eta}$	Generalized acceleration due to bending	m/sec^2

SYMBOL	DEFINITION	UNIT
λ_{Yj}	Displacement of j^{th} lateral slosh mass m_{Sj} in the $X_j^T - Y_j^T$ tank place, displacement direction parallel to the Y_j^T - axis	m
λ_{Zj}	Displacement of the j^{th} lateral slosh mass m_{Sj} in the $X_j^T - Z_j^T$ tank plane, displacement direction parallel to the Z_j^T - axis	m
λ_{Lj}	Displacement of the j^{th} longitudinal slosh mass m_{Lj} directed along the X_j^T - axis	m
$\dot{\lambda}_{Yj}$	Linear velocity of the j^{th} lateral slosh mass m_{Sj} in the $X_j^T - Y_j^T$ tank plane, velocity direction parallel to the Y_j^T - axis	m/sec
$\dot{\lambda}_{Zj}$	Linear velocity of the j^{th} lateral slosh mass in the $X_j^T - Z_j^T$ tank plane, velocity direction parallel to the Z_j^T - axis	m/sec
$\dot{\lambda}_{Lj}$	Linear velocity of the j^{th} longitudinal slosh mass m_{Lj} directed along the X_j^T - axis	m/sec
$\ddot{\lambda}_{Yj}$	Linear acceleration of the j^{th} lateral slosh mass m_{Sj} in the $X_j^T - Y_j^T$ tank plane, acceleration direction parallel to the Y_j^T - axis	m/sec^2
$\ddot{\lambda}_{Zj}$	Linear acceleration of the j^{th} lateral slosh mass m_{Sj} in the $X_j^T - Z_j^T$ tank plane, acceleration direction parallel to the Z_j^T - axis	m/sec^2
$\ddot{\lambda}_{Lj}$	Linear acceleration of the j^{th} longitudinal slosh mass m_{Lj} directed along the X_j^T - axis	m/sec^2
$\bar{L}_{Sj}$	Vector of total moments of the j^{th} tank, exciting rigid body vehicle rotation, resolved in Body coordinates	N-m
$\bar{F}_{Sj}$	Vector of total forces of the j^{th} tank, exciting rigid body vehicle translation, resolved in Body coordinates	N

SYMBOL	DEFINITION	UNIT
$\phi_{\xi}^{T}(\bar{R}_{L_j}) = \begin{bmatrix} \phi_{1X}(\bar{R}_{L_j}) & \phi_{1Y}(\bar{R}_{L_j}) & \phi_{1Z}(\bar{R}_{L_j}) \\ \vdots & \vdots & \vdots \\ \phi_{nX}(\bar{R}_{L_j}) & \phi_{nY}(\bar{R}_{L_j}) & \phi_{nZ}(\bar{R}_{L_j}) \end{bmatrix}$	Matrix transpose of modal displacement coefficient matrix at the lower bulkhead of the j^{th} tank defined by the position vector $\bar{R}_{L_j}$ $j = 1, N_S$ where N_S is the total number of tanks considered in slosh	m/m unitless
$\phi_{\xi}^{T}(\bar{R}_{S_j}) = \begin{bmatrix} \phi_{1X}(\bar{R}_{S_j}) & \phi_{1Y}(\bar{R}_{S_j}) & \phi_{1Z}(\bar{R}_{S_j}) \\ \vdots & \vdots & \vdots \\ \phi_{nX}(\bar{R}_{S_j}) & \phi_{nY}(\bar{R}_{S_j}) & \phi_{nZ}(\bar{R}_{S_j}) \end{bmatrix}$	Matrix transpose of modal displacement coefficient matrix at the j^{th} slosh mass location defined by position vector $\bar{R}_{S_j}$ $j = 1, N_s$	m/m unitless
$[\tau]_j$	Transformation matrix to resolve j^{th} tank-referenced vectors into body-referenced vectors	unitless
ω_{SL}	Fundamental slosh modal frequency (longitudinal axis slosh mass-spring model)	rad/sec
ω_{SY}	Fundamental slosh modal frequency (yaw plane slosh mass-spring model)	rad/sec
ω_{SZ}	Fundamental slosh modal frequency (pitch plane slosh mass-spring model)	rad/sec

Section VII
RIGID BODY ROTATIONAL EQUATIONS

7.1 GENERAL

The equations of angular motion of a rigid vehicle about its center-of-gravity (CG) may be derived through the use of angular momentum conservation. The angular motion of the vehicle with respect to the earth, or inertial space, is described by Euler angles which relate this inertial frame, the Plumbline Frame, to the Body Frame.

The derivation of the equations of angular motion of a rigid vehicle and the development of the required coordinate transformation is outlined in the following subsections. Those equations that are boxed in by straight lines are presented in the Simulation Diagram of the Rigid Body Rotational Dynamics Module of a companion report (ref. 1).

7.2 DERIVATION OF EQUATIONS

Conservation of angular momentum states that the time rate of change of the vehicle's angular momentum about its CG is equal to the sum of the internal and external disturbance moments about the CG. The angular momentum time derivative, written in the P-frame* (Plumbline coordinates), is thus

$$\dot{\bar{H}}^P = \sum \bar{M}^P \tag{7-1}$$

The vehicle angular momentum in the B-frame* (Body coordinates) can be written as

$$\bar{H}^B = I\,\bar{\omega}^B \tag{7-2}$$

where I is the vehicle's generalized inertia tensor about its CG, referenced to the Body axes. Utilizing A^{PB*}, in the P-frame equation (7-2) becomes

$$\bar{H}^P = A^{PB}\,\bar{H}^B = A^{PB}\,I\,\bar{\omega}^B \tag{7-3}$$

See subsection 7.3, Coordinate Transformations.

Equation (7-1) then becomes

$$\dot{\bar{H}}^P = \dot{A}^{PB}\, I\, \bar{\omega}^B + A^{PB}\, \dot{I}\, \bar{\omega}^B + A^{PB}\, I\, \dot{\bar{\omega}}^B = \sum A^{PB}\, \bar{M}^B \tag{7-4}$$

and since

$$\dot{A}^{PB} = A^{PB}\, \tilde{\omega}^B \tag{7-5}$$

then

$$\dot{\bar{H}}^P = A^{PB}\, (\tilde{\omega}^B\, I\, \bar{\omega}^B + \dot{I}\, \bar{\omega}^B + I\, \dot{\bar{\omega}}^B) = A^{PB} \sum \bar{M}^B \tag{7-6}$$

It is assumed that I changes slowly enough to neglect the $\dot{I}$ term. Then equation (7-6) becomes

$$\sum \bar{M}^B = I\, \dot{\bar{\omega}}^B + \tilde{\omega}^B\, I\, \bar{\omega}^B \tag{7-7}$$

An explicit solution of the rigid vehicle angular acceleration about its CG can be determined from equation (7-7) as

$$\dot{\bar{\omega}}^B = I^{-1}\, (\sum \bar{M}^B - \tilde{\omega}^B\, I\, \bar{\omega}^B) \tag{7-8}$$

Considering the disturbance moments $\bar{M}_A^B$ (aerodynamics), $\bar{M}_E^B$ (engine inertia), $\bar{M}_S^B$ (propellant slosh), and $\bar{M}_T^B$ (engine thrust), one can write

$$\boxed{\dot{\bar{\omega}}^B = I^{-1}\, (\bar{M}_A^B + \bar{M}_E^B + \bar{M}_S^B + \bar{M}_T^B - \tilde{\omega}^B\, I\, \bar{\omega}^B)} \tag{7-9}$$

Equation (7-9) provides an algebraic solution for the rigid vehicle angular acceleration about its CG. Angular velocity may be determined by the integration

$$\boxed{\bar{\omega}^B = \int_0^t \dot{\bar{\omega}}^B\, dt + \bar{\omega}^B(0)} \tag{7-10}$$

7.3 COORDINATE TRANSFORMATIONS

Since it is necessary to describe the angular motion of the vehicle with respect to the earth, a coordinate transformation of body angular rates (ω_X^B, ω_Y^B, ω_Z^B) to Euler rates ($\dot{\Phi}$, $\dot{\Theta}$, $\dot{\Psi}$) is needed.

7.3.1 Plumbline to Body (P–to–B)

The P-frame (Plumbline) having coordinate axes X^P, Y^P, Z^P, is shown in Figure 7-1 (Detail A). A right-hand rotation about the Y^P-axis (Figure 7-1, Detail B) through an angle Θ can be represented by the transformation

$$\begin{bmatrix} X' \\ Y' \\ Z' \end{bmatrix} = \begin{bmatrix} \cos\Theta & 0 & -\sin\Theta \\ 0 & 1 & 0 \\ \sin\Theta & 0 & \cos\Theta \end{bmatrix} \begin{bmatrix} X^P \\ Y^P \\ Z^P \end{bmatrix} = [\Theta]_2 \begin{bmatrix} X^P \\ Y^P \\ Z^P \end{bmatrix} \tag{7-11}$$

Note that $\dot{\Theta}$ is on the Y' axis (Figure 7-1, Detail B).

A similar right-hand rotation about the Z'-axis (Figure 7-1, Detail C) through an angle Ψ can be represented by the transformation

$$\begin{bmatrix} X'' \\ Y'' \\ Z'' \end{bmatrix} = \begin{bmatrix} \cos\Psi & \sin\Psi & 0 \\ -\sin\Psi & \cos\Psi & 0 \\ 0 & 0 & 1 \end{bmatrix} \begin{bmatrix} X' \\ Y' \\ Z' \end{bmatrix} = [\Psi]_3 \begin{bmatrix} X' \\ Y' \\ Z' \end{bmatrix} \tag{7-12}$$

Note that $\dot{\Psi}$ is on the Z'' axis (Figure 7-1, Detail C).

A final right-hand rotation about the X''-axis (Figure 7-1, Detail D) through an angle Φ can be represented by the transformation

$$\begin{bmatrix} X^B \\ Y^B \\ Z^B \end{bmatrix} = \begin{bmatrix} 1 & 0 & 0 \\ 0 & \cos\Phi & \sin\Phi \\ 0 & -\sin\Phi & \cos\Phi \end{bmatrix} \begin{bmatrix} X'' \\ Y'' \\ Z'' \end{bmatrix} = [\Phi]_1 \begin{bmatrix} X'' \\ Y'' \\ Z'' \end{bmatrix} \tag{7-13}$$

Note that $\dot{\Phi}$ is on the X^B axis (Figure 7-1, Detail D).

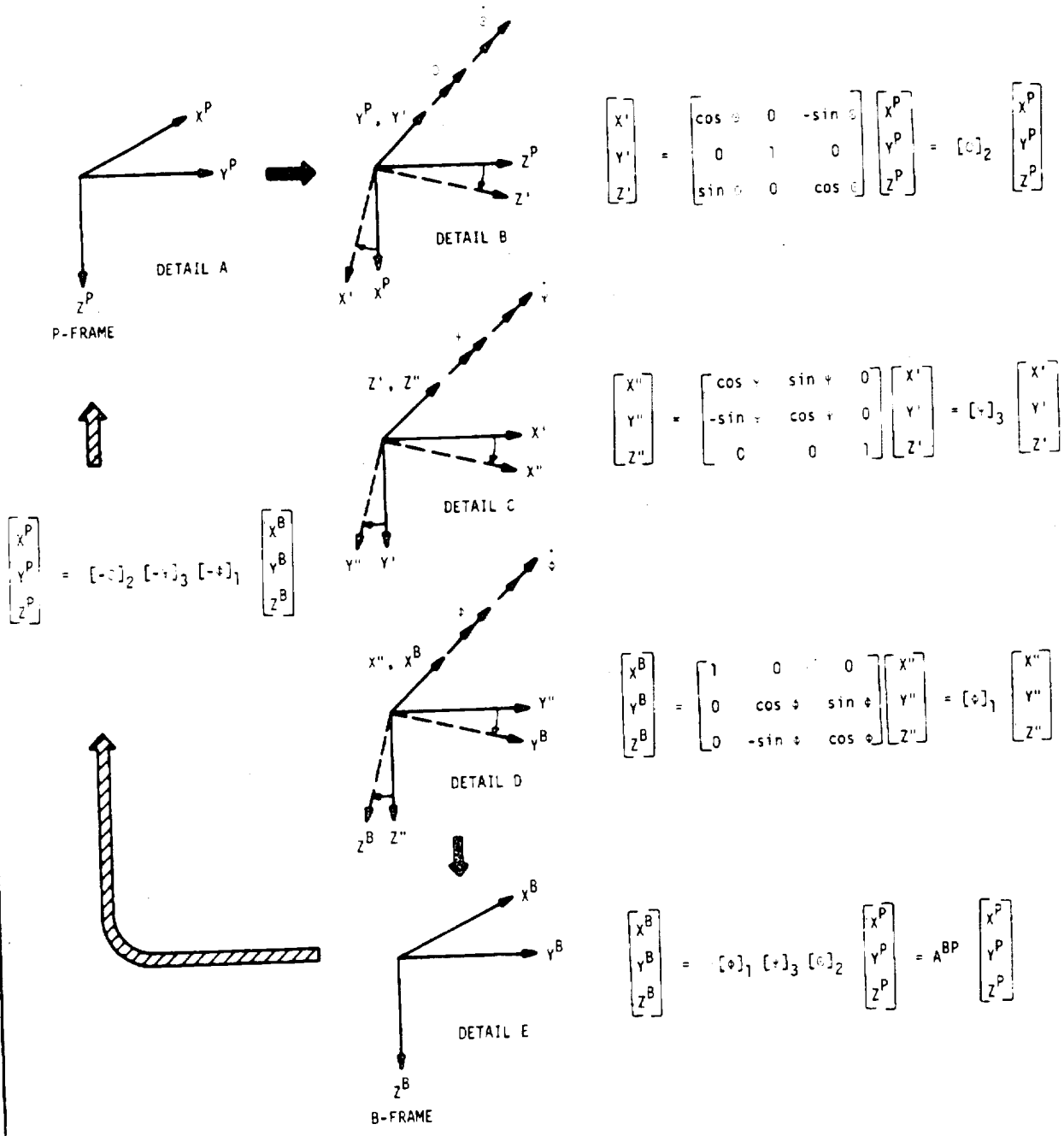

Figure 7-1. PLUMBLINE ➡ BODY AND BODY ➡ PLUMBLINE TRANSFORMATIONS

The three successive rotations of equations (7-11), (7-12), and (7-13) provide a transformation matrix that relates a vector $\bar{a}^P$ in the P-frame to the vector $\bar{a}^B$ in the B-frame as follows:

$$\bar{a}^B = [\Phi]_1 [\Psi]_3 [\Theta]_2 \bar{a}^P = A^{BP} \bar{a}^P \tag{7-14}$$

7.3.2 Euler Rates to Body Rates

Refer to Figure 7-1 and observe that the Euler rate vectors $\dot{\Phi}$, $\dot{\Psi}$, and $\dot{\Theta}$* are directed along the X^B, Z", and Y'-axes, respectively. Body rates may be written in terms of Euler rates as follows:

$$\begin{bmatrix} \omega_X^B \\ \omega_Y^B \\ \omega_Z^B \end{bmatrix} = \begin{bmatrix} I \end{bmatrix} \begin{bmatrix} \dot{\Phi} \\ 0 \\ 0 \end{bmatrix} + [\Phi]_1 \begin{bmatrix} 0 \\ 0 \\ \dot{\Psi} \end{bmatrix} + [\Phi]_1 [\Psi]_3 \begin{bmatrix} 0 \\ \dot{\Theta} \\ 0 \end{bmatrix} \tag{7-15}$$

where

$$\begin{bmatrix} I \end{bmatrix} \begin{bmatrix} \dot{\Phi} \\ 0 \\ 0 \end{bmatrix} = \begin{bmatrix} 1 & 0 & 0 \\ 0 & 1 & 0 \\ 0 & 0 & 1 \end{bmatrix} \begin{bmatrix} \dot{\Phi} \\ 0 \\ 0 \end{bmatrix} = \begin{bmatrix} 1 \\ 0 \\ 0 \end{bmatrix} \dot{\Phi} \tag{7-16}$$

$$[\Phi]_1 \begin{bmatrix} 0 \\ 0 \\ \dot{\Psi} \end{bmatrix} = \begin{bmatrix} 1 & 0 & 0 \\ 0 & \cos\Phi & \sin\Phi \\ 0 & -\sin\Phi & \cos\Phi \end{bmatrix} \begin{bmatrix} 0 \\ 0 \\ \dot{\Psi} \end{bmatrix} = \begin{bmatrix} 0 \\ \sin\Phi \\ \cos\Phi \end{bmatrix} \dot{\Psi} \tag{7-17}$$

$$[\Phi]_1 [\Psi]_3 \begin{bmatrix} 0 \\ \dot{\Theta} \\ 0 \end{bmatrix} = \begin{bmatrix} 1 & 0 & 0 \\ 0 & \cos\Phi & \sin\Phi \\ 0 & -\sin\Phi & \cos\Phi \end{bmatrix} \begin{bmatrix} \cos\Psi & \sin\Psi & 0 \\ -\sin\Psi & \cos\Psi & 0 \\ 0 & 0 & 1 \end{bmatrix} \begin{bmatrix} 0 \\ \dot{\Theta} \\ 0 \end{bmatrix} \tag{7-18}$$

It should be noted that $\dot{\Phi}$, $\dot{\Psi}$, and $\dot{\Theta}$ are not orthogonal vectors.

$$= \begin{bmatrix} \cos\Psi & \sin\Psi & 0 \\ -\sin\Psi\cos\Phi & \cos\Psi\cos\Phi & \sin\Phi \\ \sin\Psi\sin\Phi & -\cos\Psi\sin\Phi & \cos\Phi \end{bmatrix} \begin{bmatrix} 0 \\ \dot{\Theta} \\ 0 \end{bmatrix} \tag{7-19}$$

$$= \begin{bmatrix} \sin\Psi \\ \cos\Psi\cos\Phi \\ -\cos\Psi\sin\Phi \end{bmatrix} \dot{\Theta} \tag{7-20}$$

Equations (7-16), (7-17), and (7-20) are combined to form the Euler rate-to-Body rate transformation

$$\begin{bmatrix} \omega_X^B \\ \omega_Y^B \\ \omega_Z^B \end{bmatrix} = \begin{bmatrix} 1 & \sin\Psi & 0 \\ 0 & \cos\Psi\cos\Phi & \sin\Phi \\ 0 & -\cos\Psi\sin\Phi & \cos\Phi \end{bmatrix} \begin{bmatrix} \dot{\Phi} \\ \dot{\Theta} \\ \dot{\Psi} \end{bmatrix} \tag{7-21}$$

7.3.3 Body Rates to Euler Rates

The Body rate-to-Euler rate transformation can be determined by writing the inverse relation to equation (7-21) as follows:

$$\begin{bmatrix} \dot{\Phi} \\ \dot{\Theta} \\ \dot{\Psi} \end{bmatrix} = \frac{1}{\cos\Psi} \begin{bmatrix} \cos\Psi & -\sin\Psi\cos\Phi & \sin\Psi\sin\Phi \\ 0 & \cos\Phi & -\sin\Phi \\ 0 & \cos\Psi\sin\Phi & \cos\Psi\cos\Phi \end{bmatrix} \begin{bmatrix} \omega_X^B \\ \omega_Y^B \\ \omega_Z^B \end{bmatrix} \tag{7-22}$$

Euler angles are determined by integrating equation (7-22) as follows:

$$\phi = \int_0^t \dot{\phi}\, dt + \phi(0)$$

$$\theta = \int_0^t \dot{\theta}\, dt + \theta(0) \qquad (7\text{-}23)$$

$$\psi = \int_0^t \dot{\psi}\, dt + \psi(0)$$

7.4 GLOSSARY OF TERMS

SYMBOL	DEFINITION	UNIT
$\bar{a}$	Any arbitrary vector (See equation (7-14))	arbitrary
A^{BP}	Coordinate transformation from Plumbline-to-Body Frame	unitless
A^{PB}	Coordinate transformation from Body-to-Plumbline Frame	unitless
$\bar{H}$	Vehicle's vector angular momentum	$\frac{kg\text{-}m^2}{sec}$
$\dot{\bar{H}}$	Time rate of change of $\bar{H}$	$\frac{kg\text{-}m^2}{sec^2}$
I	Vehicle's generalized inertia tensor about its CG, referenced to Body axes	$kg\text{-}m^2$
$\dot{I}$	Time rate of change of I	$\frac{kg\text{-}m^2}{sec}$
$\bar{M}$	Any disturbance moment acting on the vehicle CG	$\frac{kg\text{-}m^2}{sec^2}$
$\bar{M}_A$	Total aerodynamic moment acting on the vehicle CG	$\frac{kg\text{-}m^2}{sec^2}$

SYMBOL	DEFINITION	UNIT
$\bar{M}_E$	Total moment due to the engines' inertial force acting on the vehicle CG	$\frac{kg\text{-}m^2}{sec^2}$
$\bar{M}_S$	Total slosh moment acting on the vehicle CG	$\frac{kg\text{-}m^2}{sec^2}$
$\bar{M}_T$	Total engine thrust moment acting on the vehicle CG	$\frac{kg\text{-}m^2}{sec^2}$
θ	Euler rotation about the Y^P axis	rad
$\dot{\theta}$	Time rate of change of θ	$\frac{rad}{sec}$
ϕ	Euler rotation about the X^B axis	rad
$\dot{\phi}$	Time rate of change of ϕ	$\frac{rad}{sec}$
ψ	Euler rotation about the Z' axis	rad
$\dot{\psi}$	Time rate of change of ψ	$\frac{rad}{sec}$
$\bar{\omega}$	Vehicle's vector angular velocity	$\frac{rad}{sec}$
$\dot{\bar{\omega}}$	Vehicle's vector angular acceleration	$\frac{rad}{sec^2}$
$\tilde{\omega}$	Skew-symmetric ω matrix: equivalent to the vector cross product operation "$\bar{\omega}$ x ( )"	$\frac{rad}{sec}$

Section VIII
AERODYNAMICS

8.1 INTRODUCTION

Accurate determination of a boost vehicle response to winds and other disturbances during atmospheric flight requires an aerodynamics method which includes local angle-of-attack effects. Accurate response determination including loads ensures the full utilization of the structural and control capability of the boost vehicle. Finally, full use of vehicle capability results in greater payloads and operational flexibility.

This section presents the development of equations needed to calculate the aerodynamic forces and moments acting on a rigid (Aero Option 1) and a flexible (Aero Option 2) vehicle during boost flight through the earth's atmosphere.

8.2 RIGID BODY VEHICLE (AERO OPTION 1)

8.2.1 Velocity Vector

8.2.1.1 Wind Velocity Vector, $\bar{V}_w^P$. Environmental winds acting on the vehicle are represented by a wind velocity vector acting at the vehicle CG. Components of the wind velocity vector resolved in Plumbline coordinates can be determined by

$$\bar{V}_W^P = \begin{bmatrix} V_{WX}^P \\ V_{WY}^P \\ V_{WZ}^P \end{bmatrix} = \begin{bmatrix} 0 \\ -V_W \sin (A_w - A_{ZL}) \\ -V_W \cos (A_w - A_{ZL}) \end{bmatrix} \qquad (8\text{-}1)$$

where

V_W = f(h) Magnitude of wind velocity at vehicle CG. Table lookup.

A_W = f(h) Wind direction angle measured from north at vehicle CG. Table lookup.

h = Altitude of vehicle CG above surface of the earth

Observe in equation (8-1) that the environmental winds are given only Y and Z velocity components in the Plumbline coordinate system. This is equivalent to specifying that winds are parallel to the earth's surface at the launch site.

8.2.1.2 Relative Velocity Vector at Vehicle CG, $\bar{V}_R^B$. The relative velocity vector (See Figure 8-1) at the Vehicle CG, resolved in Body coordinates, is

$$\bar{V}_R^B = [A^{PB}]^T (\bar{V}_E^P - \bar{V}_W^P) \tag{8-2}$$

where

$[A^{PB}]^T$ = Matrix transpose of the Plumbline-to-Body coordinate transformation

$\bar{V}_E^P$ = Vehicle velocity vector at the vehicle CG relative to the Earth's surface, resolved in Plumbline (P-frame) coordinates

$\bar{V}_W^P$ = Wind velocity vector resolved in Plumbline coordinates (from equation (8-1)

8.2.2. Calculation of Total α and σ

Reference to equation (8-2) and Figure 8-1 permits one to formulate total α (angle-of-attack at vehicle CG) and σ (angle measured from the vehicle yaw plane to a plane that contains the relative velocity vector and the vehicle X^B-axis) in terms of Body-resolved velocity components as follows:

$$\alpha = \cos^{-1}\left(\frac{V_{RX}^B}{|\bar{V}_R^B|}\right) \tag{8-3}$$

$$\sigma = \tan^{-1}\left(\frac{V_{RZ}^B}{V_{RY}^B}\right) \tag{8-4}$$

If aircraft related angles of attack (α') and sideslip (β') are desired, then

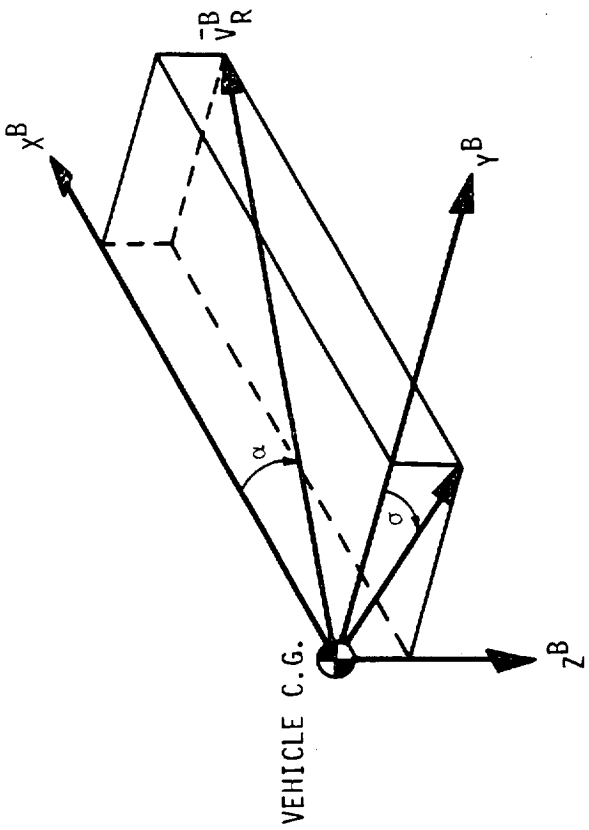

$$\alpha = \cos^{-1}\left(V_{RX}^B / |\bar{V}_R^B|\right)$$

$$\sigma = \tan^{-1}\left(V_{RZ}^B / V_{RY}^B\right)$$

Figure 8-1. ORIENTATION OF THE RELATIVE VELOCITY VECTOR WITH BODY COORDINATE AXES

$$\alpha' = \tan^{-1}\left(\frac{V^B_{RZ}}{V^B_{RX}}\right) \tag{8-5}$$

$$\beta' = \tan^{-1}\left(\frac{V^B_{RY}\cos\alpha'}{V^B_{RX}}\right) \tag{8-6}$$

8.2.3 Mach Number and Dynamic Pressure

Mach number can be determined by

$$M = \frac{|\bar{V}^B_R|}{a} \tag{8-7}$$

where a, the speed of sound at altitude h, can be determined by table lookup as follows:

$$a = f(h) \tag{8-8}$$

Dynamic pressure can be determined by

$$q = \frac{1}{2}\rho\,|\bar{V}^B_R|^2 \tag{8-9}$$

where ρ, the atmospheric density at altitude h, can be determined by table lookup as follows:

$$\rho = f(h) \tag{8-10}$$

8.2.4 Total Aero Coefficients

Changes (called ΔC's) in aero force and moment coefficients are assumed to be linear with respect to control surface deflections (called δ's). These changes are formulated as a truncated form of Taylor's formula for a function of three variables, δ_a, δ_e, and δ_r:

$$\Delta C = f(\delta_a, \delta_e, \delta_r) \tag{8-11}$$

where

δ_a = aileron deflection

δ_e = elevator deflection

δ_r = rudder deflection.

The general form of aero force and moment coefficient equations for a rigid body vehicle (Aero Option 1) is shown in equation (8-12).

$$C_\gamma = C_\gamma^o + \overbrace{\frac{\partial C_\gamma}{\partial \delta_a}\delta_a + \frac{\partial C_\gamma}{\partial \delta_e}\delta_e + \frac{\partial C_\gamma}{\partial \delta_r}\delta_r}^{\Delta C_\gamma} \qquad (8\text{-}12)$$

where

γ = X, Y, Z, ℓ, m, n

a = aileron

e = elevator

r = rudder.

Replacing the partial derivatives in equation (8-12) by standard aero derivative notation results in the somewhat simpler form shown in equation (8-13)

$$C_\gamma = C_\gamma^o + \overbrace{C_{\gamma_{\delta_a}}\delta_a + C_{\gamma_{\delta_e}}\delta_e + C_{\gamma_{\delta_r}}\delta_r}^{\Delta C_\gamma} \qquad (8\text{-}13)$$

where the indices γ, a, e, and r were defined above.

8.2.4.1 Control Surfaces in Null or Reference Position. Aero force and moment coefficients at the vehicle aero static reference point defined by position vector $\bar{R}_A^B$ (see Figure 8-2) for the case of all control surfaces in the null (δ's=0) or reference (δ's = δ^o's) position are represented by the first term of equation (8-13). This term would be determined from a 3-D table lookup as follows:

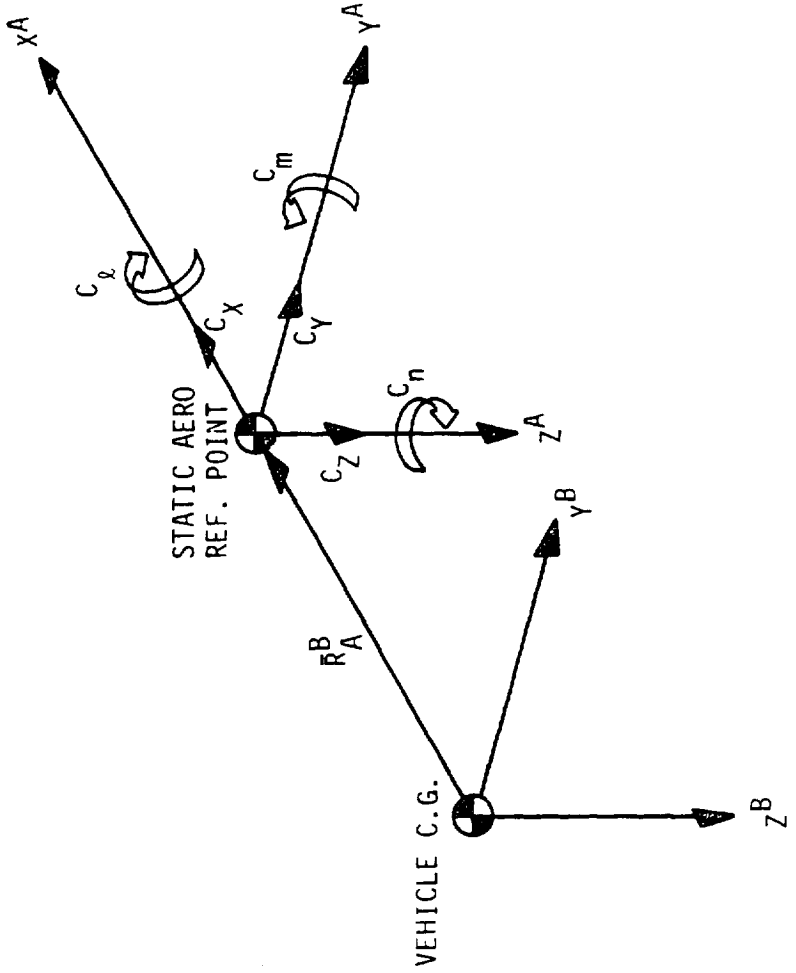

NOTE: X^A, Y^A, Z^A AXES PARALLEL TO X^B, Y^B, Z^B. X^A AND X^B AXES ARE NOT REQUIRED TO BE COLINEAR.

Figure 8-2. AERODYNAMIC COORDINATE RELATIONSHIP FOR TOTAL AERODYNAMIC COEFFICIENTS

$$C_Y = C_Y^O = f(M, \alpha, \upsilon) \tag{8-14}$$

or, in the case where angles-of-attack and sideslip are used,

$$C_Y = C_Y^O = f(m, \alpha', \beta') \tag{8-15}$$

A typical 3-D lookup table for $C_{Y=Z}$ is shown in Figure 8-3.

8.2.4.2 Control Surfaces Deflected. Aero force and moment coeficients, equation (8-14), will change as control surfaces (aileron, elevator, rudder) are deflected. It is assumed that these changes are linear with respect to control surface deflections (called δ's), and that these changes can be formulated as a truncated form of Taylor's formula for a function of three variables δ_a, δ_e, and δ_r. These changes, called ΔC's, represented by the latter part of equation (8-13), are

$$\Delta C_Y = C_{Y_{\delta_a}} \delta_a + C_{Y_{\delta_e}} \delta_e + C_{Y_{\delta_r}} \delta_r \tag{8-16}$$

The approach that would be used for updating total aero coefficients, using equations (8-14) and (8-16), is shown in Figure 8-4.

8.2.5 Total Aero Forces and Moments

The total aero vector force and moment can be determined by

$$\bar{F}_A^B = \begin{bmatrix} F_{AX}^B \\ F_{AY}^B \\ F_{AZ}^B \end{bmatrix} = q\,S \begin{bmatrix} C_X \\ C_Y \\ C_Z \end{bmatrix} \tag{8-17}$$

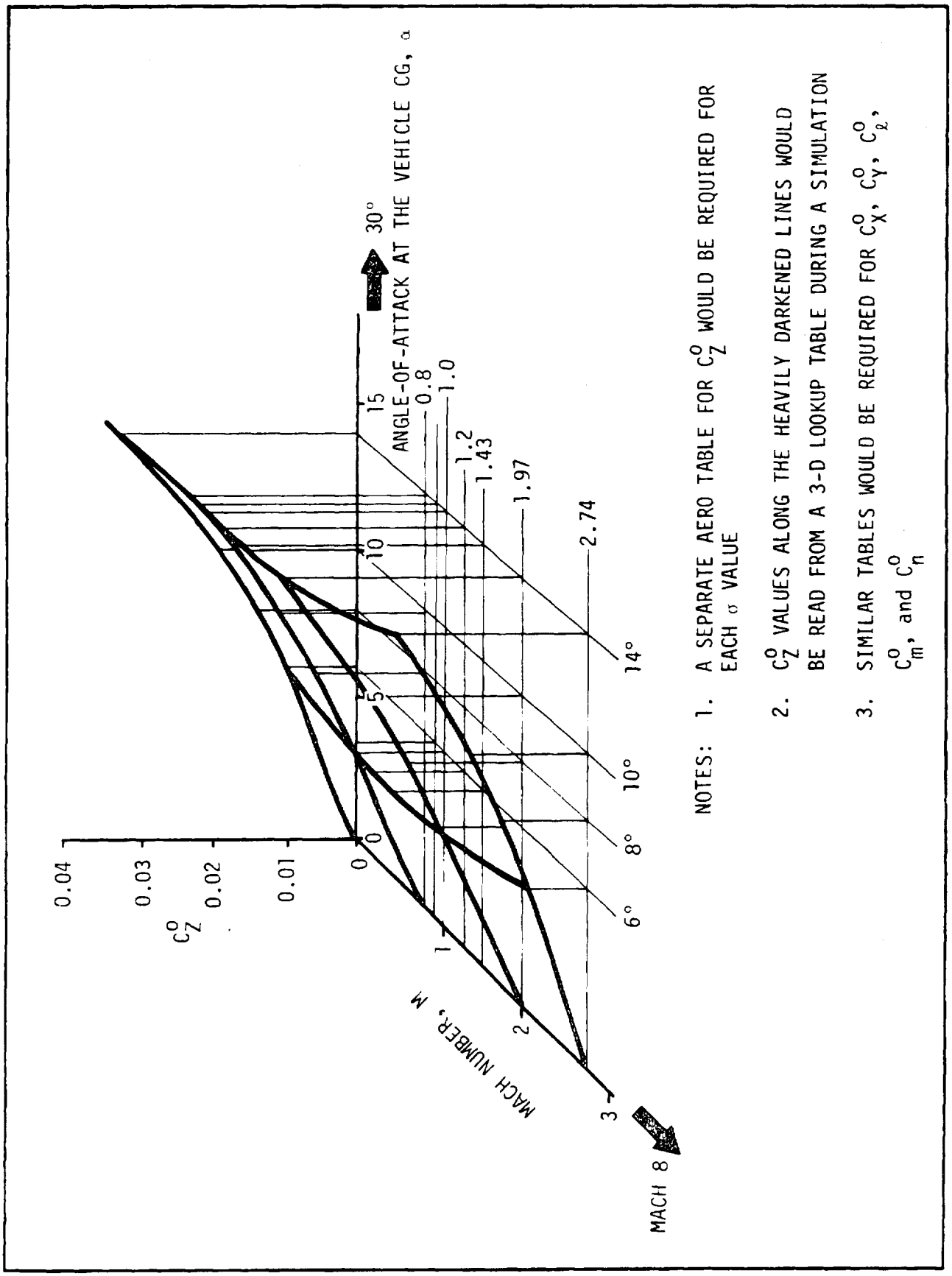

Figure 8-3. TYPICAL AERO FORCE COEFFICIENT 3-D TABLE THAT WOULD BE USED IN THE RIGID BODY AERO OPTION

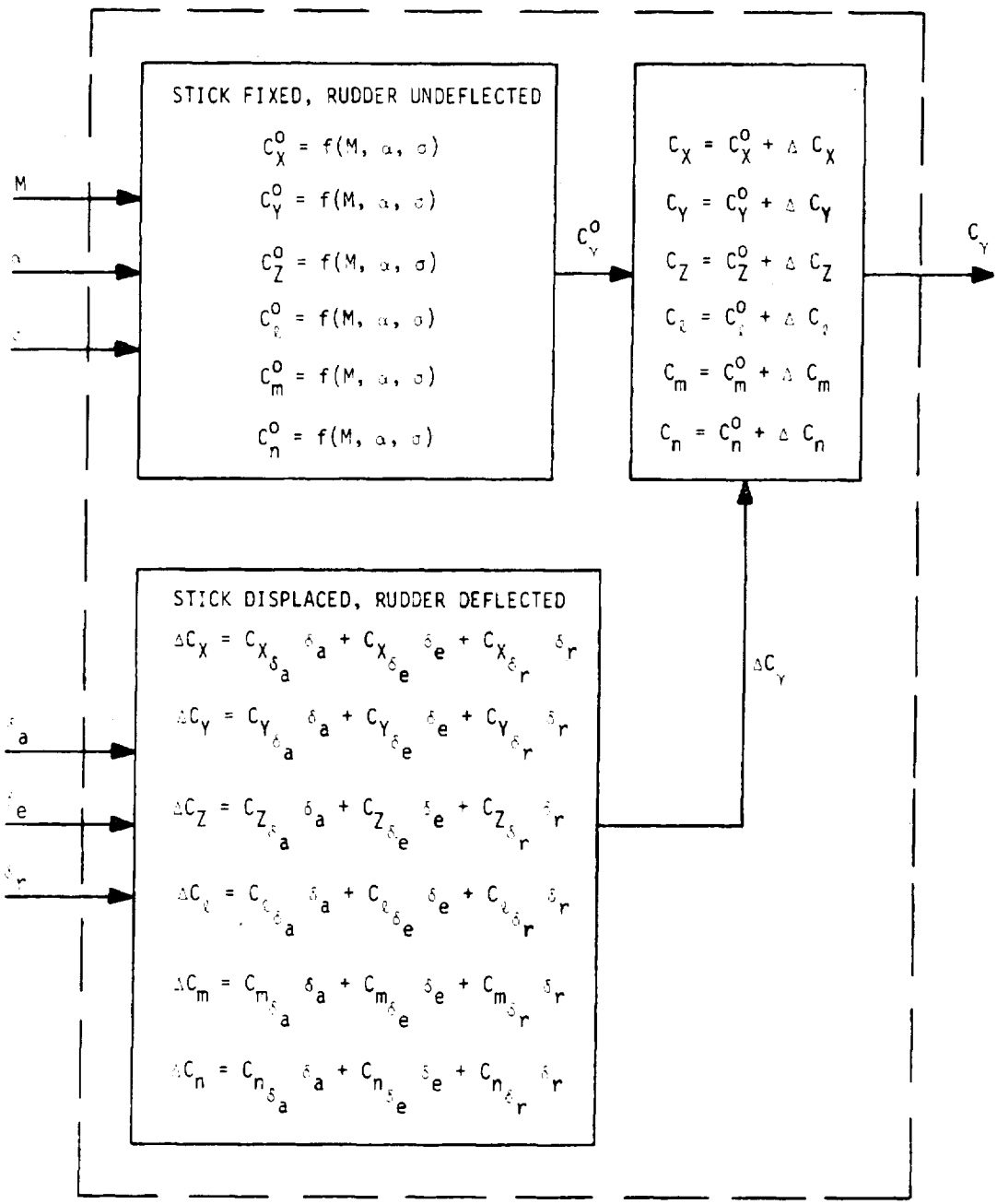

Figure 8-4. APPROACH USED FOR UPDATING TOTAL AERO COEFFICIENTS USED IN THE RIGID BODY AERO OPTION

$$\bar{M}_A^B = \begin{bmatrix} M_{AX}^B \\ M_{AY}^B \\ M_{AZ}^B \end{bmatrix} = q\,\bar{C}\,S \begin{bmatrix} C_\ell \\ C_m \\ C_n \end{bmatrix} + \begin{bmatrix} R_{AY}^B F_{AZ}^B - R_{AZ}^B F_{AY}^B \\ R_{AZ}^B F_{AX}^B - R_{AX}^B F_{AZ}^B \\ R_{AX}^B F_{AY}^B - R_{AY}^B F_{AX}^B \end{bmatrix} \qquad (8\text{-}18)$$

where

q = Dynamic pressure at vehicle CG

S = Reference area

$\bar{C}$ = Reference length

$$\bar{R}_A^B = \begin{bmatrix} R_{AX}^B \\ R_{AY}^B \\ R_{AZ}^B \end{bmatrix}$$ Components of the position vector of the static aero reference point, resolved in Body coordinates

The method for calculating aero forces and moments in the rigid body aero option is shown in Figure 8-5.

8.3 FLEXIBLE BODY VEHICLE (AERO OPTION 2)

8.3.1 Velocity Vectors

8.3.1.1 Wind Velocity Vector, $\bar{V}_{W_{\beta j}}^P$. Environmental winds acting on the vehicle are represented by wind velocity vectors acting at various aero stations on the fuselage, wing, horizontal stabilizer, and vertical stabilizer. Components of these wind velocity vectors, resolved in Plumbline coordinates, are given in equation (8-19).

$$\bar{V}_{W_{\beta j}}^P = \begin{bmatrix} V_{W_\beta X_j}^P \\ V_{W_\beta Y_j}^P \\ V_{W_\beta Z_j}^P \end{bmatrix} = \begin{bmatrix} 0 \\ -V_{W_{\beta j}} \sin\left(A_{W_{\beta j}} - A_{ZL}\right) \\ -V_{W_{\beta j}} \cos\left(A_{W_{\beta j}} - A_{ZL}\right) \end{bmatrix} \qquad (8\text{-}19)$$

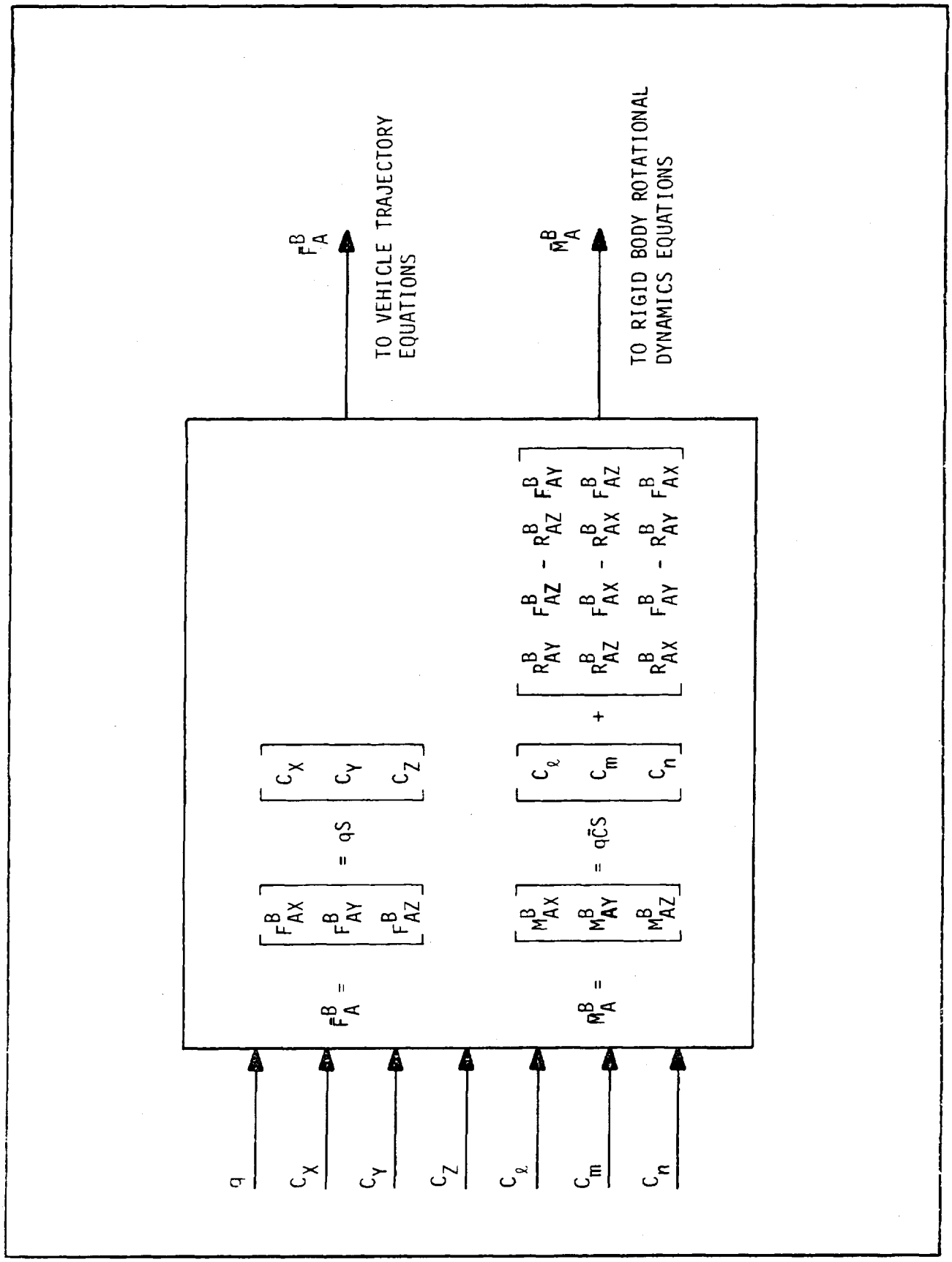

Figure 8-5. AERO FORCES AND MOMENTS CALCULATED IN THE RIGID BODY AERO OPTION

where

$V_{W_{\beta j}} = f(h_{\beta j})$ Magnitude of wind velocity at the j^{th} aero station of the β - body

$A_{W_{\beta j}} = f(h_{\beta j})$ Wind direction angle measured from north at j^{th} aero station of the β-body.

and $h_{\beta j}$, the altitude of j^{th} aero station of the β-body above the surface of the earth, can be determined by

$$h_{\beta j} = h + R^B_{A_\beta X_j} \cos\theta + R^B_{A_\beta Z_j} \sin\theta \qquad (8\text{-}20)$$

where

h = Altitude of vehicle CG above surface of the Earth

$R^B_{A_\beta X_j}$, $R^B_{A_\beta Z_j}$ = X and Z components of the vector $\bar{R}^B_{A_{\beta j}}$ (See Figure 8-6) where $\beta = f, w, h, j$.

θ = Pitch Euler angle.

8.3.1.2 Local Relative Velocity Vector, $\bar{V}^B_{A_{\beta j}}$. Components of the local relative velocity vector at various aero stations, resolved in Body coordinates, are determined by equation (8-21).

$$\bar{V}^B_{A_{\beta j}} = \begin{bmatrix} V^B_{A_\beta X_j} \\ V^B_{A_\beta Y_j} \\ V^B_{A_\beta Z_j} \end{bmatrix} = [A^{PB}]^T \begin{bmatrix} V^P_{EX} - V^P_{W_\beta X_j} \\ V^P_{EY} - V^P_{W_\beta Y_j} \\ V^P_{EZ} - V^P_{W_\beta Z_j} \end{bmatrix} \qquad (8\text{-}21)$$

where

$[A^{PB}]^T$ = Matrix transpose of the Plumbline-to-Body coordinate transformation

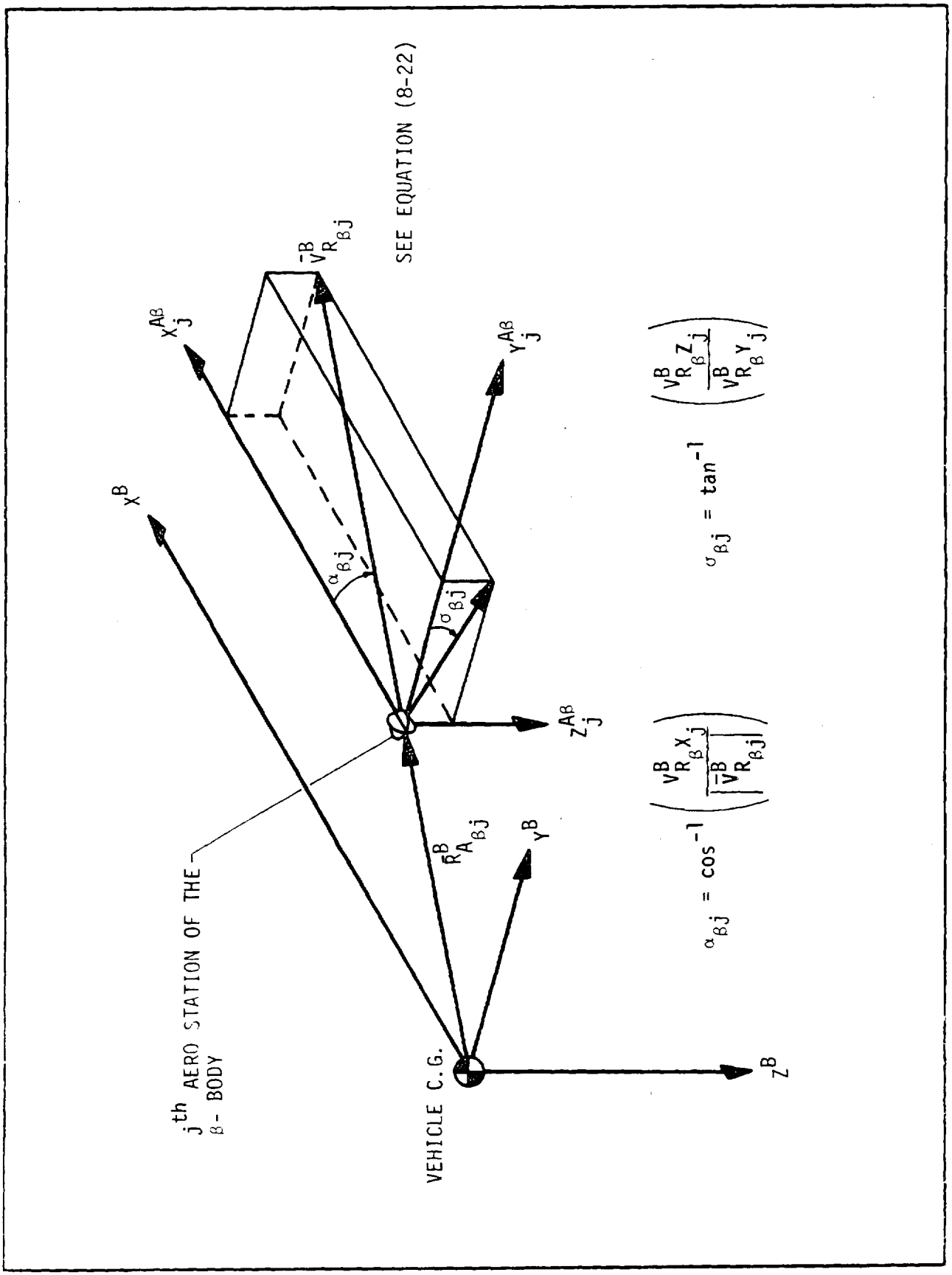

Figure 8-6. TYPICAL AERO STATION SHOWING ORIENTATION OF THE RELATIVE VELOCITY VECTOR WITH BODY COORDINATE AXES

$$\bar{V}_E^P = \begin{bmatrix} V_{EX}^P \\ V_{EY}^P \\ V_{EZ}^P \end{bmatrix}$$

Components of the vehicle velocity vector at vehicle CG relative to the earth's surface, resolved in Plumbline coordinates.

8.3.1.3 Local Relative Vehicle Velocity Vector, $\bar{V}^B_{R_{\beta j}}$, With Bending. Components of the local relative vehicle velocity vector with bending at various aero stations, resolved into Body coordinates, are determined by equation (8-22).

$$\bar{V}^B_{R_{\beta j}} = \begin{bmatrix} V^B_{R_\beta X_j} \\ V^B_{R_\beta Y_j} \\ \\ \\ V^B_{R_\beta Z_j} \end{bmatrix} = \begin{bmatrix} V^B_{A_\beta X_j} + \omega^B_Y R_{A_\beta Z_j} - \omega^B_Z R_{A_\beta Y_j} \\ V^B_{A_\beta Y_j} + \omega^B_Z R_{A_\beta X_j} - \omega^B_X R_{A_\beta Z_j} + \sum_{i=1}^{n} \phi_{iY}(\bar{R}_{A_{\beta j}})\dot{\eta}_i \\ - V^B_{RX} \sum_{i=1}^{n} \phi'_{iZ}(\bar{R}_{A_{\beta j}})\eta_i \\ V^B_{A_\beta Z_j} + \omega^B_X R_{A_\beta Y_j} - \omega^B_Y R_{A_\beta X_j} + \sum_{i=1}^{n} \phi_{iZ}(\bar{R}_{A_{\beta j}})\dot{\eta}_i \\ + V^B_{RX} \sum_{i=1}^{n} \phi'_{iY}(R_{A_{3j}})\eta_i \end{bmatrix} \quad (8\text{-}22)$$

where

ω^B_X, ω^B_Y, ω^B_Z = X,Y,Z components of the vehicle angular rate

$R_{A_\beta X_j}$, $R_{A_\beta Y_j}$, $R_{A_\beta Z_j}$ = X,Y,Z components of position vector $\bar{R}^B_{A_{\beta j}}$

$\sum_{i=1}^{n} \phi_{iY}(\bar{R}_{A_{\beta j}})\dot{\eta}_i$ = velocity in the positive Y^B - direction due to bending

$\sum_{i=1}^{n} \phi_{iZ}(\bar{R}_{A_{\beta j}})\,\dot{r}_i$ = velocity in the positive Z^B - direction due to bending

$\sum_{i=1}^{n} \phi'_{iY}(\bar{R}_{A_{\beta j}})\,r_i$ = rotation about the positive Y^B - axis due to bending

$\sum_{i=1}^{n} \phi'_{iZ}(\bar{R}_{A_{\beta j}})\,r_i$ = rotation about the positive Z^B - axis due to bending.

8.3.2 Calculation of Local α and σ

Reference to equation (8-22) and Figure 8-6 permits one to formulate the local α and σ at the j^{th} aero station of the β-body as follows:

$$\alpha_{\beta j} = \cos^{-1}\left(\frac{V^B_{R_\beta X_j}}{|\bar{V}^B_{R_{\beta j}}|}\right) \tag{8-23}$$

$$\sigma_{\beta j} = \tan^{-1}\left(\frac{V^B_{R_\beta Z_j}}{V^B_{R_\beta Y_j}}\right) \tag{8-24}$$

If aircraft related local angles of attack ($\alpha'_{\beta j}$) and sideslip ($\beta'_{\beta j}$) are desired, then

$$\alpha'_{\beta j} = \tan^{-1}\left(\frac{V^B_{R_\beta Z_j}}{V^B_{R_\beta X_j}}\right) \tag{8-25}$$

$$\beta'_{\beta j} = \tan^{-1}\left(\frac{V^B_{R_\beta Y_j}\cos\alpha'_{\beta j}}{V^B_{R_\beta X_j}}\right) \tag{8-26}$$

8.3.3 Mach Number and Dynamic Pressure

Mach number can be determined by

$$M_{\beta j} = \frac{\left| \bar{V}^{B}_{R_{\beta j}} \right|}{a} \tag{8-27}$$

where a, the speed of sound at altitude h, can be determined by table lookup described earlier in the rigid body option (see equation (8-8)).

Dynamic pressure can be determined by

$$q_{\beta j} = \frac{1}{2} \rho \left| \bar{V}^{B}_{R_{\beta j}} \right|^{2} \tag{8-28}$$

where ρ, the atmospheric density at altitude h, can be determined by table lookup described earlier in the rigid body option (see equation (8-10)).

8.3.4 Distributed Aero Coefficients

The general form of aero force and moment coefficient equation for a flexible body (Aero Option 2) is shown in equation (8-29).

$$C_{\beta\gamma_j} = C^{o}_{\beta\gamma_j} + C_{\beta\gamma_{j_{\delta_a}}} \delta_a + C_{\beta\gamma_{j_{\delta_e}}} \delta_e + C_{\beta\gamma_{j_{\delta_r}}} \delta_r \tag{8-29}$$

where

γ = X,Y,Z,ℓ,m,n

β = f,w,h,v

f = L (left), R (right) fuselage

w = L (left), R (right) wing

h = L (left), R (right) horizontal stabilizer

v = L (left), R (right) vertical stabilizer

a,e,r = aileron, elevator, rudder

j = 1, N_{A_β}

N_{A_β} = total number of aero stations selected on the β-body

An example catamaran-type booster configuration showing typical aero stations is shown in Figure 8-7 to aid the reader in understanding the indicial notation of equation (8-29).

8.3.4.1 Control Surfaces in Null or Reference Position. Aero force and moment coefficients at the j^{th} aero station of the β-body (see Figure 8-8) are represented by the first term of equation (8-29). This term would be determined from a 3-D table lookup as follows

$$C_{\beta\gamma_j} = C^{o}_{\beta\gamma_j} = f(M_{\beta j}, \alpha_{\beta j}, \sigma_{\beta j}) \tag{8-30}$$

or, in the case where angles-of-attack ($\alpha'_{\beta j}$) and sideslip ($\beta'_{\beta j}$) are used

$$C_{\beta\gamma_j} = C^{o}_{\beta\gamma_j} = f(M_{\beta j}, \alpha'_{\beta j}, \beta'_{\beta j}) \tag{8-31}$$

A typical 3-D lookup table for $C_{\beta Z_j}$ is shown in Figure 8-9.

8.3.4.2 Control Surfaces Deflected. Aero force and moment coefficients, equation (8-30), will change as control surfaces (aileron, elevator, rudder) are deflected. It is assumed that these changes are linear with respect to control surface deflections called δ's, and that these changes can be formulated as a truncated form of Taylor's formula for a function of three varables, δ_a, δ_e, and δ_r. These changes, called ΔC's represented by the latter part of equation (8-29), are

$$\Delta C_{\beta\gamma_j} = C_{\beta\gamma_{j_{\delta_a}}} \delta_a + C_{\beta\gamma_{j_{\delta_e}}} \delta_e + C_{\beta\gamma_{j_{\delta_r}}} \delta_r \tag{8-32}$$

The approach that would be used for updating distributed aero coefficients using equations (8-30) and (8-32) is shown in Figure 8-10.

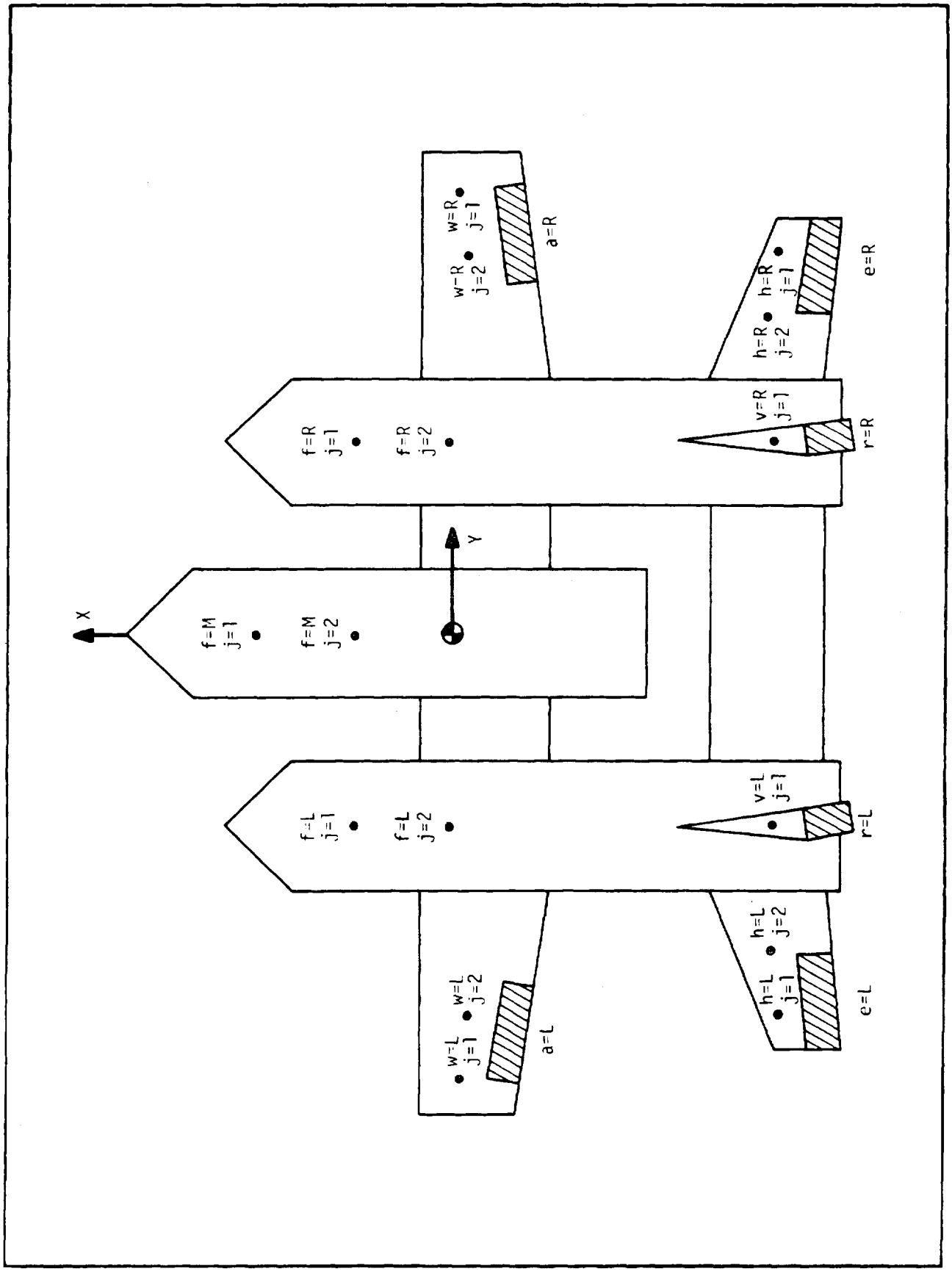

Figure 8-7. EXAMPLE CATAMARAN BOOSTER CONFIGURATION SHOWING TYPICAL AERO STATIONS

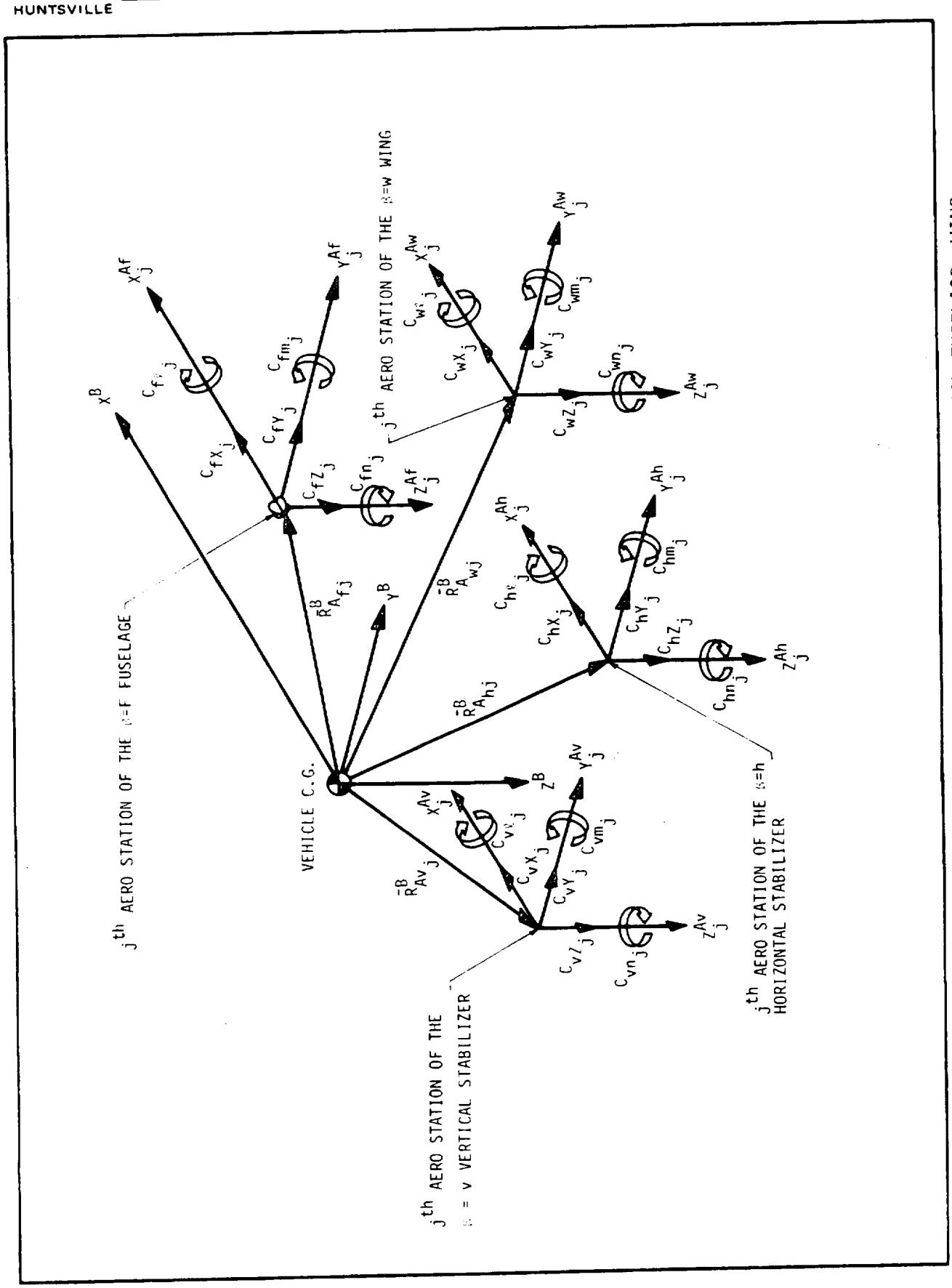

Figure 8-8. DISTRIBUTED AERO COORDINATE SYSTEM SHOWING TYPICAL FUSELAGE, WING, HORIZONTAL STABILIZER, AND VERTICAL STABILIZER AERO STATIONS

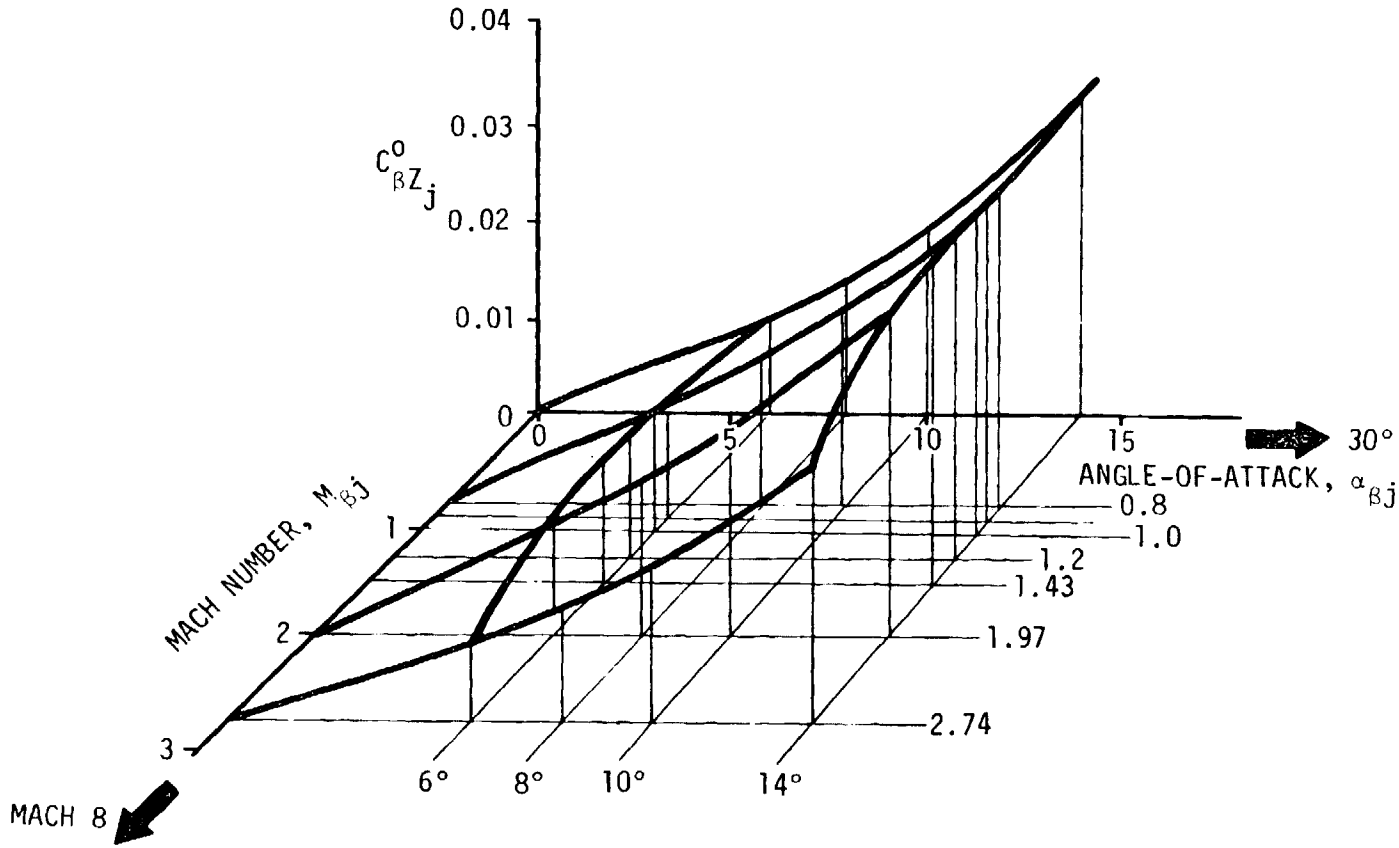

NOTES:

1. COMPARE NOTATION WITH THAT OF THE RIGID BODY AERO OPTION SHOWN IN Figure 8-3.
2. A SEPARATE AERO TABLE FOR $C^{o}_{\beta Z_j}$ WOULD BE REQUIRED FOR EACH $\sigma_{\beta j}$ VALUE.
3. $C_{\beta Z_j}$ VALUES ALONG THE HEAVILY-DARKENED LINES WOULD BE READ FROM A 3-D LOOKUP TABLE DURING A SIMULATION
4. SIMILAR TABLES WOULD BE REQUIRED FOR $C^{o}_{\beta X_j}$, $C^{o}_{\beta Y_j}$, $C^{o}_{\beta \ell_j}$, $C^{o}_{\beta m_j}$, and $C^{o}_{\beta n_j}$

Figure 8-9. TYPICAL AERO FORCE COEFFICIENT 3-D GRAPH THAT WOULD BE USED IN THE FLEXIBLE BODY AERO OPTION

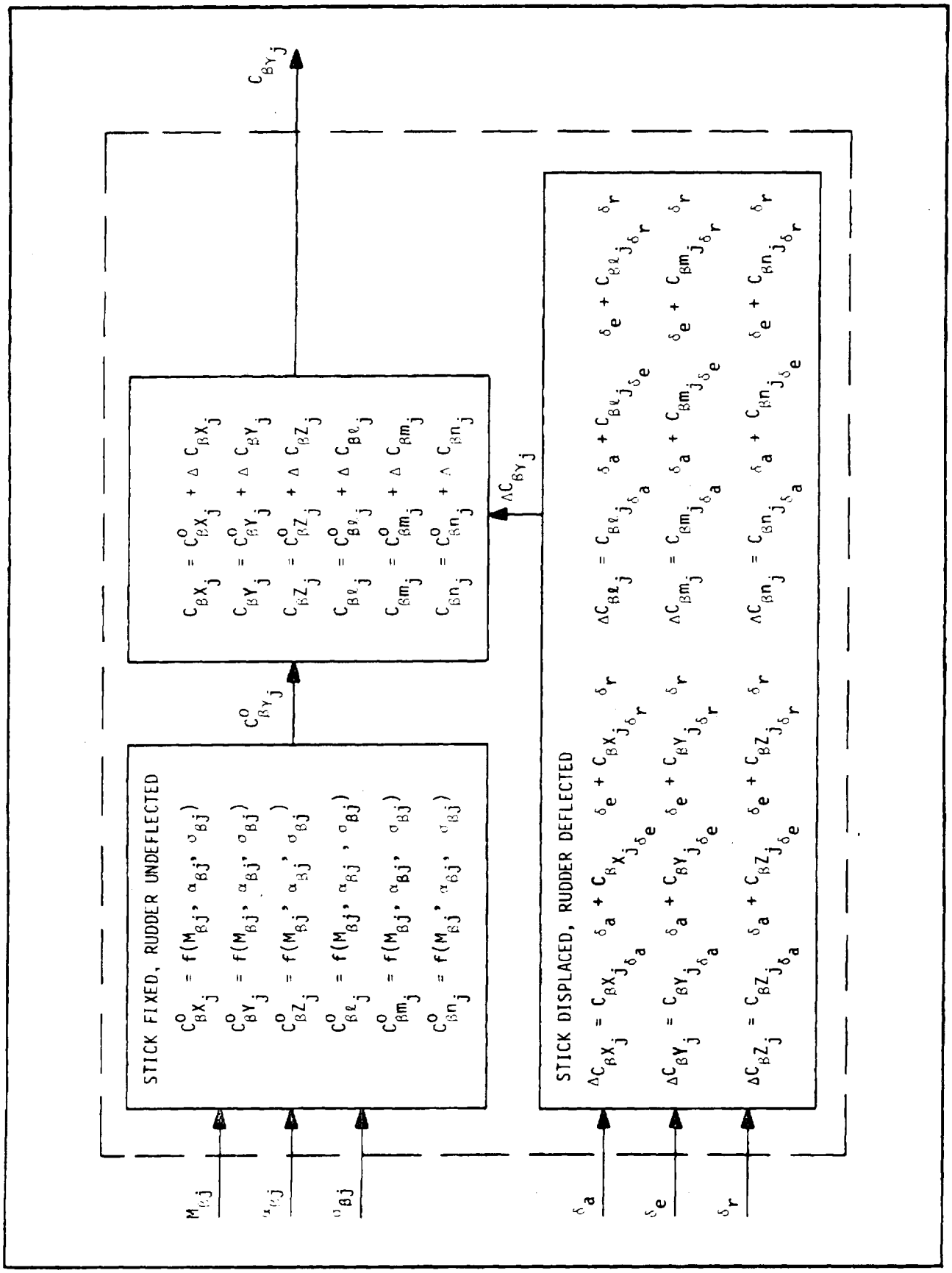

Figure 8-10. APPROACH USED FOR UPDATING DISTRIBUTED AERO COEFFICIENTS IN THE FLEXIBLE BODY AERO OPTION

8.3.5 Distributed Aero Forces and Moments

The method for calculating aero forces and moments in the flexible body aero option is shown in Figure 8-11.

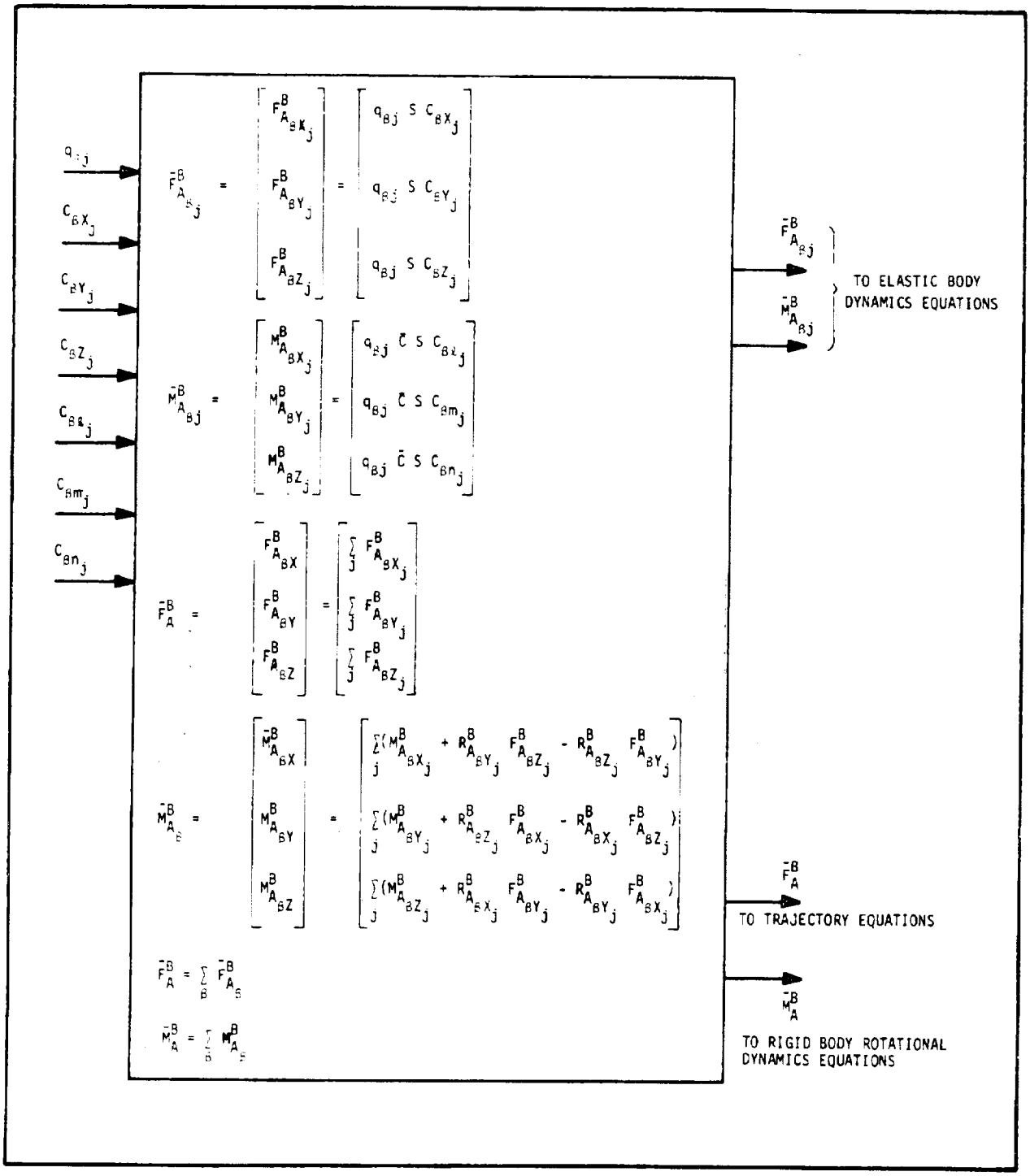

Figure 8-11. AERO FORCES AND MOMENTS CALCULATED IN THE FLEXIBLE BODY AERO OPTION

Section IX
PROPULSION AND ENGINE DYNAMICS

9.1 INTRODUCTION

Advanced aerospace vehicles currently being considered for earth-orbit shuttle tasks fall into two-stage boost, multiple-engined booster/multiple-engined orbiter configuration categories. Further, for any one given vehicle, the multiple engines may or may not be the same type or size. To develop equations suitable for simulating the propulsion and engine dynamics in a flight dynamics simulation of these vehicles during boost-phase flight requires, among other things, a general formulation applicable to various multi-engined configured vehicles.

This section presents the derivation of propulsion and engine dynamics equations. The formulation, which makes extensive use of matrix and vector algebra, includes 3-D elastic body vehicle effects, and is presented in a form suitable for application to digital or hybrid simulations.

9.2 PROPULSION

9.2.1 Engine Thrust Profile

Generally, in vehicle flight dynamics simulations the magnitude of thrust for one or all engines is furnished for input data purposes as a thrust profile determined as a function of time. The magnitude of a basic thrust profile for the j^{th} engine as a function of flight time may be approximated by the following equation

$$F'_{Tj} = F_{TREFj} + (P_{REFj} - P_A)A_{EXj} + K_{1j}\left(\frac{A^B_X}{A_G} - A_{GREF}\right) + K_{2j}\left(\frac{A^B_X}{A_G} - A_{GREF}\right)^2 \qquad (9\text{-}1)$$

where

F_{TREF_j} = Reference thrust of the j^{th} engine

P_{REF_j} = Reference pressure of the j^{th} engine

P_A = Ambient pressure at vehicle CG

A_{EX_j} = Exit area of the j^{th} engine

A_G = Magnitude of gravitational acceleration acting on the vehicle CG

A_X^B = Vehicle x-axis component of the acceleration vector $\bar{A}^B$

A_{GREF} = Reference gravity constant

K_{1j} = Linear adjustment constant of thrust due to acceleration for the j^{th} engine

K_{2j} = Quadratic adjustment constant of thrust due to acceleration for the j^{th} engine.

The magnitude of the thrust of the j^{th} engine can be expressed by a product of the basic thrust profile F'_{T_j} and a function f_j suitably formulated to alter the basic thrust profile to simulate thrust variations and malfunctions. For example, the form

$$\boxed{F_{T_j} = F'_{T_j}\,[f_j(t - t_{CO_j})]} \qquad (9\text{-}2)$$

may be used to simulate a decaying thrust profile as a function of time from the j^{th} engine cutoff time t_{CO_j}. Observe that the subscripted general thrust profile function in equation (9-2) provides a capability to simulate the thrust malfunctions such as single and multiple engines cutoff in a specified sequence.

9.2.2 Body Resolved Thrust Components

The engine thrust force F_{T_j} of the j^{th} engine has body-resolved components F_{TX_j}, F_{TY_j}, and F_{TZ_j} as shown in Figure 9-1.

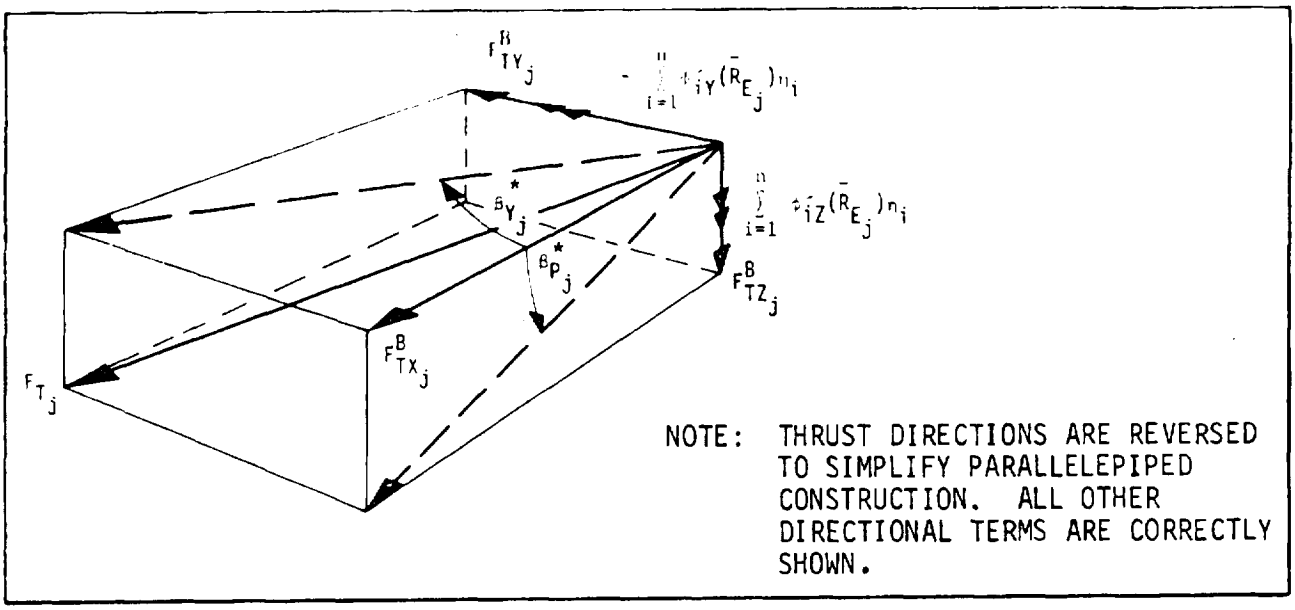

Figure 9-1. ENGINE THRUST F_{T_J} RESOLVED INTO BODY-FRAME COORDINATES

The engine gimbal angles in the pitch (P subscript) and yaw (Y subscript) planes can be expressed in terms of thrust components as follows:

$$\tan\left(\beta^*_{P_j} + \sum_{i=1}^{n} \phi'_{iY}(\bar{R}_{E_j})r_i\right) = \frac{-F^B_{TZ_j}}{F^B_{TX_j}} \tag{9-3}$$

$$\tan\left(\beta^*_{Y_j} + \sum_{i=1}^{n} \phi'_{iZ}(\bar{R}_{E_j})n_i\right) = \frac{F^B_{TY_j}}{F^B_{TX_j}} \tag{9-4}$$

The thrust $F^B_{T_j}$ is

$$F^B_{T_j} = \sqrt{(F^B_{TX_j})^2 + (F^B_{TY_j})^2 + (F^B_{TZ_j})^2} \tag{9-5}$$

Substituting $F^B_{TY_j}$ and $F^B_{TZ_j}$ from equations (9-4) and (9-3) into equation (9-5), and neglecting bending terms, yields the form

$$F^B_{T_j} = \sqrt{(F^B_{TX_j})^2 + (F^B_{TX_j} \tan \beta^*_{Y_j})^2 + (F^B_{TX_j} \tan \beta^*_{P_j})^2} \qquad (9\text{-}6)$$

which reduces to

$$F^B_{T_j} = F^B_{TX_j} \sqrt{1 + \tan^2 \beta^*_{Y_j} + \tan^2 \beta^*_{P_j}} \qquad (9\text{-}7)$$

9.2.2.1 Thrust Forces that Drive Vehicle Translation. Use of equations (9-3), (9-4), and (9-7) and reference to Figure 9-1 are all that is necessary to determine the body-resolved thrust components. These components are as follows:

$$\bar{F}^B_{T_j} = \begin{bmatrix} F^B_{TX_j} \\ F^B_{TY_j} \\ F^B_{TZ_j} \end{bmatrix} = \begin{bmatrix} \dfrac{F^B_{T_j}}{\sqrt{1 + \tan^2 \beta^*_{Y_j} + \tan^2 \beta^*_{P_j}}} \\ F^B_{TX_j} [\tan (\beta^*_{Y_j} + \sum_{i=1}^{n} \phi'_{iZ}(\bar{R}_{E_j}) \eta_i)] \\ -F^B_{TX_j} [\tan (\beta^*_{P_j} + \sum_{i=1}^{n} \phi'_{iY}(\bar{R}_{E_j}) \eta_i)] \end{bmatrix} \qquad (9\text{-}8)$$

where the terms $\sum_{i=1}^{n} \phi'_{iZ} (\bar{R}_{E_j}) \eta_i$ and $\sum_{i=1}^{n} \phi'_{iY} (\bar{R}_{E_j}) \eta_i$ represent the rotation (due to vehicle bending) at the engine attach point in the engine yaw and pitch plane, respectively. Equation (9-8) provides both rigid body or flexible body options since all that is needed is to delete or retain the rotational terms due to bending.

Total vector force produced by N_E engines is determined by summing the individual forces of each engine as follows:

$$\bar{F}_T^B = \sum_{j=1}^{N_E} \bar{F}_{T_j}^B \tag{9-9}$$

9.2.2.2 Thrust Forces that Drive Vehicle Bending. Equation (9-9) is satisfactory for driving the trajectory equations but not the elastic body equations. Engine thrust forces used to drive vehicle bending are essentially lateral thrust forces at the engine attach point in the Y and Z directions; these thrust forces, identified by a subscript (b), are determined as follows:

$$\bar{F}_{T(b)_j}^B = \begin{bmatrix} F_{T(b)X_j}^B \\ F_{T(b)Y_j}^B \\ F_{T(b)Z_j}^B \end{bmatrix} = \begin{bmatrix} 0 \\ F_{TX_j}^B \tan \beta_{Y_j}^* \\ -F_{TX_j}^B \tan \beta_{P_j}^* \end{bmatrix} \tag{9-10}$$

It should be noted that this force drives vehicle bending at the j^{th} engine attach point and that it is not summed over N_E engines prior to going to elastic body vehicle equations.

9.2.2.3 Thrust Vector Moments that Drive Rigid Body Rotation. The vector force $\bar{F}_{T_j}^B$ produces a moment about the vehicle CG as follows:

$$\bar{M}_{T_j}^B = [(\bar{R}_{E_j} - \bar{R}) + \bar{\xi}(\bar{R}_{E_j})] \times \bar{F}_{T_j}^B \tag{9-11}$$

where

$\bar{R}_{E_j} - \bar{R}$ = Position vector of the j^{th} engine attach point with respect to the vehicle CG

$\bar{\xi}(\bar{R}_{E_j})$ = Vector displacement at the j^{th} engine attach point produced by vehicle bending.

Total vector moment produced by N_E engines is determined by summing the individual moments of each engine as follows:

$$\bar{M}_T^B = \sum_{i=1}^{N_E} \bar{M}_{T_j}^B \tag{9-12}$$

9.2.2.4 Thrust Vector Moments That Drive Vehicle Bending. The vector force $\bar{F}_{T(b)_j}^B$ does not produce a moment about the j^{th} engine attach point, therefore

$$\bar{M}_{T(b)_j}^B = 0 \tag{9-13}$$

The vector moment in equation (9-13) is zero because the vector force of equation (9-10), for any arbitrary engine gimbal angle, will be directed through the engine attach point.

9.3 ENGINE DYNAMICS

The equations of motion of the gimbaling engine* are derived using an energy approach and the Lagrange equations. The system under consideration is assumed to be uncoupled, i.e., the equations are derivable for each plane of motion in a separate form; and the Lagrangian of the system is a quadratic of the generalized velocities with no contribution from a potential function associated with local or absolute deformations.

As a matter of convenience only the equations associated with the yaw plane (X-Y plane, see Figure 9-2) will be derived; pitch plane (X-Z plane) equations will be presented intuitively from the yaw-plane derivation.

The deflected configuration of the missile in the yaw plane (X-Y plane) is shown in Figure 9-2. Most of the notation is self-explanatory in this drawing.

---

* *The subscript j used to identify the j^{th} engine has been dropped to simplify derivations.*

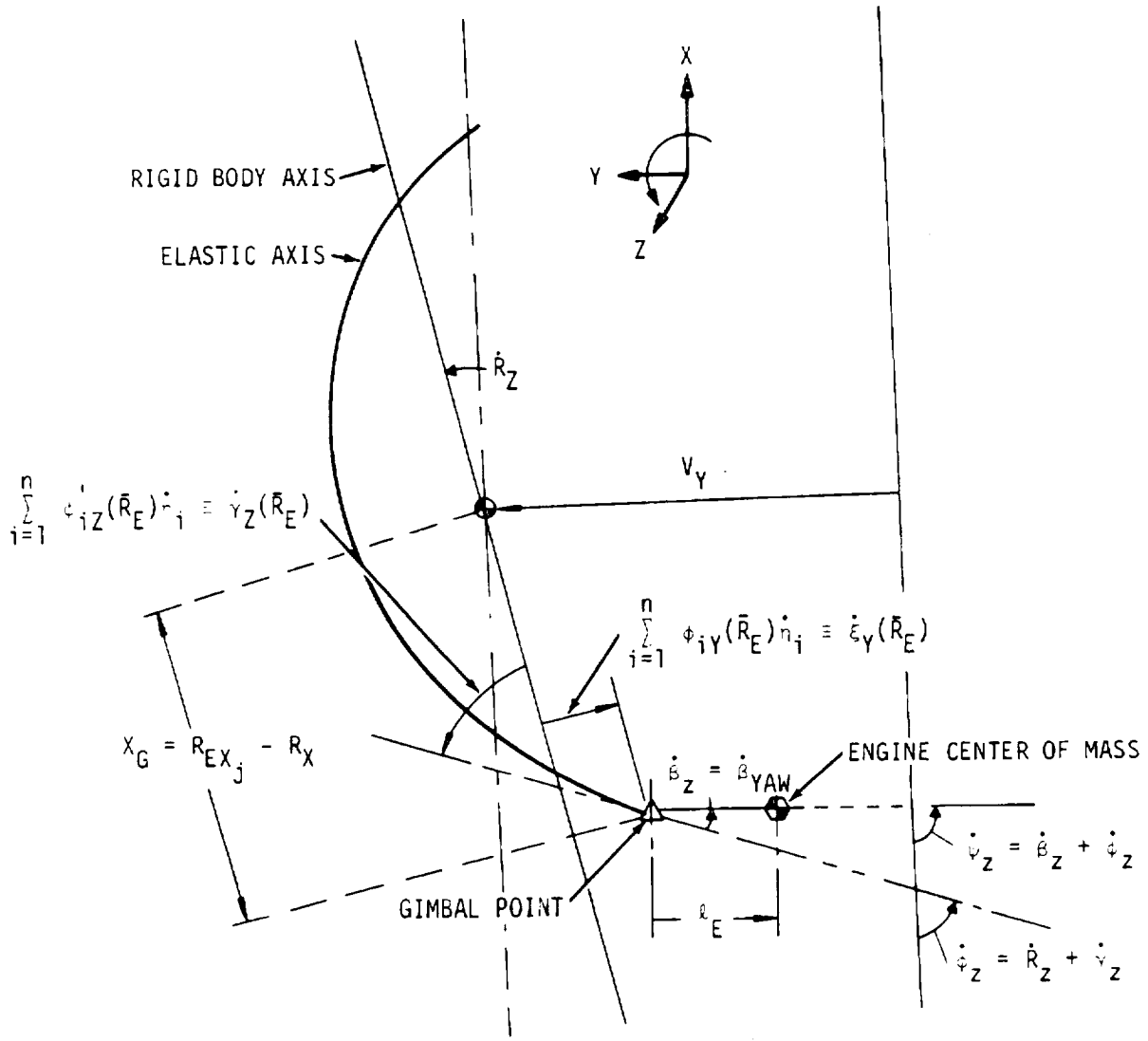

Figure 9-2. YAW PLANE MISSILE RATE OF DEFLECTION CONFIGURATION

The total angular rate at the center of mass of the engine is:

$$\dot{\psi}_z = \dot{\beta}_z + \dot{R}_Z + \dot{\gamma}_Z(\bar{R}_E) \tag{9-14}$$

and the total linear velocity of the center of mass of the engine is equal to:

$$\dot{\alpha} = \dot{\Delta}_G - \ell_E \dot{\psi}_z \tag{9-15}$$

where $\dot{\Delta}_G$, the linear velocity at the gimbal, is determined by

$$\dot{\Delta}_G = V_Y - X_G \dot{R}_Z + \dot{\xi}_Y(\bar{R}_E) \tag{9-16}$$

Substitution of equations (9-14) and (9-16) into (9-15) yields

$$\dot{\alpha} = V_Y - X_G \dot{R}_Z + \xi_Y(\bar{R}_E) - \ell_E \beta_z - \ell_E \dot{R}_Z - \ell_E \dot{\gamma}_Z(\bar{R}_E) \tag{9-17}$$

Observe that the term $-X_G \dot{R}_Z$ is the Y-component ($Z_G \dot{R}_X$ assumed zero) of the vector cross product $\bar{X} \times \dot{\bar{R}}$, and that ℓ_E is positive in the direction shown in Figure 9-2, so that the Y-component of $\bar{\ell} \times \dot{\bar{\psi}}$ is positive in these equations.

The total kinetic energy of the gimbaling engine is then

$$T_E = \frac{1}{2} m_E [V_Y - X_G \dot{R}_Z + \dot{\xi}_Y(\bar{R}_E) - \ell_E \dot{\beta}_z - \ell_E \dot{R}_Z - \ell_E \dot{\gamma}_Z(\bar{R}_E)]^2$$

$$+ \frac{1}{2} I_{EZ} [\dot{\beta}_z + \dot{R}_Z + \dot{\gamma}_Z(\bar{R}_E)]^2 \tag{9-18}$$

where m_E is the engine mass, and I_{EZ} is the engine inertia about the Z axis passing through the engine center of mass. For the case of a kinetic-energy Lagrangian, the equations of motion of the system are determined by the modified Lagrange equation:

$$\frac{d}{dt}\left(\frac{\partial T}{\partial \dot{q}_i}\right) = 0 \tag{9-19}$$

where the generalized velocities $q_i = \dot{R}_Z$, V_Y, $\dot{\xi}_Y(\bar{R}_E)$, $\dot{\gamma}_Z(\bar{R}_E)$, $\dot{\beta}_z$ are associated with rigid body rotation, rigid body translation, bending translation, rotation due to bending, and gimbaling engine, respectively.

9.3.1 Rigid Body Translation and Forces

The derivation of rigid body translation will give those forces due to the gimbaling engine that excite rigid body translation.

Using the kinetic energy expression, equation (9-18), in equation (9-19) and performing the indicated operations for $\dot{q}_i = V_Y$ results in the following expression:

$$m_E\left[\frac{d}{dt}\left(V_Y - X_G\dot{R}_Z - \ell_e\dot{R}_Z\right)\right] - m_e\,\ell_E\,\ddot{\beta}_z + m_e\,\ddot{\xi}_Y(\bar{R}_E) - m_E\,\ell_E\,\ddot{\gamma}_Z(\bar{R}_E) = 0 \tag{9-20}$$

where

$$\frac{d}{dt}V_Y = A_Y^B + \omega_Z^B V_X - \omega_X^B V_Z \cong A_Y^B \tag{9-21}$$

and

$$X_G\frac{d}{dt}(\dot{R}_Z) \cong X_G\,\dot{\omega}_Z^B \tag{9-22}$$

Similarly

$$\ell_e\frac{d}{dt}(\dot{R}_Z) \cong \ell_E\,\dot{\omega}_Z^B \tag{9-23}$$

hence equation (9-20) becomes, after rearranging,

$$m_e A_Y^B = m_E X_G \dot{\omega}_Z^B + m_E \ell_E \dot{\omega}_Z^B + m_E \ell_E \ddot{\beta}_z - m_E \ddot{\xi}_Y(R_E) + m_E \ell_E \ddot{\gamma}_z(R_E) \qquad (9\text{-}24)$$

where the terms on the right side of the equality represent forces due to the gimbaling engine that drives rigid-body translation. If the terms that couple rigid body rotation with rigid body translation are neglected (since these effects are included in the rigid body equations) and the coupling between bending and rigid body motion are considered negligible, the right side of equation (9-24) can be expressed as follows:

$$F_{EY}^B = m_E \ell_E \ddot{\beta}_z - m_E \ddot{\xi}_Y(\bar{R}_E) + m_E \ell_E \ddot{\gamma}_Z(\bar{R}_E) \qquad (9\text{-}25)$$

From a similar analysis, the forces due to gimbaling associated with the roll and pitch planes are presented below.

$$F_{EX}^B = - m_E \ddot{\xi}_X(\bar{R}_E) \qquad (9\text{-}26)$$

$$F_{EZ}^B = - m_E \ell_E \ddot{\beta}_y - m_E \ell_E \ddot{\gamma}_Y(\bar{R}_E) - m_E \ddot{\xi}_Z(\bar{R}_E) \qquad (9\text{-}27)$$

Equations (9-25) through (9-27) represent simplified and reduced components of the general vector force due to the j^{th} gimbaling engine:

$$\bar{F}_{E_j}^B = m_{E_j} \left\{ (\bar{R}_{E_{CG_j}} - \bar{R}_{E_j}) \times [\ddot{\bar{\beta}}_j + \ddot{\bar{\gamma}}(\bar{R}_{E_j})] - \ddot{\bar{\xi}}(\bar{R}_{E_j}) \right\} \qquad (9\text{-}28)$$

where

m_{e_j} = Mass of j^{th} engine

$\bar{R}_{E_{CG_j}} - \bar{R}_{E_j}$ = Position vector of j^{th} engine CG with respect to engine attach point

$\ddot{\bar{\xi}}(\bar{R}_{E_j})$ = Acceleration vector (due to vehicle bending) at the j^{th} engine attach point

$\ddot{\bar{\gamma}}(\bar{R}_{E_j})$ = Angular acceleration (due to vehicle bending) at the j^{th} engine attach point.

The vector $(\bar{R}_{E_{CG_j}} - \bar{R}_{E_j})$ is defined as

$$\bar{R}_{E_{CG_j}} - \bar{R}_{E_j} = \begin{bmatrix} R_{E_{CGX_j}} - R_{EX_j} \\ R_{E_{CGY_j}} - R_{EY_j} \\ R_{E_{CGZ_j}} - R_{EZ_j} \end{bmatrix} = \begin{bmatrix} \ell_{E_j} \cos \beta^{+}_{P_j} \cos \beta^{+}_{Y_j} \\ -\ell_{E_j} \cos \beta^{+}_{P_j} \sin \beta^{+}_{Y_j} \\ \ell_{E_j} \sin \beta^{+}_{P_j} \cos \beta^{+}_{Y_j} \end{bmatrix} \tag{9-29}$$

where ℓ_{E_j} is the distance from the attach point of the j^{th} engine to its CG and the pitch (β^{+}_{P}) and yaw (β^{+}_{Y}) angles are assumed to consist of canted $(\beta_{Pk_j}, \beta_{Yk_j})$ and misalignment $(\beta_{Pm_j}, \beta_{Ym_j})$ angles as follows:

$$\beta^{+}_{P_j} = \beta_{Pk_j} + \beta_{Pm_j} \tag{9-30}$$

$$\beta^{+}_{Y_j} = \beta_{Yk_j} + \beta_{Ym_j} \tag{9-31}$$

The total force of N_E engines is determined by summing the individual engine inertial reactive forces as follows:

$$\bar{F}^{B}_{E} = \sum_{j=1}^{N_E} \bar{F}^{B}_{E_j} \tag{9-32}$$

9.3.2 Rigid Body Rotation and Moments

The derivation of rigid body rotation will give those moments due to the gimbaling engine that excite rigid body rotation.

In equation (9-19) if $\dot{q}_i = \dot{R}_Z$, the expression below follows:

$$m_E \frac{d}{dt}\left(X_G^2 \dot{R}_Z + \ell_E^2 \dot{R}_Z - V_Y X_G - \ell_E V_Y + 2 \ell_E X_G \dot{R}_Z\right) + I_{EZ} \frac{d}{dt}(\dot{R}_Z)$$

$$+ m_E \left[-X_G \ddot{\xi}_Y(\bar{R}_E) + \ell_E X_G \ddot{\beta}_z + X_G \ell_E \ddot{\gamma}_Z(\bar{R}_E) + \ell_e \ddot{\xi}_Y(\bar{R}_E) + \ell_e^2 \ddot{\beta}_z + \ell_E^2 \ddot{\gamma}_Z(\bar{R}_E)\right]$$

$$+ I_{EZ}\left[\ddot{\beta}_z + \ddot{\gamma}_Z(\bar{R}_E)\right] = 0 \qquad (9\text{-}33)$$

where, after using the approximations stated in equations (9-21) through (9-23) and some slight rearrangement of terms, equation (9-33) can be rewritten as follows:

$$\left[m_E (X_G + \ell_E)^2 + I_{EZ}\right] \dot{\omega}_Z^B = m_E (X_G + \ell_E) A_Y^B + m_E \left[X_G \ddot{\xi}_Y(\bar{R}_E) - \ell_E X_G \ddot{\beta}_z\right.$$

$$\left. - X_G \ell_E \ddot{\gamma}_Z(\bar{R}_E) + \ell_E \ddot{\xi}_Y(\bar{R}_E) - \ell_E^2 \ddot{\beta}_z - \ell_E^2 \ddot{\gamma}_Z(\bar{R}_E)\right] - I_{EZ}\left[\ddot{\beta}_Z + \ddot{\gamma}_Z(\bar{R}_E)\right] \qquad (9\text{-}34)$$

where, as a matter of convenience, the coupling between the rigid body motion terms $(m_E(X_G + \ell_E) A_Y^B)$ and between bending and rigid motion, will be neglected. Observe that equations (9-25) and (9-34) show that the right side of equation (9-34) can be easily rewritten as follows:

$$M_{EZ}^B = -F_{EY}^B \ell_E + m_E\{X_G \ddot{\xi}_Y(\bar{R}_E) - \ell_E X_G[\ddot{\beta}_z + \ddot{\gamma}_Z(\bar{R}_E)]\} - I_{EZ}[\ddot{\beta}_z + \ddot{\gamma}_Z(\bar{R}_E)] \qquad (9\text{-}35)$$

Expanding the analysis to the general case where the gimbal location is specified by a position vector with components along 3 axes, and interchanging component names, the total moments from the 3 axes can be written as follows:

$$M^B_{EX} = -I_{EX}\ddot{\gamma}_X(\bar{R}_E) + (R_{EY} - R_Y)\ddot{\xi}_Z(\bar{R}_E) - (R_{EZ} - R_Z)\ddot{\xi}_Y(\bar{R}_E) \tag{9-36}$$

$$M^B_{EY} = \ell_E F^B_{EZ} - I_{EY}[\ddot{\beta}_Y + \ddot{\gamma}_Y(\bar{R}_E)] - m_E(R_{EX} - R_X)\left\{[\ddot{\beta}_y + \ddot{\gamma}_Y(\bar{R}_E)]\ \ell_E + \ddot{\xi}_Z(\bar{R}_E)\right\}$$
$$+ m_E\ (R_{EZ} - R_Z)\ \ddot{\xi}_X(\bar{R}_E) \tag{9-37}$$

$$M^B_{EZ} = -\ell_E F^B_{EY} - I_{EZ}\ [\ \ddot{\beta}_z + \ddot{\gamma}_Z(\bar{R}_E) + m_E\ (R_{EX} - R_X)\left\{-[\ddot{\beta}_z + \ddot{\gamma}_Z(\bar{R}_E)]\ \ell_E + \ddot{\xi}_Y(\bar{R}_E)\right\}$$
$$- m_E(R_{EY} - R_Y)\ \ddot{\xi}_X(\bar{R}_E) \tag{9-38}$$

Equations (9-36) through (9-38) represent components of the general vector moment due to the j^{th} gimbaling engine written as follows:

$$\bar{M}^B_{E_j} = (\bar{R}_{E_j} - \bar{R}) \times \bar{F}^B_{E_j} - I_{E_j}\ [\ddot{\bar{\beta}}_j + \ddot{\bar{\gamma}}(\bar{R}_{E_j})] \tag{9-39}$$

where

$$\bar{R}_{E_j} - \bar{R} = \begin{bmatrix} R_{EX_j} - R_X \\ R_{EY_j} - R_Y \\ R_{EZ_j} - R_Z \end{bmatrix} \tag{9-40}$$

$$I_{E_j} = \begin{bmatrix} I_{EX_j} & 0 & 0 \\ 0 & I_{EY_j} & 0 \\ 0 & 0 & I_{EZ_j} \end{bmatrix} \tag{9-41}$$

Total vector moment produced by N_E engines is determined by summing the individual moments of each engine as follows:

$$\bar{M}_E^B = \sum_{j=1}^{N_E} \bar{\ell} \, \bar{M}_{E_j}^B \tag{9-42}$$

9.3.3 Bending Translation and Forces

In equation (9-19) if $\dot{q}_i = \dot{\xi}_Y(\bar{R}_E)$, the expression below follows:

$$m_E \frac{d}{dt} (V_Y - X_G \dot{R}_Z - \ell_E \dot{R}_Z) + m_E [\ddot{\xi}_Y(\bar{R}_E) - \ell_E \ddot{\beta}_z - \ell_E \ddot{\gamma}_Z(\bar{R}_E)] = - F_{E(b)Y}^B \tag{9-43}$$

Upon using the simplification previously stipulated and approximations of equations (9-21) through (9-23), equation (9-43) reduces to

$$- m_E A_Y^B = m_E(X_G + \ell_E) \dot{\omega}_Z^B + F_{EY}^B \doteq F_{E(b)Y}^B \tag{9-44}$$

Equation (9-44) represents the force exciting bending in the yaw plane. By a similar analysis, the forces that drive bending in the roll and pitch plane may be determined, and all force components may be combined to form the general vector force due to the j^{th} gimbaling engine. This force, which drives bending at the j^{th} engine attach point, is as follows:

$$\bar{F}_{E(b)_j}^B = \bar{F}_{E_j}^B - m_{E_j} [(\bar{R}_{E_{CG_j}} - \bar{R}) \times \dot{\bar{\omega}}^B] - m_{E_j} \bar{A}^B \tag{9-45}$$

$$= \bar{F}_{E_j}^B + \bar{F}_{E_j}^{B*} \tag{9-46}$$

where

$\dot{\bar{\omega}}^B$ = Angular acceleration vector at the rigid body vehicle CG.

The vector force $F_{E_j}^{B*}$ appears in equation (9-45) because of the assumed form of the 3-D modal data. Since it has been assumed that 3-D modal data

were generated by using a vehicle bending model that excluded engine mass, engine inertial reactive forces produced by rigid body vehicle angular acceleration must be included in the force equations that drive bending.

Substituting the skew-symmetric matrix

$$\tilde{\dot{\omega}} = \begin{bmatrix} 0 & -\dot{\omega}_Z^B & \dot{\omega}_Y^B \\ \dot{\omega}_Z^B & 0 & -\dot{\omega}_X^B \\ -\dot{\omega}_Y & \dot{\omega}_Z^B & 0 \end{bmatrix} \tag{9-47}$$

to facilitate vector cross product operations and employing the anti-commutative property of vector cross products permit rearrangement of equation (9-45) to the form shown below:

$$\boxed{\bar{F}^B_{E(b)_j} = \bar{F}^B_{E_j} + m_{E_j}\left[\dot{\tilde{\omega}}\,(\bar{R}_{E_{CG_j}} - \bar{R}) - \bar{A}^B\right]} \tag{9-48}$$

Equation (9-48) may be simplified by writing the vector $(\bar{R}_{E_{CG_j}} - \bar{R})$ as follows:

$$(\bar{R}_{E_{CG_j}} - \bar{R}) = (\bar{R}_{E_{CG_j}} - \bar{R}_{E_j}) + (\bar{R}_{E_j} - \bar{R}) \tag{9-49}$$

Inserting equation (9-49) into equation (9-48) and substituting for $\bar{F}^B_{E_j}$ from equation (9-28) produces the following equation:

$$\bar{F}^B_{E(b)_j} = m_{E_j}\left\{(\bar{R}_{E_{CG_j}} - \bar{R}_{E_j}) \times [\ddot{\bar{\beta}}_j + \ddot{\bar{\gamma}}(\bar{R}_{E_j})] - \ddot{\bar{\xi}}(\bar{R}_{E_j})\right\}$$

$$+ m_{E_j}\left\{\dot{\tilde{\omega}}\,(\bar{R}_{E_{CG_j}} - \bar{R}_{E_j}) + \dot{\tilde{\omega}}(\bar{R}_{E_j} - \bar{R}) - \bar{A}^B\right\} \tag{9-50}$$

Finally, equation (9-50) can be rearranged to render the form

$$\bar{F}^{B}_{E(b)_j} = m_{e_j} \left\{ (\bar{R}_{E_{CG_j}} - \bar{R}_{E_j}) \times [-\dot{\bar{\omega}}^{B} + \ddot{\bar{\beta}}_j + \ddot{\bar{\gamma}}(R_{E_j})] \right.$$

$$\left. + \dot{\bar{\omega}}(\bar{R}_{E_j} - \bar{R}) - \ddot{\bar{\xi}}(\bar{R}_{E_j}) - \bar{A}^{B} \right\} \qquad (9\text{-}51)$$

It should be noted that this force drives bending at the j^{th} engine attach point and that it is not summed over N_E engines prior to going to elastic body equations (Section II).

9.3.4 Bending Rotation and Moments

In equation (9-19) if $\dot{q}_i = \dot{\gamma}_Z(\bar{R}_E)$ it follows that

$$m_E \frac{d}{dt}(-\ell_E V_Y + X_G \ell_E \dot{R}_Z + \ell_E^2 \dot{R}_Z) + I_{E_Z} \frac{d}{dt}(\dot{R}_Z)$$

$$+ m_E[\ell_E^2 \ddot{\gamma}_Z(\bar{R}_E) - \ell_E \ddot{\xi}_Y(\bar{R}_E) + \ell_E^2 \ddot{\beta}_z]$$

$$+ I_{EZ}[\ddot{\gamma}_Z(\bar{R}_E) + \ddot{\beta}_z] = - M_{E(b)Z} \qquad (9\text{-}52)$$

Equation (9-52) reduces to

$$m_E \ell_E A^{B}_Y - \ell_E F^{B}_{E(b)Y} - I_{EZ}[\ddot{\gamma}_Z(\bar{R}_E) + \ddot{\beta}_z - \dot{\omega}^{B}_Z] \equiv M_{E(b)Z} \qquad (9\text{-}53)$$

Equation (9-53) represents the moment exciting bending in the yaw plane. By a similar analysis, the moments that drive bending in the roll and pitch plane may be determined, and all components may be combined to form the vector moment that drives vehicle bending at the j^{th} engine attach point:

$$\boxed{\bar{M}^{B}_{E(b)_j} = (\bar{R}_{E_{CG_j}} - \bar{R}_{E_j}) \times \bar{F}^{B}_{E(b)_j} - I_{E_j}[\ddot{\bar{\beta}}_j + \ddot{\bar{\gamma}}(\bar{R}_{E_j}) + \dot{\bar{\omega}}^{B}]} \qquad (9\text{-}54)$$

Section X
VEHICLE LOADS

10.1 GENERAL

Suitable formulation for determining vehicle loads at the k^{th} fuselage station due to forces and moments at the j^{th} fuselage station is presented. A separate, but similar in form, formulation would be required for determining loads at selected wing, horizontal stabilizer, and vertical stabilizer stations. This formulation would be finalized after a shuttle vehicle candidate had been selected.

Formulation presented contains the following main features and assumptions:

- The fuselage is segmented by station, and loads are computed at the junctions of the stations (see Figure 10-1).
- Aerodynamic drag distribution is computed in this module. This is done because drag forces are slowly varying and thus have little effect on flexible body vibrations.
- It assumes a lumped mass approximation to the vehicle structure. Vehicle is segmented by station into mass panels.
- It assumes sectionalized aero distributions.
- Inertial loads are computed.
- Torsional moments are neglected.
- Load station must coincide with a junction of fuselage mass panels and aero panels.
- Second-order effects resulting from static or dynamic displacements of the slosh masses or structure from equilibrium are neglected.
- Load equations must be modified for load stations within liquid propellant tanks.
- Load stations are numbered consecutively from the rear of the vehicle.

The loads are computed as a linear combination of individual loads produced by aerodynamics, slosh, and vehicle inertia.

10.2 BENDING MOMENTS

Bending moments on the fuselage are computed about the pitch and yaw axes only. Torsional moments associated with the vehicle roll axis are not computed.

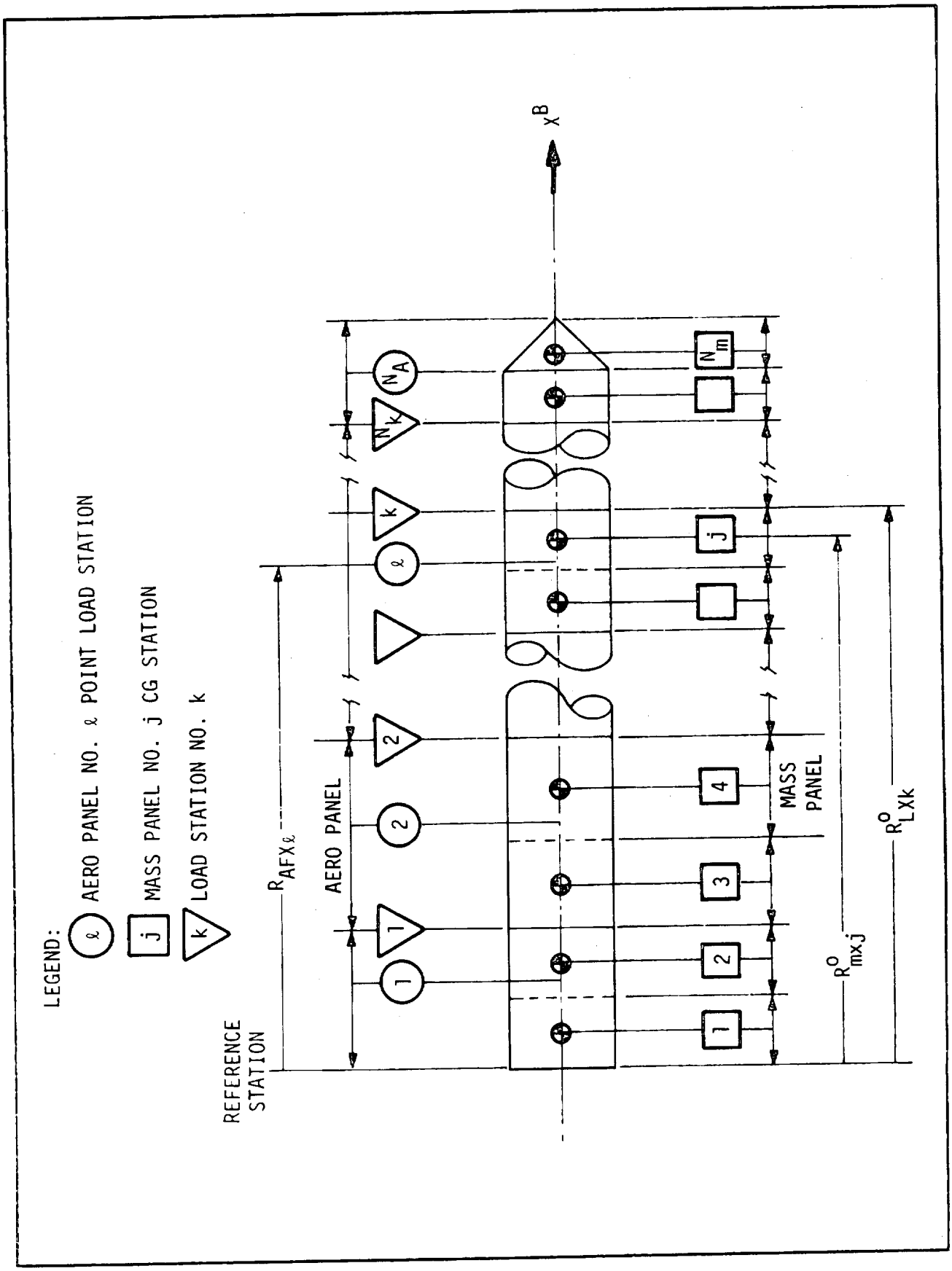

Figure 10-1. FUSELAGE LOAD STATION RELATIONSHIP WITH AERO AND MASS PANEL BREAKDOWN

The general expression for bending moments at the fuselage k^{th} load station is:

$$\overline{BM}_k = \sum_{j=①}^{N_{A_f}} [(\bar{R}^B_{A_{fj}} - \bar{R}^B_{L_{fk}}) \times \bar{F}^B_{A_{fj}} + \bar{M}^B_{A_{fj}}] + \sum_{j=②}^{N_S} [(\bar{R}^B_{S_j} - \bar{R}^B_{Lk}) \times \bar{F}^B_{S_j} + \bar{M}^B_{S_j}] - \sum_{j=③}^{N_m} [m_j(\bar{R}^B_{m_j} - \bar{R}^B_{Lk}) \times \bar{a}^B_j] \quad (10\text{-}1)$$

where the vector $\overline{BM}_k$ is of the form

$$\overline{BM}_k = \begin{bmatrix} 0 \\ BM_{Yk} \\ BM_{Zk} \end{bmatrix} \quad (10\text{-}2)$$

and the term $\bar{a}^B_j$ is the total acceleration due to vehicle dynamics, and is of the form shown below:

$$\bar{a}^B_j = \begin{bmatrix} A^B_X \\ A^B_Y \\ A^B_Z \end{bmatrix} + \begin{bmatrix} 0 & -\dot{\omega}^B_Z & \dot{\omega}^B_Y \\ \dot{\omega}^B_Z & 0 & -\dot{\omega}^B_X \\ -\dot{\omega}^B_Y & \dot{\omega}^B_X & 0 \end{bmatrix} \begin{bmatrix} R^B_{mXj} \\ R^B_{mYj} \\ R^B_{mZj} \end{bmatrix} + \begin{bmatrix} 0 \\ \sum_{i=1}^{n} \phi_{iY}(\bar{R}_{mj})\ddot{\eta}_i \\ \sum_{i=1}^{n} \phi_{iZ}(\bar{R}_{mj})\ddot{\eta}_i \end{bmatrix} \quad (10\text{-}3)$$

The lower limit in the summations shown in equation (10-1) are defined as follows:

- ① takes the value of j that satisfies the relation $R^B_{AfX_j} \geq R^B_{LX_k}$
- ② takes the value of j that satisfies the relation $R^B_{SX_j} \geq R^B_{LX_k}$
- ③ takes the value of j that satisfies the relation $R^B_{MX_j} \geq R^B_{LX_k}$

10.3 SHEAR FORCES

Shearing forces for the pitch and yaw planes are computed as a linear combination of the forces associated with aerodynamics, slosh, and inertia of the vehicle. The general expression is:

$$\overline{VF}_k = \sum_{j=①}^{N_{A_f}} \bar{F}^B_{A_{fj}} + \sum_{j=②}^{N_S} \bar{F}^B_{Sj} - \sum_{j=③}^{N_m} m_j \bar{a}^B_j \qquad (10\text{-}4)$$

where the vector $\overline{VF}_k$ has the form

$$VF_k = \begin{bmatrix} 0 \\ VF_{Yk} \\ VF_{Zk} \end{bmatrix} \qquad (10\text{-}5)$$

The axial force at the fuselage k^{th} load station has the form:

$$AF_k = \sum_{j=①}^{N_{Af}} F^B_{AfX_j} - \sum_{j=③}^{N_m} m_j a^B_{Xj} \qquad (10\text{-}6)$$

where $F^B_{AfX_j}$ is the drag force at the k^{th} load station, and is computed as follows:

$$F^B_{AfX_j} = q\ S\ C_{fX_j} \qquad (10\text{-}7)$$

where:

- q = Dynamic pressure at vehicle CG
- S = Reference area
- C_{fX_j} = Aerodynamic drag coefficient at the fuselage j^{th} aero station (table lookup).

10.4 GLOSSARY OF TERMS

SYMBOL	DEFINITION	UNIT
$\bar{a}^B_j = \begin{bmatrix} a^B_{X_j} \\ a^B_{Y_j} \\ a^B_{Z_j} \end{bmatrix}$	Total acceleration vector of the j^{th} mass, resolved in Body coordinates $j = 1, N_m$	m/sec^2
$\bar{A}^B = \begin{bmatrix} A^B_X \\ A^B_Y \\ A^B_Z \end{bmatrix}$	Acceleration vector of the vehicle CG due to body forces, resolved in Body coordinates	m/sec^2
AF_k	Axial force acting at the k^{th} load station $k = 1, N_k$	N
$\overline{BM}_k = \begin{bmatrix} 0 \\ BM_{Yk} \\ BM_{Zk} \end{bmatrix}$	Bending moment acting at the k^{th} load station $k = 1, N_k$	N-m
$C_{fX_j} = f(M)$	Sectional aerodynamic drag coefficient at the fuselage j^{th} aero station $j = 1, N_A$	unitless
$\bar{F}^B_{A_{fj}} = \begin{bmatrix} 0 \\ F_{AY_{fj}} \\ F_{AZ_{fj}} \end{bmatrix}$	Vector force at the fuselage j^{th} aero station, resolved in Body coordinates $j = 1, N_A$	N
$\bar{F}^B_{Sj} = \begin{bmatrix} F^B_{SX_j} \\ F^B_{SY_j} \\ F^B_{SZ_j} \end{bmatrix}$	Vector force at the j^{th} tank lateral slosh mass, resolved in Body coordinates $j = 1, N_S$	N

SYMBOL	DEFINITION	UNIT
m_j	Mass of the j^{th} mass panel $j = 1, N_m$	kg
M	Mach number	unitless
$\bar{M}^B_{Af_j} = \begin{bmatrix} M^B_{AfX_j} \\ M^B_{AfY_j} \\ M^B_{AfZ_j} \end{bmatrix}$	Vector moment of the j^{th} aero station resolved in Body coordinates $j = 1, N_S$	N-m
$\bar{M}^B_{S_j} = \begin{bmatrix} M^B_{SX_j} \\ M^B_{SY_j} \\ M^B_{SZ_j} \end{bmatrix}$	Vector moment of the j^{th} tank lateral slosh mass, resolved in Body coordinates $j = 1, N_S$	N-m
n	Number of bending modes being considered	unitless
q	Dynamic pressure at vehicle CG	N/m^2
$\bar{R}^B_{Af_j} = \begin{bmatrix} R^B_{AfX_j} \\ R^B_{AfY_j} \\ R^B_{AfZ_j} \end{bmatrix}$	Position vector from the Body origin (vehicle CG) to the j^{th} aero station $j = 1, N_A$	m
$\bar{R}^B_{Lk} = \begin{bmatrix} R^B_{LXk} \\ 0 \\ 0 \end{bmatrix}$	Position vector of the k^{th} load station, resolved in Body coordinates $k = 1, N_k$	m
$\bar{R}^B_{m_j} = \begin{bmatrix} R^B_{mX_j} \\ R^B_{mY_j} \\ R^B_{mZ_j} \end{bmatrix}$	Position vector of the j^{th} mass CG, resolved in Body coordinates $j = 1, N_m$	m

SYMBOL	DEFINITION	UNIT
S	Reference area	m^2
$\overline{VF}_k = \begin{bmatrix} 0 \\ VF_{Yk} \\ VF_{Zk} \end{bmatrix}$	Vector shear force acting at the k^{th} load station $k = 1, N_k$	N
$\ddot{\eta} = \begin{bmatrix} \ddot{\eta}_1 \\ \ddot{\eta}_2 \\ \vdots \\ \ddot{\eta}_n \end{bmatrix}$	Vehicle bending mode generalized acceleration	m/sec^2
$\phi_{iY}(\bar{R}_{m_j})$	Modal displacement Y^B coefficient for the i^{th} mode at the j^{th} mass panel location, defined by $\bar{R}_{m_j}$ $i = 1, n$ $j = 1, N_m$	unitless
$\phi_{iZ}(\bar{R}_{m_j})$	Nodal displacement Z^B coefficient for the i^{th} mode at the j^{th} mass panel location, defined by $\bar{R}_{m_j}$ $i = 1, n$ $j = 1, N_m$	unitless
$\dot{\omega}^B = \begin{bmatrix} \dot{\omega}^B_X \\ \dot{\omega}^B_Y \\ \dot{\omega}^B_Z \end{bmatrix}$	Angular acceleration vector of the vehicle, resolved in Body coordinates	rad/sec^2

Section XI
GUIDANCE AND CONTROL EQUATIONS

11.1 GENERAL

This section outlines the development of the equations used in the Guidance and Control Module of reference 1. The equations developed are based on an "open-loop" type scheme; steering signals are generated in the form of pitch and yaw commands such that the error resulting by comparing the actual vehicle attitude with a programmed time-varying attitude is minimized. Formulation in the Guidance and Control Module is given in a completely general form so that for any particular case the number of gimbaling engines and the number of active control surfaces can be easily changed by simply modifying a program control variable. Also, as a matter of generality, transfer functions associated with the control variables are left in finite product form, and the gains associated with control laws are also completely arbitrary. Control laws for both gimbaling engines and control surfaces are shown to be of the same kind; however, related gains are arbitrary. A functional block diagram of the guidance and control scheme is shown in Figure 11-1.

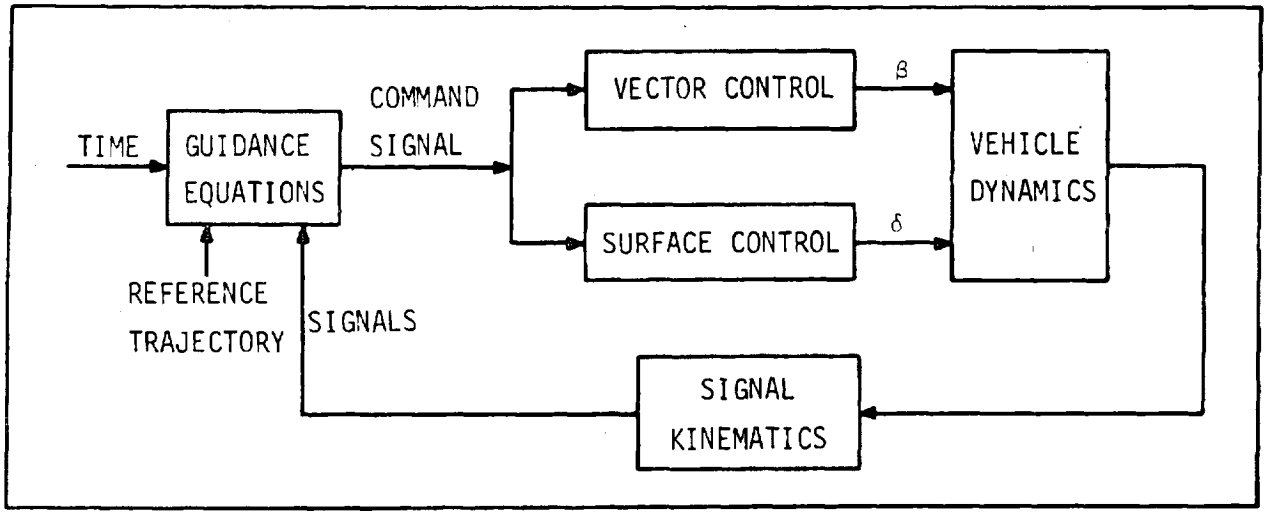

Figure 11-1. FUNCTIONAL BLOCK DIAGRAM OF CONTROL SYSTEM

The derivation of the guidance and control based on the open-loop scheme, reduces to the task of showing how the feedback signals used in the control system are calculated. The vehicle must then contain the necessary sensors to detect the translational, rotational, and vibrational motion of the vehicle. The commonly employed sensors are the rate-gyro, position gyro, and accelerometer.

11.2 ASSUMPTIONS AND APPROXIMATIONS

In developing formulation suitable for simulating G&C dynamics and malfunctions, two fundamental guidelines were established. These are:

- Formulation must be sufficiently flexible to effect desired changes in control and steering laws and their associated gains.
- Formulation must be sufficiently general to consider both thrust vector and aero control for a variety of vehicle candidates.

Significant assumptions/approximations made in equation formulation (and modularization) and unique features are as follows:

- Guidance is based on an open-loop scheme
- Control laws for thrust vector and aero control are presented in a general form containing control gains (to be furnished as parametric inputs when vehicle configuration data becomes available) and filtered sensor output signals.
- Distribution laws for thrust vector and aero control are presented in a general form, containing gains to be determined by location geometry of the j^{th} engine and k^{th} control surface.
- 3-D modal data at sensor stations are considered.
- Number of integrations will depend on order of actuator-engine transfer functions.
- Control filters are given in general form.

11.3 SIGNAL KINEMATICS

Feedback signals used in the control and distribution laws are computed in this section. For purposes of simulation it is desirable to compute these signals as they would be sensed by the proper sensors in the vehicle; thus by superposition of the translation, rotation, and bending motion at a particular location associated with the sensor location, it is possible to duplicate what this sensor would detect during flight of the vehicle.

The effects of 'sensor dynamics' are not considered in this simulation in the sense that there is no input to the program that results from some signal detected by a sensor. Sensor subscript notation is shown in Table 11-1.

Table 11-1. SENSOR SUBSCRIPT NOTATION

SUBSCRIPT	SENSOR STATION
q = a	ACCELEROMETER AT VEHICLE STATION LOCATED BY POSITION VECTOR $\bar{R}_a$
q = p	INERTIAL PLATFORM AT VEHICLE STATION LOCATED BY POSITION VECTOR $\bar{R}_p$
q = r	RATE GYRO AT VEHICLE STATION LOCATED BY POSITION VECTOR $\bar{R}_r$
q = v	VELOCITY METER AT VEHICLE STATION LOCATED BY POSITION VECTOR $\bar{R}_v$

The acceleration feedback is computed by summing the acceleration at the vehicle CM, the linear acceleration at the location of the accelerometer due to angular acceleration, and acceleration due to bending at the accelerometer location. The effects of the centripetal acceleration of the form $\tilde{\omega}^B \tilde{\omega}^B R_a^B$ are not considered. Then, the total acceleration at the accelerometer location is given by the expressions.

$$
\begin{aligned}
A_{sX} &= A_X^B + \dot{\omega}_Y^B R_{aZ}^B - \dot{\omega}_Z^B R_{aY}^B + \sum_{i=1}^{n} \phi_{iX}(\bar{R}_a) \ddot{\eta}_i \\
A_{sY} &= A_Y^B + \dot{\omega}_Z^B R_{aX}^B - \dot{\omega}_X^B R_{aZ}^B + \sum_{i=1}^{n} \phi_{iY}(\bar{R}_a) \ddot{\eta}_i \\
A_{sZ} &= A_Z^B + \dot{\omega}_X^B R_{aY}^B - \dot{\omega}_Y^B R_{aX}^B + \sum_{i=1}^{n} \phi_{iZ}(\bar{R}_a) \ddot{\eta}_i
\end{aligned}
\qquad (11\text{-}1)
$$

The velocity feedback is computed by a linear combination of the following terms: velocity vector of the vehicle CM, velocity at the velocity meter

resulting from vehicle angular velocity, and velocity due to bending. The necessary computations are shown below as follows:

$$\bar{V}^B = [A^{PB}]^T \dot{\bar{R}}^P$$

$$V_{sX} = V_X^B + \omega_Y^B R_{vZ}^B - \omega_Z^B R_{vY}^B + \sum_{i=1}^{n} \phi_{iX}(\bar{R}_v)\, \dot{\eta}_i$$

$$V_{sY} = V_Y^B + \omega_Z^B R_{vX}^B - \omega_X^B R_{vZ}^B + \sum_{i=1}^{n} \phi_{iY}(\bar{R}_v)\, \dot{\eta}_i \qquad (11\text{-}2)$$

$$V_{sZ} = V_Z^B + \omega_X^B R_{vY}^B - \omega_Y^B R_{vX}^B + \sum_{i=1}^{n} \phi_{iZ}(\bar{R}_v)\, \dot{\eta}_i$$

The attitude rate signals are computed by adding to the vehicle angular rates the angular rates at the rate-gyro locations due to bending:

$$\omega_{sX} = \omega_X^B + \sum_{i=1}^{n} \phi'_{iX}(\bar{R}_r)\, \dot{\eta}_i$$

$$\omega_{sY} = \omega_Y^B + \sum_{i=1}^{n} \phi'_{iY}(\bar{R}_r)\, \dot{\eta}_i \qquad (11\text{-}3)$$

$$\omega_{sZ} = \omega_Z^B + \sum_{i=1}^{n} \phi'_{iZ}(\bar{R}_r)\, \dot{\eta}_i$$

The attitude feedback signals are computed by adding the slopes due to bending, measured at the position gyro locations, to the attitude error that results by comparing the actual vehicle attitude with a programmed time-dependent attitude. The attitude error in Plumbline coordinate frame is given by

$$\Phi_\varepsilon = \Phi_c(t) - \Phi$$

$$\Theta_\varepsilon = \Theta_c(t) - \Theta \qquad (11\text{-}4)$$

$$\Psi_\varepsilon = \Psi_c(T) - \Psi$$

These signals, resolved in Body coordinates and combined with bending effects, yield attitude signals of the form shown below:

$$\Phi_s = \Phi_\varepsilon + \Psi_\varepsilon s\Psi - \sum_{i=1}^{n} \phi'_{iX}(\bar{R}_p)\,\eta_i$$

$$\Theta_s = \Theta_\varepsilon c\Phi\, c\Psi + \Psi_\varepsilon s\Phi - \sum_{i=1}^{n} \phi'_{iY}(\bar{R}_p)\,\eta_i \qquad (11\text{-}5)$$

$$\Psi_s = -\Theta_\varepsilon s\Phi\, c\Psi + \Psi_\varepsilon c\Phi - \sum_{i=1}^{n} \phi'_{iZ}(\bar{R}_p)\,\eta_i$$

11.4 FILTERS

Flight control filters shape the 'sensed' signals to achieve phase and gain stabilization. Filter subscript notation is shown in Table 11-2.

Table 11-2. FILTER SUBSCRIPT NOTATION

SUBSCRIPT	FILTER	FUNCTION
k = AX	$[F_{AX}]$	FILTERS FOR VEHICLE ACCELERATION SENSOR OUTPUTS A_{sx}, A_{sy}, AND A_{sz}
k = AY	$[F_{AY}]$	
k = AZ	$[F_{AZ}]$	
k = VX	$[F_{VX}]$	FILTERS FOR VEHICLE VELOCITY SENSOR OUTPUTS V_{sx}, V_{sy}, AND V_{sz}
k = VY	$[F_{VY}]$	
k = VZ	$[F_{VZ}]$	
k = ωx	$[F_{\omega x}]$	FILTERS FOR VEHICLE ANGULAR VELOCITY SENSOR OUTPUTS ω_{sx}, ω_{sy}, AND ω_{sz}
k = ωy	$[F_{\omega y}]$	
k = ωz	$[F_{\omega z}]$	
k = ϕ	$[F_{\phi}]$	FILTERS FOR VEHICLE ATTITUDE SENSOR OUTPUTS Φ_s, Θ_s, AND Ψ_s
k = θ	$[F_{\theta}]$	
k = ψ	$[F_{\psi}]$	

For translational acceleration:

$$\boxed{\begin{aligned} A_{FX} &= [F_{AX}]\ A_{sX} \\ A_{FY} &= [F_{AY}]\ A_{sY} \\ A_{FZ} &= [F_{AZ}]\ A_{sZ} \end{aligned}} \qquad (11\text{-}6)$$

For translational velocity:

$$\boxed{\begin{aligned} V_{FX} &= [F_{VX}]\ V_{sX} \\ V_{FY} &= [F_{VY}]\ V_{sY} \\ V_{FZ} &= [F_{VZ}]\ V_{sZ} \end{aligned}} \qquad (11\text{-}7)$$

For attitude rate:

$$\boxed{\begin{aligned} \omega_{FX} &= [F_{\omega X}]\ \omega_{sX} \\ \omega_{FY} &= [F_{\omega Y}]\ \omega_{sY} \\ \omega_{FZ} &= [F_{\omega Z}]\ \omega_{sZ} \end{aligned}} \qquad (11\text{-}8)$$

For attitude error:

$$\boxed{\begin{aligned} \Phi_F &= [F_{\phi}]\ \Phi_s \\ \Theta_F &= [F_{\theta}]\ \Theta_s \\ \Psi_F &= [F_{\psi}]\ \Psi_s \end{aligned}} \qquad (11\text{-}9)$$

11.5 CONTROL AND DISTRIBUTION LAW

The basic function of the control law is to generate steering signals, engine gimbal commands, and control surface deflections in response to error signals so that the vehicle follows a set of constraints.

11.5.1 Thrust Vector Control

11.5.1.1 Engine Commands. The control law for the j^{th} engine is of the form:

ROLL:

$$\beta_{R_j} = a_{OR_j}\,\Phi_F + a_{1R_j}\,\omega_{FX}$$

PITCH:

$$\beta_{P_j} = a_{OP_j}\,\Theta_F + a_{1P_j}\,\omega_{FY} + g_{1P_j}\,V_{FZ} + g_{2P_j}\,A_{FZ} \qquad (11\text{-}10)$$

YAW:

$$\beta_{Y_j} = a_{OY_j}\,\Psi_F + a_{1Y_j}\,\omega_{FZ} + g_{1Y_j}\,V_{FY} + g_{2Y_j}\,A_{FY}$$

Pitch and yaw engine actuator commands are generated by combining the control angles of equation (11-10) as functional relations of the engine location

$$\beta_{cy_j} = K_{1Y_j}\,\beta_{P_j} + K_{2Y_j}\,\beta_{R_j}$$

$$\beta_{cz_j} = K_{1Z_j}\,\beta_{Y_j} + K_{2Z_j}\,\beta_{R_j} \qquad (11\text{-}11)$$

where the distribution gains K_{1Y_j}, K_{2Y_j}, K_{1Z_j}, and K_{2Z_j} are determined by geometry of the engine location. Actuator and engine transfer functions may be combined to determine the actual engine gimbal angle deflection, as shown in Figure 11-2.

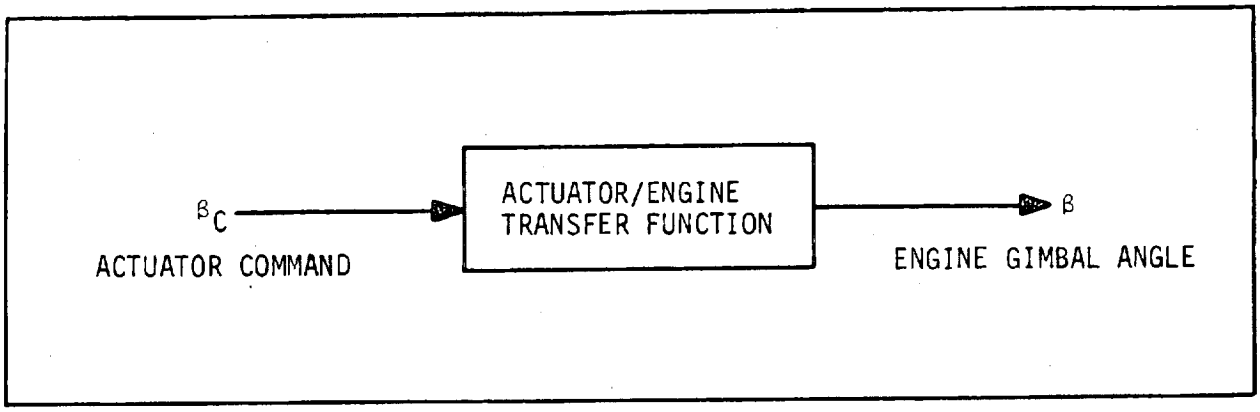

Figure 11-2. SIMPLIFIED BLOCK DIAGRAM FOR ENGINE DEFLECTION

Pitch and yaw gimbal angle deflections for the j^{th} engine, using pitch and yaw combined actuator/engine transfer functions, are given as follows:

$$\beta_{y_j} = Y_{AE_j}(S)\ \beta_{cy_j}$$

$$\beta_{z_j} = Z_{AE_j}(S)\ \beta_{cz_j} \qquad (11\text{-}12)$$

11.5.1.2 Engine Actuator Failure. Formulation used in the simulation is sufficiently flexible to simulate an engine actuator failure. Flight time at which failure is to occur is input and at this time the engine command will be set equal to the failed gimbal angle. Actuator malfunction for any number of engines may be specified in a completely arbitrary form.

11.5.2 Aero Surface Control

11.5.2.1 Control Surface Commands. The control law for the k^{th} control surface is of the form

ROLL

$$\delta_{R_k} = b_{OR_k}\,\phi_F + b_{1R_k}\,\omega_{FX}$$

PITCH

$$\delta_{Pk} = b_{OP_k}\,\theta_F + b_{1P_k}\,\omega_{FY} + d_{1P_k}\,V_{FZ} + d_{2P_k}\,A_{FZ} \qquad (11\text{-}13)$$

YAW

$$\delta_{Yk} = b_{OY_k}\,\psi_F + b_{1Y_k}\,\omega_{FZ} + d_{1Y_k}\,V_{FY} + d_{2Y_k}\,A_{FY}$$

Pitch and yaw control surface actuator commands are generated by combining the control angles shown in equation (11-13) as functional relations of the control surface location and function (aileron, elevator, rudder).

$$\delta_{ca_k} = K_{3X_k}\,\delta_{R_k}$$

$$\delta_{ce_k} = K_{3Y_k}\,\delta_{P_k} + K_{4Y_k}\,\delta_{R_k} \qquad (11\text{-}14)$$

$$\delta_{cr_k} = K_{3Z_k}\,\delta_{Y_k} + K_{4Z_k}\,\delta_{R_k}$$

where the distribution gains K_{3X_k}, K_{3Y_k}, K_{3Z_k}, K_{4Y_k}, and K_{4Z_k} are determined by the location and function of the k^{th} control surface. The actual control surface deflection is also based upon the block diagram shown in Figure 11-2. Thus, the actual control surface deflection for the k^{th} element is given as follows:

$$\boxed{\begin{aligned} \delta_{a_k} &= Y_{a_k}(S)\,\delta_{ca_k} \\ \delta_{e_k} &= Y_{e_k}(S)\,\delta_{ce_k} \\ \delta_{r_k} &= Y_{r_k}(S)\,\delta_{cr_k} \end{aligned}} \qquad (11\text{-}15)$$

11.5.2.2 Control Surface Actuator Failure. The case where a control surface actuator fails may also be simulated. As in the engine actuator failure the flag that indicates when actuator failure occurs is time. At this time of failure, the control surface command will be set equal to the failed control surface deflection angle. Thereafter the dynamics associated with the failed control surface cease to exist, and control via this control surface is lost.

11.6 GLOSSARY OF TERMS

SYMBOL	DEFINITION	UNIT
$\bar{A}^B = \begin{bmatrix} A_X^B \\ A_Y^B \\ A_Z^B \end{bmatrix}$	Acceleration vector of the vehicle CG due to body forces, resolved in Body coordinates	m/sec^2
$[A^{PB}]$	Coordinate transformation from Body coordinates to Plumbline coordinates	unitless
A_{sX}, A_{sY}, A_{sZ}	Vehicle acceleration signals	m/sec^2
A_{FX}, A_{FY}, A_{FZ}	Filtered output signals A_{sX}, A_{sY}, A_{sZ}	m/sec^2

Actuator/Engine Transfer Functions

$Y_{AE_j}(S) = Y_{A_j}(S)\,Y_{E_j}(S)$	Combined actuator-engine transfer function for the j^{th} engine, Y-axis command	unitless
$Z_{AE_j}(S) = Z_{A_j}(S)\,Z_{E_j}(S)$	Combined actuator-engine transfer function for the j^{th} engine, Z-axis command	unitless

SYMBOL	DEFINITION	UNIT
Control Surface Transfer Functions		
Y_{a_k}	Combined actuator-control surface transfer function for the k^{th} control surface, X-axis command (ailerons)	unitless
Y_{e_k}	Combined actuator-control surface transfer function for the k^{th} control surface, Y-axis command (elevators)	unitless
Y_{r_k}	Combined actuator-control surface transfer function for the k^{th} control surface, Z-axis command (rudder)	unitless
Control Law Gains - Thrust Vector Control		
a_{OR_j}	Attitude gain, roll	rad/rad-unitless
a_{1R_j}	Attitude rate gain, roll	sec
a_{OP_j}	Attitude gain, pitch	unitless
a_{1P_j}	Attitude rate gain, pitch	sec
a_{OY_j}	Attitude gain, yaw	unitless
a_{1Y_j}	Attitude rate gain, yaw	sec
g_{1P_j}	Lateral velocity gain, Z-axis	rad-sec/m
g_{2P_j}	Lateral acceleration gain, Y-axis	$rad-sec^2/m$
g_{1Y_j}	Lateral velocity gain, Z-axis	rad-sec/m
g_{2Y_j}	Lateral acceleration gain, Y-axis	$rad-sec^2/m$

SYMBOL	DEFINITION	UNIT
	Control Law Gains - Aero Surface Control	
b_{OR_k}	Attitude gain, roll	rad/rad-unitless
b_{1R_k}	Attitude rate gain, roll	sec
b_{OP_k}	Attitude gain, pitch	unitless
b_{1P_k}	Attitude rate gain, pitch	sec
d_{1P_k}	Lateral velocity gain, Z-axis	rad-sec/m
d_{2P_k}	Lateral acceleration gain, Z-axis	rad-sec^2/m
b_{OY_k}	Attitude gain, yaw	unitless
b_{1Y_k}	Attitude rate gain, yaw	sec
d_{1Y_k}	Lateral velocity gain, Y-axis	rad-sec/m
d_{2Y_k}	Lateral acceleration gain, Y-axis	rad-sec^2/m
	Distribution Law Gains - Thrust Vector Control	
K_{1Y_j}	Pitch gain used in pitch "beta command" equation β_{cy_j} Gain determined by geometry of the j^{th} engine location	unitless
K_{2Y_j}	Roll gain used in pitch "beta command" equation β_{cy_j}	unitless
K_{1Z_j}	Yaw gain used in yaw "beta command" equation β_{cz_j}	unitless
K_{2Z_j}	Roll gain used in yaw "beta command" equation β_{cz_j}	unitless
	Distribution Law Gains - Aero Surface Control	
K_{3X_k}	Roll gain used in roll δ_{ca_k} (k^{th} aileron)	unitless

SYMBOL	DEFINITION	UNIT
K_{3Y_k}	Pitch gain used in pitch equation δ_{ce_k} (k^{th} elevator)	unitless
K_{3Z_k}	Yaw gain used in yaw equation δ_{cr_k} (k^{th} rudder)	unitless
K_{4Y_k}	Roll gain used in pitch equation δ_{ce_k} (k^{th} elevator)	unitless
K_{4Z_k}	Roll gain used in yaw equation δ_{cr_k} (k^{th} rudder)	unitless
$[F_k]$	General form of filter for the k^{th} sensor output	unitless

$$[F_k] = \frac{\prod_{\ell=1}^{m} (S - Z_{1k})}{\prod_{\ell=1}^{n} (S - P_{1k})} \qquad n \geq m$$

$\bar{R}^B_q = \begin{bmatrix} R^B_{qX} \\ R^B_{qY} \\ R^B_{qZ} \end{bmatrix}$	Position vector of sensor location q (q = a,p,r,v) resolved in Body coordinates	m
$\dot{\bar{R}}^P = \begin{bmatrix} \dot{R}^P_X \\ \dot{R}^P_Y \\ \dot{R}^P_Z \end{bmatrix}$	Velocity vector of the vehicle CG, relative to the Plumbline Frame origin, resolved in Plumbline coordinates	m/sec
$\bar{V}^B = \begin{bmatrix} V^B_X \\ V^B_Y \\ V^B_Z \end{bmatrix}$	Velocity vector of the vehicle CG relative to the Plumbline Frame origin, resolved in Body reference frame	m/sec
V_{sX}, V_{sY}, V_{sZ}	Vehicle velocity signals	m/sec
V_{Fx}, V_{FY}, V_{FZ}	Filtered output signals V_{sX}, V_{sY}, V_{sZ}	m/sec

SYMBOL	DEFINITION	UNIT
$\beta_{R_j}, \beta_{P_j}, \beta_{Y_j}$	Thrust control angles for roll, pitch, and yaw	rad
$\beta_{cy_j}, \beta_{cz_j}$	Engine actuator "beta commands" for pitch, yaw	rad
$\ddot{\bar{\beta}}_j = \begin{bmatrix} 0 \\ \ddot{\beta}_{y_j} \\ \ddot{\beta}_{z_j} \end{bmatrix} \triangleq \begin{bmatrix} 0 \\ \ddot{\beta}_{P_j} \\ \ddot{\beta}_{Y_j} \end{bmatrix}$	Gimbal angular acceleration vector of the j^{th} engine	rad
$\bar{\beta}_j = \begin{bmatrix} 0 \\ \beta_{y_j} \\ \beta_{z_j} \end{bmatrix} \triangleq \begin{bmatrix} 0 \\ \beta_{P_j} \\ \beta_{Y_j} \end{bmatrix}$	Gimbal angle vector of the j^{th} engine	rad
$\delta_{a_k}, \delta_{e_k}, \delta_{r_k}$	Control surfaces control angles for the k^{th} aileron, elevator, and rudder	rad
$\delta_{ca_k}, \delta_{ce_k}, \delta_{cr_k}$	Control surface actuators - "delta commands" for roll, pitch, and yaw	rad
$\ddot{\bar{\delta}}_k = \begin{bmatrix} \ddot{\delta}_{X_k} \\ \ddot{\delta}_{Y_k} \\ \ddot{\delta}_{Z_k} \end{bmatrix}$	Control surface angular acceleration vector of the k^{th} control surface	rad/sec^2
$\bar{\delta}_k = \begin{bmatrix} \delta_{X_k} \\ \delta_{Y_k} \\ \delta_{Z_k} \end{bmatrix}$	Control surface vector of the k^{th} control surface	rad

SYMBOL	DEFINITION	UNIT
$\bar{\eta} = \begin{bmatrix} \eta_1 \\ \eta_2 \\ \vdots \\ \eta_n \end{bmatrix}$	Vehicle bending mode generalized displacement	m
$\ddot{\bar{\eta}} \begin{bmatrix} \ddot{\eta}_1 \\ \ddot{\eta}_2 \\ \vdots \\ \ddot{\eta}_n \end{bmatrix}$	Vehicle bending mode generalized acceleration	m/sec^2
θ	Pitch-Euler attitude angle	rad
$\theta_C = \theta(t)$	Pitch-nominal commanded attitude	rad
θ_F	Pitch-filtered Euler attitude error feedback	rad
θ_S	Pitch unfiltered Euler attitude error feedback	rad
Φ	Roll-Euler attitude angle	rad
$\Phi_C = \Phi(t)$	Roll-nominal commanded attitude	rad
Φ_F	Roll-filtered Euler attitude error feedback	rad
Φ_S	Roll-unfiltered Euler attitude error feedback	rad
$\Phi_\xi(\bar{R}_q) = \begin{bmatrix} \phi_{1X}(\bar{R}_q) & \cdots & \phi_{nX}(\bar{R}_q) \\ \phi_{1Y}(\bar{R}_q) & \cdots & \phi_{nY}(\bar{R}_q) \\ \phi_{1Z}(\bar{R}_q) & \cdots & \phi_{nZ}(\bar{R}_q) \end{bmatrix}$	General form for matrix of modal <u>displacement</u> coefficients at sensor location q	unitless
$\Phi_\gamma(\bar{R}_q) = \begin{bmatrix} \phi'_{1X}(\bar{R}_q) & \cdots & \phi'_{nX}(\bar{R}_q) \\ \phi'_{1Y}(\bar{R}_q) & \cdots & \phi'_{nY}(\bar{R}_q) \\ \phi'_{1Z}(\bar{R}_q) & \cdots & \phi'_{nZ}(\bar{R}_q) \end{bmatrix}$	General form for matrix of modal <u>rotational</u> coefficients at sensor location q	rad/m

SYMBOL	DEFINITION	UNIT
Ψ	Yaw-Euler attitude angle	rad
$\Psi_C = \Psi(t)$	Yaw-nominal commanded attitude	rad
Ψ_F	Yaw-filtered Euler attitude error feedback	rad
Ψ_S	Yaw-unfiltered Euler attitude error feedback	rad
$\dot{\omega}^B = \begin{bmatrix} \dot{\omega}_X^B \\ \dot{\omega}_Y^B \\ \dot{\omega}_Z^B \end{bmatrix}$	Angular acceleration vector of the vehicle, resolved in Body coordinates	rad/sec^2
$\omega^B = \begin{bmatrix} \omega_X^B \\ \omega_Y^B \\ \omega_Z^B \end{bmatrix}$	Angular velocity vector of the vehicle, resolved in Body coordinates	rad/sec
$\omega_{sX}, \omega_{sY}, \omega_{sZ}$	Vehicle angular rate signals	rad/sec
$\omega_{FX}\ \omega_{FY}\ \omega_{FZ}$	Filtered output signals ω_{sX}, ω_{sY}, ω_{sZ}	rad/sec

Section XII
CONCLUSIONS AND RECOMMENDATIONS

The overall objective of the project has been to derive a space vehicle 6-D trajectory with 3-D elastic body vehicle dynamics. It is felt that the formulation presented in Sections II through XI meets this objective. Specific requirements met are:

- Vehicle subsystem equations use 3-D modal data
- Subsystem equations are developed in modular form having flexibility and option characteristics
- The modularized formulation possesses inter-modular compatibility
- Trajectory equations are 6-D
- Different types of earth gravitational models may be considered, and
- All documentation of the modularized subsystem equations is presented in a form amenable to analog/digital simulation.

As in all large sets of equations designed to be used in simulating a problem of interest additional refinements may be added to the equations as the problem complexity increases. Table 12-1 presents a tabulated summary of conclusions on the present equations and recommendations for future refinements.

Table 12-1. CONCLUSIONS AND RECOMMENDATIONS

EQUATIONS	CONCLUSIONS	RECOMMENDATIONS
ELASTIC BODY (SECTION II)	EXTENSIVE USAGE OF MATRIX AND VECTOR ALGEBRA HAS ELIMINATED LENGTHY REPETITION OF EQUATIONS FOR EACH MODE. FORMULATION IS COMPATIBLE WITH ASSUMPTION THAT 3-D MODAL DATA, TO BE FURNISHED AT A LATER DATE, WILL BE GENERATED BY USING A BENDING MODEL WHOSE TOTAL MASS INCLUDES (1) EMPTY AIRFRAME, (2) NON-SLOSH PROPELLANTS, AND (3) SLOSH PROPELLANTS (FROZEN); AND EXCLUDES ENGINE MASSES.	ADDITIONAL STUDY SHOULD BE DIRECTED TOWARD INVESTIGATING COMPATIBILITY OF ALTERNATE TYPES OF MODAL DATA WITH EQUATIONS OF MOTION AND RELATED SLOSH-BENDING INTERACTION.
VEHICLE TRAJECTORY (SECTION III)	PRESENT EQUATIONS ARE ADEQUATE. ADDITIONAL FORCES COULD BE EASILY ADDED USING THE PRESENT FORMULATION.	NONE
INITIALIZATION (SECTION IV)	EQUATIONS PROVIDE BOTH INITIALIZATION AND REPETITIVE RE-INITIALIZATION. DIFFERENT EARTH MODELS ARE PROVIDED BY PARAMETER ASSIGNMENTS. THERE ARE NO DYNAMIC VARIABLE INPUTS REQUIRED; THE ONLY OUTPUTS ARE CONSTANT PARAMETERS.	NO PARTICULAR RECOMMENDATION APPEARS APPLICABLE AT PRESENT. ADDITIONAL REFINEMENTS COULD BE ADDED TO EQUATIONS AS NEEDED.
GRAVITATION (SECTION V)	PRESENT EQUATIONS ARE ADEQUATE TO COVER A WIDE RANGE OF MODELS.	NONE
PROPELLANT SLOSH (SECTION VI)	FORMULATION WHICH CONSIDERS EFFECTS OF VEHICLE LATERAL AND ANGULAR ACCELERATIONS WILL SUITABLY MODEL THE FUNDAMENTAL SLOSH MODE IN EACH PROPELLANT TANK OF A MULTI-TANK CONFIGURED VEHICLE. PROPELLANT TANKS DISORIENTED WITH RESPECT TO THE VEHICLE COORDINATE FRAME MAY BE CONSIDERED. EQUATIONS VALID FOR • NORMAL AND HIGH-g SLOSH MODELS • PROPERLY SEATED PROPELLANTS • UNCOUPLED SLOSH PLANES • SMALL MISALIGNMENTS OF TANK LONGITUDINAL AXIS AND VEHICLE ACCELERATION VECTOR	ADDITIONAL STUDY OF PROPELLANT SLOSH MODELS FOR EXTREME TANK GEOMETRIES AND ORIENTATION SHOULD BE INITIATED. SLOSH IN TANKS THAT ARE LOCATED AT CONSIDERABLE DISTANCES FROM THE VEHICLE CG AND ITS INFLUENCE ON VEHICLE DYNAMICS SHOULD BE INVESTIGATED. PARTICULAR EMPHASIS SHOULD BE PLACED ON (1) THE DEVELOPMENT OF MATHEMATICAL MODELS FOR LIQUID SLOSHING IN AXISYMMETRIC TANKS WITH LONGITUDINAL AXES GREATLY MISALIGNED TO THE VEHICLE ACCELERATION VECTOR, (2) COUPLING OF SLOSH PLANES, AND (3) SPECIALIZATION OF EXISTING FORMULATION TO, OR DEVELOPMENT OF NEW FORMULATION FOR, LOW-g MODELS.
RIGID BODY ROTATION (SECTION VII)	FORMULATION IS ADEQUATE FOR CURRENT SIMULATION REQUIREMENTS. ADDITIONAL VECTOR MOMENTS SUCH AS THOSE PRODUCED BY GYROSCOPIC EFFECTS OF ROTATING MACHINERY MAY BE EASILY INTEGRATED INTO THE EQUATIONS.	NONE

Table 12-1. CONCLUSIONS AND RECOMMENDATIONS (CONCLUDED)

EQUATIONS	CONCLUSION	RECOMMENDATIONS
AERODYNAMICS (SECTION VIII)	FORMULATION FOR DETERMINING AERO FORCES ACTING ON RIGID AND FLEXIBLE SHUTTLE VEHICLES DURING FLIGHT THROUGH THE EARTH'S ATMOSPHERE INVOLVES CONSIDERABLE "LOOKUPS AND BOOKKEEPING". COMPUTER SIMULATION WILL PROBABLY BE HANDICAPPED BY EXCESSIVE COMPUTER CORE STORAGE REQUIREMENTS AND SLOW RUN TIME.	USING AN ALTERNATE APPROACH TO THAT CURRENTLY BEING UTILIZED IN THE AERODYNAMICS MODULE, DEVELOP A LESS TEDIOUS FORMULATION AMENABLE TO A SIMULATION THAT HAS A RIGID BODY OPTION AND A FLEXIBLE BODY OPTION FOR TREATING BENDING-AERO EFFECTS.
PROPULSION AND ENGINE DYNAMICS (SECTION IX)	GENERAL FORMULATION IS ADEQUATE BUT MAY REQUIRE A LARGE NUMBER OF ENGINE POSITION VECTORS AND CROSS PRODUCT OPERATIONS FOR A MULTI-ENGINE VEHICLE.	CONSIDER SIMPLIFYING ASSUMPTIONS AND APPROXIMATIONS THAT MAY BE VALID FOR VEHICLES POSSESSING A NUMBER OF SYMMETRICAL PROPERTIES. THIS WOULD REDUCE ALGEBRAIC OPERATIONS CONSIDERABLY.
LOADS (SECTION X)	FORMULATION PROVIDES FOR LOADS DETERMINATION AT FUSELAGE STATIONS ONLY.	EXTEND FORMULATION TO PROVIDE LOADS DETERMINATION AT ARBITRARILY SELECTED STATIONS.
GUIDANCE AND CONTROL (SECTION XI)	GENERAL FORMULATION PROVIDES CAPABILITY FOR IMPLEMENTING CHANGES IN CONTROL LAW GAINS AND DISTRIBUTION LAW GAINS AS REQUIRED.	ADDITIONAL FORMULATION SHOULD BE DEVELOPED TO (1) PROVIDE AN ADEQUATE CONTROL LAW ASSOCIATED WITH AERO CONTROL SURFACES, (2) INCLUDE ANGLE-OF-ATTACK FEEDBACK IN PRESENT FORMULATION FOR APPLICATION TO LOAD RELIEF STUDIES USING THRUST VECTOR CONTROL AND CONTROL SURFACES, AND (3) CONSIDER CONTROL SURFACE SUPPRESSION OF VIBRATIONS ASSOCIATED WITH VEHICLE BENDING.

Section XIII

REFERENCES

1. Aramayo, G. A., et al., "Modularized Flight Dynamics Simulation (Boost Phase)", Interim Report, Northrop-Huntsville TR-795-9-679, December 1969.

2. Northrop-Huntsville Technical Proposal, "Derivation of Equations for a 6-D Trajectory with 3-D Elastic Body Vehicle Dynamics", PS-795-9-553 (NHP-69-16), 27 May 1969.

3. Northrop-Huntsville Technical Proposal, "Derivation, Modularization, and Computer Application of Equations for a 6-D Trajectory with 3-D Elastic Body Vehicle Dynamics", PS-795-9-650 (NHP-69-32), 3 November 1969.

4. Brothers, J. R., et al., "Modularized Rotational Simulation", Northrop-Huntsville TR-795-9-542, May 1969.